LBL-16420
c.2

Lawrence Berkeley Laboratory
UNIVERSITY OF CALIFORNIA

Physics, Computer Science & Mathematics Division

RECEIVED
LAWRENCE
BERKELEY LABORATORY
SEP 27 1983
LIBRARY AND
DOCUMENTS SECTION

JET CROSS SECTIONS IN ELECTRON-POSITRON ANNIHILATION

S.R. Sharpe
(Ph.D. Thesis)

August 1983

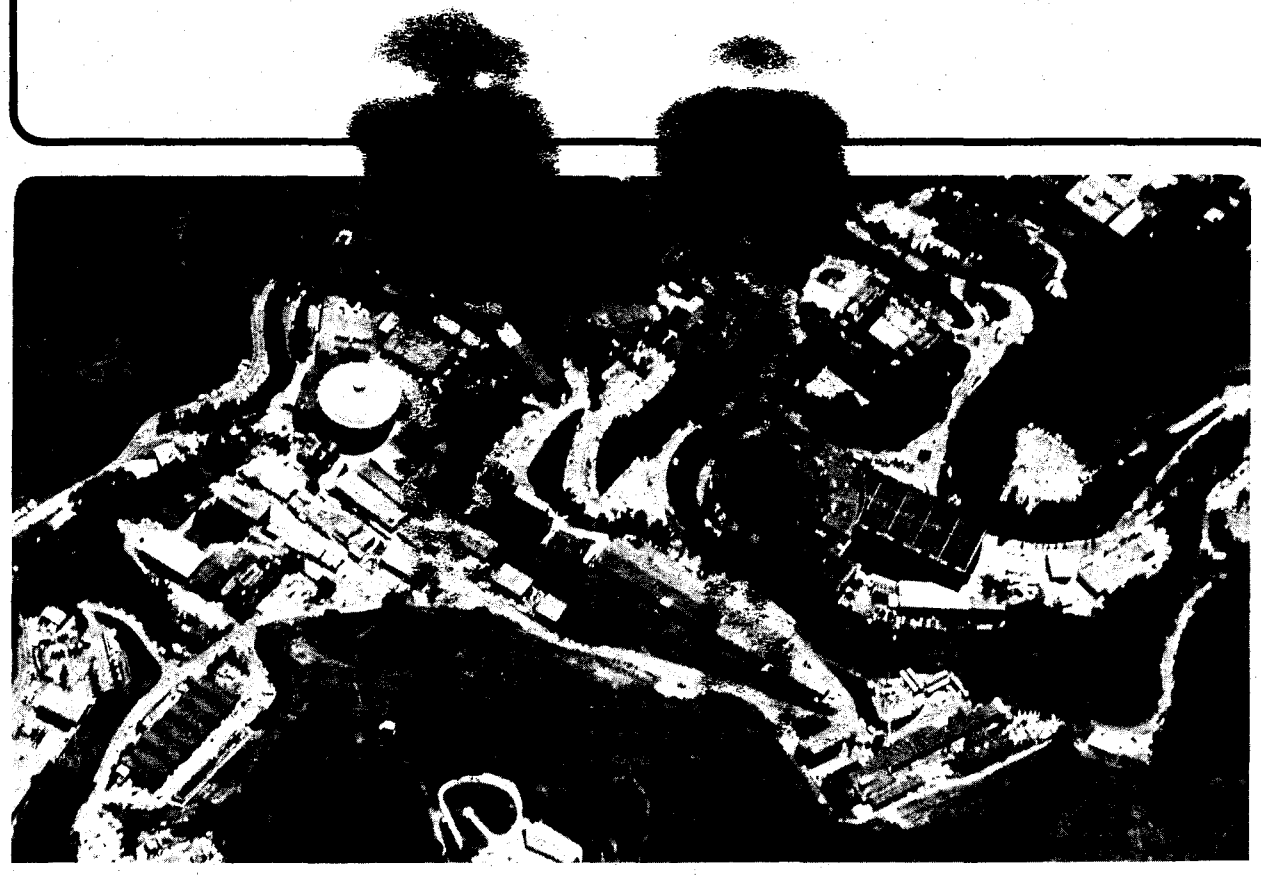

Prepared for the U.S. Department of Energy under Contract DE-AC03-76SF00098

LBL-16420
c.2

DISCLAIMER

This document was prepared as an account of work sponsored by the United States Government. While this document is believed to contain correct information, neither the United States Government nor any agency thereof, nor the Regents of the University of California, nor any of their employees, makes any warranty, express or implied, or assumes any legal responsibility for the accuracy, completeness, or usefulness of any information, apparatus, product, or process disclosed, or represents that its use would not infringe privately owned rights. Reference herein to any specific commercial product, process, or service by its trade name, trademark, manufacturer, or otherwise, does not necessarily constitute or imply its endorsement, recommendation, or favoring by the United States Government or any agency thereof, or the Regents of the University of California. The views and opinions of authors expressed herein do not necessarily state or reflect those of the United States Government or any agency thereof or the Regents of the University of California.

August 1982 LBL-16420

JET CROSS SECTIONS IN ELECTRON-POSITRON ANNIHILATION

Stephen Roger Sharpe

Ph.D. Thesis

Lawrence Berkeley Laboratory

and

Department of Physics

University of California

Berkeley, California, 94720 U.S.A.

This work was supported by the Director, Office of Energy Research, Office of High Energy and Nuclear Physics, Division of High Energy Physics of the U.S. Department of Energy under Contract DE-AC03-76SF00098.

JET CROSS SECTIONS IN ELECTRON-POSITRON ANNIHILATION

Stephen Roger Sharpe

ABSTRACT

There are few, if any, detailed tests of QCD at present. I discuss the problems associated with testing QCD and argue that the three jet angular distribution in electron-positron annihilation is a good quantity to use because it minimizes the sensitivity to non-perturbative effects and provides a test of the detailed structure of QCD. However, for such a test to be possible, the perturbation expansion must be well behaved. I present a calculation of the perturbative corrections using two different generalizations of the Sterman-Weinberg two-jet cross section. I argue that because of the uncertainties in our understanding of hadronization it is necessary that the corrections to both these cross sections be small. In presenting the results I use the recent proof of Mukti and Sterman that all the logarithms can be resummed. I find that at Z-factory energies there is a substantial region of parameters defining the jets for which the correction is small, but that there is no such region at PEP/PETRA energies. This problem at PEP/PETRA energies is made worse by the results of a study of the effects of hadronization. Using a simple model I find very significant effects at PEP/PETRA energies that would make a test difficult. These effects do not, however, present problems at Z-factory energies. I conclude that, even if there are further theoretical advances, testing QCD at PEP/PETRA energies using the three-jet angular distribution will be very difficult. However, this distribution can be used to test QCD in a detailed way at Z-factory energies. The corrected results, furthermore, show a systematic difference from the lowest order result that may be measurable at Z-factory energies. If this effect could be measured it would provide a yet more detailed test of QCD, testing, for example, the three gluon coupling.

ACKNOWLEDGMENTS

This work owes a great debt to Michael Chanowitz who provided much encouragement, many crucial discussions, and happy hours on the tennis court. He has given me a fine example to emulate.

I have also benefitted greatly from discussions with Robert Cahn and Ian Hinchliffe.

My interests have been kept from coming too narrow by lively conversations with many people at LBL and elsewhere. I thank particularly Alan Axelrod, Ghassan George Batrouni, Veit Elser, Mark Soldate and Andrew Strominger. I also thank Jim Andrews for showing me how to hit a home run, Bill Moses for teaching me how to sink a handjam, and Rem van Tyen whose search for the ultimate chocolate mousse has been an inspiration.

I give many thanks to Luanne Neumann for patiently typing this thesis.

I thank Susan Fidelman, Luanne Neumann and Betty Sublett for making the atmosphere at LBL so relaxed and friendly.

Finally, most is owed to Mary Whitlock Blundell for making my life so happy.

CONTENTS

1. INTRODUCTION 1

2. PERTURBATIVE CROSS SECTIONS FOR e^+e^- ANNIHILATION 6

3. CALCULATING THE LOGARITHMS AND CONSTANTS 21

4. NUMERICAL EVALUATION OF NON-SINGULAR PARTS 42

5. RESULTS 51

(a) Straightforward Analysis 51

(b) Hadronization 54

(c) Improved results 63

6. CONCLUSIONS 70

REFERENCES 72

TABLES 76

FIGURE CAPTIONS 78

FIGURES 81

1. INTRODUCTION

The last 15 years have seen a great revival of field theories. We now have, in addition to the fantastically successful Quantum Electrodynamics (QED), the weak interaction theory of Glashow, Salam, Ward and Weinberg (listed alphabetically), and the candidate for the strong interaction theory, Quantum Chomodyamics (QCD). The evidence for the Weinberg-Salam model (to return to common parlance), apart from the Higgs sector, is now very compelling - compelling enough for the Nobel committee! That for QCD is, in constrast, a huge mass of qualitative and semi quantitative data. As an example consider the status of scaling violations in deep inelastic scattering. There is general experimental agreement that there are such violations but there is significant disagreement on their magnitude and thus on the value of the strong coupling constant α_s.[1] Furthermore there is very little conclusive evidence that the running coupling constant of QCD actually runs. It is fair to say that most, nearly all perhaps, theoretical particle physicists think that QCD is the correct theory of strong interactions, but it remains true that there is little detailed quantitative evidence.

Given this situation it is important to search for further, more quantitative tests of QCD, and the work presented here is an attempt to find such a test. The only calculational tools available are weak coupling perturbation theory and non-perturbative lattice methods. The latter, though very important, are at a primitive stage and are only useful for determining the static properties of particles. For calculating scattering amplitudes there is only perturbation theory. Furthermore perturbation theory is only applicable at high energies. This lack of theoretical tools is, of course, the reason why it has been so hard to test QCD.

I shall use QCD perturbation theory to investigate the structure of the hadronic final states in electron-positron annihilation. The essential asssumption necessary in all applications of perturbation theory is that in processes involving large momentum transfers and, thus, short distance interactions one can calculate cross sections using quarks and

gluons (which I shall generically call partons) rather than hadrons. This assumption is reasonable because, firstly, QCD has a running coupling constant which though weak at short distances becomes strong at long distances so that one can conceive of long distance effects being strong enough to confine quarks and gluons while short distance interactions are weak. And, secondly, non-perturbative effects appear to be associated with a fixed scale - the radius of the proton, the limited transverse momentum in hadronic jets - and are suppressed by powers of this scale divided by the momentum transfer at large momentum transfers. These two reasons are no doubt related - the non-perturbative scale is roughly that energy at which the coupling constant becomes strong - but this connection is not understood in detail.

The assumption that perturbation theory can be used is, then, reasonable at "high enough" energies. However, one must determine for any given process what "high enough" precisely means. There are two ways in which the application of perturbation theory can become invalid, corresponding to the two arguments for the use of perturbation theory given above. Firstly the coupling constant must be small enough that perturbation theory is convergent. Following general usage, convergent is meant here in the loosest possible way, namely that the second term in the series is smaller by a reasonable amount than the first. Secondly, the quantity that one is calculating should be insensitive to "hadronization", i.e. the process of "conversion" of quarks and gluons into hadrons. Even if the quantity appears naively to involve a large energy scale, suggesting that non-perturbative effects should be suppressed, this is not always the case. One must be very careful in the choice of the quantity to use. An example, relevant to what follows, is that if one defines a jet in perturbation theory using a cone then one must beware because a real hadronic jet is much more like a tube. The scale characterizing the perturbative jet is $E_{jet}\,\delta$, where δ is the cone half-angle,whereas that for the non-perturbative jet is the average transverse momentum, $\langle p_t \rangle$. However, the condition $E_{jet}\,\delta >> \langle p_t \rangle$ does not imply that non-perturbative effects are small because hadronization distributes the energy of the jet among several particles. The angles of these particles relative to the jet axis will thus be larger than $\langle p_t \rangle / E_{jet}$ and may be comparable

to δ. Although this effect decreases with increasing jet energy, a detailed analysis by Furmanski[2] has shown that such effects are important even at LEP (large electron-position facility) energies. Clearly as one looks in a more detailed way at the perturbative predictions for any process the problem of sensitivity to hadronization becomes more acute. For example, interference effects during the "conversion" of partons to particles can change the detailed energy distribution in the e^+e^- final state but not the total cross section. As I am considering the details of the e^+e^- final state, I must use particular care in the choice of quantities to calculate.

A further problem in the application of perturbative QCD is the presence of singularities associated with soft momentum flows and thus with propagation over long distances. Such long distance effects cannot reasonably be described by perturbation theory and it must be either that they can be factored out or that they cancel leaving, in both cases, a quantity not dependent on any soft momenta. The first case is exemplified by deep inelastic scattering in which factorizaton in guaranteed by the renormalization group, and much effort has gone into generalizing this result to other processes, e.g. Drell-Yan production of $\mu^+\mu^-$ pairs. The second case, which is the one I shall consider in the following, includes the e^+e^- total cross section, Thrust,[3] Spherocity[4] and Sterman-Weinberg (SW) cross sections.[5] All these quantities do not contain terms like $\ell n(Q^2/\mu^2)$, where Q is the center of mass (CM) energy and μ the parton mass or off-shell-ness, although they do contain terms of the form μ^2/Q^2. The absence of $\ell nQ^2/\mu^2$ terms shows that one could calculate with all the partons offshell, $\mu \sim 1$ GeV say, thus avoiding long distance propagation in the diagrams, but still obtain the same answer as with $\mu = 0$ apart from small terms of $O(\mu^2/Q^2)$. This is the sense in which these processes are not dependent on soft momentum flows. A related point is that the quarks and gluons are off-shell in hadrons so that one should use $\mu \sim$ 1/5 - 1 GeV, but the answer obtained would not depend significantly on the choice of μ and the uncertainty in that choice. Although these quantities do not have logarithmic dependence on μ^2 Gottschalk[6] has found that the size of the perturbative corrections to Thrust-like distributions varies rapidly

with μ^2 for $\mu^2 \sim 1$ GeV^2 and $Q^2 \approx 900$ GeV^2, so that it is not clear whether at presently available energies these distributions can be reliably calculated. This last problem, which I will discuss in more detail in Section 2, does not apply, however, to the e^+e^- total cross section nor to Sterman-Weinberg cross sections.

To use perturbation theory to find tests of QCD clearly involves walking across a minefield. Furthermore after a safe traverse one may feel that one has very little left to show for one's efforts. Given this situation many have turned away (witness the increase in effort at PEP and PETRA aimed at weak interaction physics as compared to QCD related work) and others (almost all theorists) have chosen to apply their calculations ignoring all the possible pitfalls.[7] I find neither approach satisfying and have tried, in the following, to pick my way carefully across the minefield. I do come away with some positive results, although, unfortunately, I do not think that a detailed test of QCD of the type advertised above as necessary will be possible until Z-factory energies. Things are very marginal at PEP/PETRA energies though some sort of a test may be possible.

I present in this dissertation calculations of the perturbative corrections to the three jet cross-section in e^+-e^- annihilation. My strategy is to see if for suitably defined jets the corrections are small, because if they are small the lowest order angular distribution of the jets is a detailed possibly testable prediction of QCD. This angular distribution does depend on the vector nature of the gluon and on the nature of its coupling but these are essentially the same as for a photon in QED. It would be nice, therefore, to have a test which depended on the 3- and 4-gluon couplings which differentiate the non-Abelian from the Abelian theories. In fact it does appear to be possible, given the statistics of the Z-factories, and modulo various caveats which I will discuss, to perform such a test by looking for the difference in the angular distribution of the three jets from the lowest order result using certain definitions of the jets. If this result withstands the scrutiny of theorists and, most importantly, Monte-Carlo simulations of the possible sources of error, it gives an important stimulus to the study of QCD at Z-factories.

This work is presented as follows. In Section 2, I introduce the Sterman-Weinberg cross sections which I have calculated and discuss various of the "mines" that must be avoided, particularly the problem of minimizing dependence on hadronization. In Section 3, describe the analytical calculation of the most singular part of my answer. The calculations were also done by Fabricius, Kramer, Schierholz and Schmitt[8] (FKSS) and similar calculations were done by Ellis, Ross and Terano[9] (ERT) and by Vermarseren, Gaemers and Oldam.[10] I find agreement with ERT but not with FKSS, and I present arguments supporting my result. I mention these references now because there is substantial overlap between my work and that of FKSS, while I have drawn repeatedly from the results of ERT. The work presented in Section 3 is the only original matrix element calculation that I did; for the non-singular parts of the answer I used the matrix element results of FKSS and ERT and did substantial numerical work with them. Thus to a certain extent I have joined the growing ranks of the experimental theoreticians alongside the lattice calculators! The numerical calculations are outlined in Section 4, in which I present only enough to show that the problem was not entirely trivial. Section 5 contains results and is divided into three sections: naively corrected results, hadronization effects, and improved corrected results. In this section, I return to the minefield and the nitty-gritty physics of the problem. Finally, in Section 6, I present my conclusions, including a comparison of my work and approach with that of others. I should also note that some of this work was presented in a paper[11] which I shall refer to as SS below.

2. PERTURBATIVE CROSS SECTIONS FOR e^+e^- ANNIHILATION

Electron-positron annihilation experiments have provided considerable qualitative and some quantitative evidence for QCD. The size of the total hadronic cross section, appropriately smeared, agrees roughly with that predicted.[12] The presence and angular distribution of 2-jet events seen at SPEAR was a dramatic confirmation of the existence of spin 1/2 quarks and the applicability of perturbation theory.[13] The observation of clear 3-jet events at PETRA[14] and then at PEP[15] was the first direct evidence for the existence of the gluon. There is also some evidence for 4-jet events[16] at a small rate comparable to that expected by perturbation theory.

Thus we can feel confident that the naive notion of associating a primitive parton with a jet of hadrons is roughly correct. But, as discussed in the introduction, in order to find a detailed quantitative test of QCD we must consider quantities which are insensitive to long-distance processes when calculated in perturbation theory and as independent as possible of the details of hadronization. There are various quantities which have been used and approaches which have been taken. However, I will procede directly to a discussion of the S-W cross sections which I have used, and return to discuss the relative merits of the various alternate approaches.

It is worthwhile considering the 2-jet SW cross section before proceding to the 3-jet case. Sterman and Weinberg defined[5] a 2 jet configuration as one in which all of the energy but for an amount εE_{beam} or less falls into two oppositely directed cones of half angle δ which lie in calorimeters at an angle θ to the beam direction. (They actually used an ε half that defined here but I prefer this definition.) The point of this geometrical definition is that it can be applied to a perturbative configuration of any number of partons and furthermore that it is infrared finite. Loosely speaking the infrared finiteness follows because the detection criteria do not distinguish events with an extra soft parton from those without nor do they distinguish events with a group of collinear partons from those in which those parton are "combined" to form one parton. But these are the configurations which, as will be seen in detail in Section 3,

give rise to soft and collinear singularities respectively and these singularities will cancel, according to the KLN theorem,[17] since the singular parts are added with equal weight. This result has been proved to all orders by Sterman[18]. Sterman and Weinberg calculated their cross section to $O(\alpha_s)$ and found:

$$\sigma^{SW} \propto (1+\cos\Theta^2)\,[1-2C_F\,\frac{\alpha_s}{2\pi}\,(4\ln\delta\ln\varepsilon + 3\ln\delta + \frac{\pi^2}{3} - \frac{5}{2}) + O(\alpha_s\delta, \alpha_s\varepsilon) + O(\alpha_s{}^2)] \tag{2.1}$$

where $C_F = 4/3$ is the Casimir for the fundamental representation in QCD. The 1 in the square brackets in Equation 2.1 is the contribution of the lowest order qq diagram while the $O(\alpha_s)$ terms come from the virtual 1 loop $q\bar{q}$ diagrams and the $q\bar{q}g$ tree diagrams. The $\ln\delta$ and $\ln\varepsilon$ terms reflect the collinear and soft singularities respectively. The constant terms, independent of ε and δ, are also a product of the singularities since non-singular integrands would give a vanishing result as $\varepsilon, \delta \rightarrow 0$. The $O(\alpha_s\varepsilon, \alpha_s\delta)$ terms were calculated by others[19] and found to be small for nearly all ε and δ. Notice, finally, that for small δ and ε the logarithms grow large and the perturbation expansion does not converge.

The importance of this definition and calculation was threefold. Firstly it provided a precise definition of jets in perturbation theory. Secondly it showed that 2 jet events should dominate the e^+e^- crosssection at high energies. To show this explicitly Sterman and Weinberg calculated the fraction of events satisfying their 2-jet criterion. The result is the same as the square bracket in 2.1 with the 5/2 replaced by 7/4. Thus this fraction tends asymptotically to 1 for fixed δ and ε. Thirdly, their calculation showed that the $1 + \cos^2\theta$ angular distribution, which had been measured, was a precise prediction of QCD. The $O(\alpha_s\delta, \alpha_s\varepsilon)$ terms do provide a small correction to this distribution.[20] However, Sterman and Weinberg suggest that the $1 + \cos^2\theta$ distribution is correct to all orders for the logarithms

and constants, with massless quarks. This is because helicity conservation forbids a magnetic moment term in the radiatively corrected vertex. Such a term would give rise to a constant termwith a $1\text{-}\cos^2\theta$ angular distribution at $O(\alpha_s{}^2)$ for massive quarks. They also pointed out that their definition could be easily generalized to multijet events.

How does hadronization effect this successful perturbative prediction? Experimentally one selects two jet events by making a cut on thrust or a similar quantity, or by a cluster algorithm, and one must assume that this corresponds in some way to the partonic SW cross section. It will not correspond to a SW cross secton with a particular ε and δ but, rather, to a weighted average of such distributions. One might argue that one should include a weighting for perturbative configurations with the cones not back to back.[21] This, however, would not change the conclusions. Assuming such a weighting function then the $1 + \cos^2\theta$ distribution is a prediction after hadronization as long as there is very little weight in the small ε and δ region where the perturbation expansion is not convergent. Recent results have, however, almost removed this caveat. Mukti and Sterman[22] have shown that <u>all</u> the logarithms of ε and δ can be exponentiated or absorbed into the scale of α_s. This means, as will be discussed in more detail in Section 5, that a leading logarithm summation can be performed[23] and is reasonable even when the non-leading logarithms become large. Once the logs can be summed the remaining correction terms in 2.1 are small and so δ and ε can be made much smaller. The limit now comes from the requirement that $Q\delta >> \Lambda$, where Λ is the perturbative scale of QCD, so that $\alpha_s(Q\delta) < 1$. A similar restriction applies to ε. This new restriction ensures that the SW cross section does not depend on the infrared regions of perturbative diagrams. These lower limits on δ and ε are small even for jets at SPEAR energies. Thus most experimental criteria will not have significant weight inside the disallowed region, and so the $1 + \cos^2\theta$ distribution is, for such criteria, a prediction resting only on the assumption that perturbation theory can be used at all.

The perturbative "jets" of SW are very different from non-perturbative jets.[5] For fixed ε in order to keep the fraction of 2- jet events fixed as E_{beam} varies one has to vary δ like

$E_{beam}^{-0.25}$. Infact when δ gets smaller than ε one must use a modified definition proposed by Rakow and Webber[21] and then δ falls more slowly than any power of E. These results will remain valid if the logarithms are summed for not too small ε and δ.

These properties of the perturbative jets are to be compared with a non-perturbative jet with limited transverse momentum and a rapidity plateau of constant height for which a similarly defined δ falls like $1/E_{jet}$ up to logarithms. It might seem, therefore, that the SW definition is too restrictive, there perhaps being perturbative structure inside the SW cones. Of course, to study this rigorously, one would have to use a multijet SW cross section. However, the exponentiation of all logarithms and the smallness of the remaining correction make it reasonable, in the two jet case at least, to use the leading logarithm approximation. Doing this, one does find more and more structure as the energy increases with increasingly many "jets within jets" being resolved.[24] However, if one makes reasonable assumptions about hadronization, this structure does not begin to show until the jets have energies of a few hundred GeV and is not fully manifest until one has TeV jets.[25] Thus at PEP/PETRA or Z-factory energies one is not losing information by studying fixed angle SW jets. I have studied 3-jet processes but only for three widely separated jets each of fixed opening angle. I have not considered possible structure within these "large" jets.

A related point is that it might seem possible to use the variation of σ_{SW} with δ and ε, i.e. the jet broadening, to test QCD. However, because of hadronization, such a test is hopeless at PEP/PETRA energies and difficult at Z-factory energies, as was shown by Furmanski.[2] He compared the fraction of SW 2-jet events obtained using the leading-logarithm-summed perturbative result and using a fixed transverse momentum, independent emission model of a non-perturbative jet. He also combined perturbative and non-perturbative results in a simple way to look at "realistic" jets. He found that at PEP/PETRA energies the non-perturbative broadening dominates. The situation improves as the jet energy increases, but even for a 100 GeV jet the value of δ for which half the events are accepted is roughly equal for perturbative and non-perturbative jets, although for larger δ ($\delta \geq 20^0$) the perturbative component of the

realistic jets may be measurable. Thus for the 15-40 GeV jets in three jet events at Z-factory energies it will not be possible to measure the perturbative jet broadening. This suprisingly large hadronization effect, is, as discussed in the introduction, due to the mismatch of cones and tubes.

Thus it does not seem possible, even at Z-factory energies, to study the detailed structure of jets. Furmanski does define ratios of SW cross sections that are less sensitive to hadronization, but this insensitivity is dependent to some extent on his model of a "realistic" jet. To avoid much of the dependence on the details of hadronization, one can, instead, consider the 3-jet cross section and study the angular distribution of these jets. The importance of considering the angular distribution is that although hadronization will broaden the jets it will leave their directions nearly unchanged. The advantage of the 3 jet cross section over that for 2 jets is that the dependence of the cross section on the two additional degrees of freedom (the angles between the jets in the event plane) is sensitive to the nature of the QCD coupling of quarks and gluons. This is in contrast to the angular distribution with respect to the beam direction which for both 2 and 3 jets reflects the electomagnetic coupling of the quarks. Of course to make the notion of jets precise, one must use a generalized SW criterion, and I will present two such criteria below. In order that the 3-jet cross section and associated angular distribution be measurable the $O(\alpha_s)$ corrections to this cross section must be small. But because of the non-perturbative broadening of jets, this must be true for a range of ε and δ since, as in the 2 jet case, any experimental jet finding algorithm will correspond to a weighted average of perturbative SW cross sections. Notice that I am not interested in the detailed ε and δ dependence of the cross section, which, as discussed above, cannot be measured, but only in the region of ε and δ for which the correction is small. However, it may be, as in the 2 jet case, that the <u>shape</u> of the $O(\alpha_s)$ <u>corrected</u> angular distribution is nearly independent of ε and δ for a range of these parameters. Furthermore, unlike the 2-jet case, there is no reason why this corrected distribution should be the same as the lowest order result. In fact, there is such a systematic difference and this difference may

be measurable, providing a yet more detailed test of QCD . All of these points are discussed in more detail in the remainder of this section and in Section 5.

The lowest order contribution to the three jet cross section comes from the Born qqg diagrams which are shown in Figure 2.1. These were calculated by Ellis, Gaillard and Ross,[26] who suggested that the partons should be interpreted as jets and that the angular distribution should be measurable. They found the result:

$$\frac{d^2\sigma}{dx_1 dx_2} = \sigma_0 C_F \frac{\alpha_s}{2\pi} \frac{x_1^2 + x_2^2}{(1-x_1)(1-x_2)} \tag{2.2}$$

where x_1, x_2 are the quark and antiquark energies scaled by the beam energy, and σ_0 is the lowest order e^+e^- total cross section. However, as explained above, this must be interpreted as the lowest order contribution to a 3-jet SW cross section, and, if this is to be claimed as a prediction of QCD, the corrections must be calculated and shown to be small. I have calculated the corrections using two different definitions of the SW 3-jet cross section. The first definition, which I shall call the "energies" case, is that a perturbative configuration contributes to the 3-jet cross section if all but a fraction $\varepsilon/2$ or less of the total energy falls into 3 cones of half angle δ. The "lost" energy is thus less than or equal to εE_{beam}. The three cones are positioned so as to maximize the total energy in them, and if the resulting energies in the cones are $E_1 > E_2 > E_3$ I define the scaled energy variables x_i' by:

$$x_i' = 2E_i/(\sum_{j=1}^{3} E_j) \qquad i=1,2,3 \tag{2.3}$$

so that $\Sigma x_i' = 2$, as for the x_i of the qqg lowest order calculation. I define the "angular distribution" to be:

$$\frac{d^2\sigma}{dx_1' dx_2'} = \sigma_0 C_F \frac{\alpha_s(Q)}{2\pi} F_1(x_1',x_2') \left(1+\frac{\alpha_s(Q)}{2\pi} F_2(x_1',x_2';\varepsilon,\delta) + O(\alpha_s^2)\right) \tag{2.4}$$

where α_s, is defined in the $\overline{MS}$ scheme, and from the calculation of Ellis, Gaillard and Ross

$$F_1(x_1',x_2') = \sum_{\substack{i,j=1 \\ i\neq j}}^{3} \frac{x_i'^2 + x_j'^2}{(1-x_i')(1-x_j')} \tag{2.5}$$

with $x_3' = 2 - x_i' - x_2'$. I have calculated the $O(\alpha_s)$ correction term, F_2.

There are a number of points to note. Firstly, I am assuming an integration over the beam direction. This leaves only the angular distribution within the plane, which is that part of the cross section that depends mainly on the QCD quark-gluon couplings. One might be worried since experimentally one cannot detect all 3-jet events and so cannot completely perform such an averaging. However, in lowest order the angular distribution in the plane, i.e. F_1, decouples from that of the normal of the plane itself and the same is true of the logarithmic terms in F_2 and at least some of the constant and $O(\varepsilon, \delta)$ terms. I assume that this happens to a sufficiently good approximation for the remaining terms so that I am justified in doing this angular averaging. In fact various results I use from ERT have been so averaged so I am forced to do this averaging anyway. Secondly, since it is not possible (certainly on an event by event basis) to distinguish quark and gluon jets, I only differentiate between the jets on the basis of their energies. This leads to the sum over permutations in (2.5). Thirdly, I use the x_i' variables rather than, say, E_1/E_{beam} and E_2/E_{beam}. This choice gives variables connected by the same kinematic relation as the lowest order variables, and is symmetric between the three jets. The most important reason for this choice, however, is that x_i' are less sensitive to hadronization. Fourthly, I should point out that the definition differs from the 2-jet SW definition in not being calorimetric because I include the injunction to position the cones so as to maximize the energy. The resulting cross section is not exactly the same, though similar, to that obtained from averaging the results from a three arm calorimeter

with cells subtending solid angle $n\delta^2$. I prefer the choice made above because it represents more closely what is actually done by experimentalists searching for jets with, for example, a cluster algorithm. The injuction to maximize total cone - energy is infact somewhat arbitrary - at the level of 4 massless partons maximizing total momentum is equivalent. Fifthly, there are constraints on ε and δ necessary for the consistency of the 3-jet criterion. The energy in the least energetic jet must be greater than $\varepsilon\, E_{beam}$ which means that $\varepsilon < x_3^{min}/(1 + x_3^{min}/2)$. For $x_i' \leq .85$ - a region I shall restrict myself to below - this implies $\varepsilon < .26$. It is also necessary that the angle between any two of the jets is never less than 2δ, otherwise the event would only contain two SW jets. This is in fact a stronger constraint than that just described, and the excluded region in the ε, δ plane is shown in Figure 5.1. Finally, there is the problem of possible cone overlap for large δ, i.e. an ambiguity in the assignment of partons to cones. I return to this point shortly.

I presented the results of a calculation of F_2 in SS. I also presented the results of an analysis of the effects of hadronization which I discuss in Section 5. There were , as I subsequently discovered, two small errors in the computer programs (errors in transcribing formulae from paper to code) I had used, but fortunately they had very little numerical effect and did not change any numbers which I present in SS. The results which I present below have been corrected for these errors. There was a more serious omission in SS which was that I had overlooked the problem of overlapping cones. Again, fortunately, this does not affect the numbers presented nor the final conclusions, though some of the intermediate results (e.g. the size of the allowed region) are slightly modified. The main result of this oversight was the lack of a discussion of the problem of cone overlap and the associated problem of the uncertainty in the choice of SW definition to be used.

The overlap problem occurs when a soft parton is approximately midway between two hard partons and the angle between it and either of the two partons is less than 2δ. This situation is illustrated in Figure 2.2 with $\delta = 25^\circ$ and $x_i' = .8$, $x_2' = .65$. Clearly whether

overlaps can occur depends on the x_i'. Later I use the restriction $x_i' \leq .85$ in which case the smallest angle betwen two jets occurs for $x_i = .85$, $x_2 = .575 = x_3$ and is $\approx 85^\circ$. Thus $\delta \leq 21^\circ$ to avoid overlaps, which is a severe restriction as will be seen in Section 5. To remove this restriction I augment the definition by associating the soft parton with the hard parton closest in angle if an ambiguity arose. This revised definition is identical to that proposed by Hagiwara,[27] and can be extended to any number of partons.

The overlap problem can be alleviated by changing the jet criterion: forcing the axes of the cones to lie along the direction of the momentum sum of the partons which they contain. Together with the injunction to maximise the energy or momentum in the cones such a definition is applicable to any numbers of partons. Changing the cone definition has no effect on configurations like that shown in Figure 2.3a, but for that shown in Fig. 2.3b the two partons will not be accepted as a jet by the new definition, although they would be by the original definition. However, if the soft parton has energy less than εE_{beam} the event would be accepted by the new criterion as a 3 jet event but with different x_i' from those obtained with the original definition. The new definition lies somewhere between the original definition with the same δ and that with δ halved, ε being the same in both cases. It increases the maximum δ not leading to overlaps by 50%.

This alleviation of the overlap problem is, however, illusory because, as I now explain, there is a genuine uncertainty in the choice of correct SW criterion. The difference between these two definitions is that they give different values of the x_i' to some partonic configurations and that other partonic configurations are accepted for a larger range of parameters of the original definition than of the revised definition. For energies high enough that hadronization is a negligable effect one could choose to use either definition experimentally. However, when hadronization is important one has to attempt to lump together partonic configurations equally likely to be accepted by an experimental jet finding criterion after hadronization, and these two definitions are possible ways of doing this. The correct way will, of course, depend upon the details of hadronization and the experimental

criterion used. To illustrate the latter point I show possible real final states for the partonic configurations of Figs. 2.3a, b in Figs. 2.3c, d respectively. An experimental cluster algorithm that clusters in the angle between particles[29] would probably treat these two configurations similarly; clustering biased towards more energetic particles[29] would more likely accept Fig.2.3c as one jet than Fig. 2.3d. Thus in the former case the original cone definition is probably more appropriate, while in the latter the revised definition should probably be used. But clearly, given our ignorance of the details of hadronization, we cannot with any certainty decide which definition to use. A reasonable way to proceed is, therefore, to require that both definitions yield small corrections. Thus I have calculated the 3 jet cross section with the revised cone definition, but also with another change which I now describe.

I make this other change because of an another problem associated with hadronization, which I discussed in SS. This is that the third jet tends to lose a greater fraction of its energy upon hadronization than the second jet, which in turn loses a greater fraction than the first jet. This problem is discussed in more detail in Section 5, but it is clear that it will lead to a systematic shift downwards in x_3' and upwards in x_1'. One may attempt to correct for this using Monte-Carlo Models of hadronization, but it would be preferable to avoid such corrections. This may be done by considering the angles between the jets rather than their energies. These angles will of course be changed by hadronization but there will be no systematic shifts because the energy lost due to hadronization is distributed symmetrically on average.

Thus my second definition, which I call the "angles" definition, uses the revised cone criterion and the angles between the jets as variables. More precisely I consider

$$\frac{d^2\sigma}{d\Theta_1 d\Theta_2} = \sigma_0 C_F \frac{\alpha_s(Q)}{2\pi} F_1(\Theta_1,\Theta_2) \left[1+\frac{\alpha_s(Q)}{2\pi} F_2(\Theta_1,\Theta_2;\varepsilon,\delta) + O(\alpha_s^2)\right] \qquad (2.6)$$

where θ_1 and θ_2 are the largest and next to largest angles between the jets when the jets are projected onto the plane in a particular way. This projection is necessary because of the energy outside the cones. I choose to project onto the plane whose normal is $\rho_1 + \rho_2 + \rho_3$, where ρ_i is the unit vector in the direction of the axis (i.e. the momentum sum) of the ith cone. This choice leaves the $u_i = (1 - \cos\theta_i)/2$ in the same ratios and I found it to be convenient for calculations. The particular choice of projection only effects the $O(\varepsilon, \delta)$ terms in F_2 and only effects these terms mildly. Thus I would expect the results and conclusions to be little effected by the precise choice of projection. Furthermore for similar reasons I expect, though I have not checked this in detail, that the major difference between the energies and angles results come from the change in the cone definition.

I will frequently convert the angles result back into the energies notation using the $x_i'(\theta_i)$ appropriate to three massless partons lying in a plane. This I do to give a uniformity of notation but also because various experimental groups[30] have defined x_i' in this way. Having done this the $F_1(x_i')$ is the same in the angles case as in the energies case (Equation 2.2).

As explained above, with this cone definition the overlap "problem" is less severe. For the region $x_i' \leq .85$ the limit on δ is $\approx 30^\circ$; for $x_i' \leq .9$, $\delta \leq 25^\circ$. These limits are sufficiently weak that I chose not to go beyond them, thus avoiding confronting the problem of altering the jet definition as in the energies case. The limits on ε are, however, more severe than in the energies case, this being the price one pays for using the angles between the jets as variables. For $x_i' \leq .85$ I find that $\varepsilon < .15 - .175$ and for $x_i' \leq .9$ I find $\varepsilon < .1 - .125$ where the range of limits on ε reflects a variation of the limit with δ, the most stringent limit being for small δ. I need not have paid this price because I could have used the energies definition with the new cone criterion, but for the reasons discussed above I prefer to use the angles between the jets as variables.

The angles calculation is, I have argued, necessary and important in order to see whether the 3-jet angular distribution can be measured at PEP/PETRA and Z-factory

energies. It is also important in providing many checks on the energies calculation with which it has a significant overlap. In fact, as I explained above, I did find some errors.

For the remainder of this section I discuss briefly other quantities that have been suggested for testing QCD in e^+e^- annihilation, and the criticisms of these tests and the SW cross sections made by various authors, particularly Gottschalk.[6]

One of the most common approaches to comparing QCD with the data has been to compare in great detail the hadronic final state of real events with those produced by a Monte-Carlo simulation including the lowest order qqg and, in some cases, the lowest order 4 parton result also. One finds a good agreement, although there are some discrepancies, with $\alpha_s = .15 - .28$ depending on the Monte-Carlo scheme.[31] There are two main objections to this approach. Firstly it clearly involves testing the Monte-Carlo model as much as testing the QCD matrix elements. This has been shown dramatically by the CELLO group who find differences in the value of α_s by factors between 1.28 and 1.67 using two different fragmentation models![31] Secondly, there is no simple way of including QCD perturbative corrections into the models. One striking consequence of this is that the 3-jet matrix element has to be cut off near the 2-jet configuration in an ad hoc way. At PEP/PETRA energies this presents little problem because of the smearing of 2-jet events by hadronization. But at Z-factory energies a gap will begin to open between the smeared 2-jet events and the most extreme 3- jet events allowed by the cut off!

This latter problem can be solved by using leading logarithm (LL) models [24,25,32,37] which exponentiate the leading singularities and thus smoothly extrapolate across the gap. These models are, however, based on certain approximations and cannot easily include corrections. They incorporate factorization of the jet evolution from the initial hard process and, because they involve degrading the virtualness of initially highly virtual partons down to some cut off q_0^2, they also factorize the perturbative from the non-perturbative jet evolution. This means that hadronization is easily incorporated, but that

non-factorizable (in the first sense) and interference correction terms are not easily included, the latter because the jet evolution is probabilistic. An exception is the recent work of Marchesini and Webber[33] who have incorporated into a LL Monte Carlo the non-factorizable terms that contain some interference contributions considered by Bassetto, Ciafaloni, Marchesini and Mueller,[34] but this relies on a special circumstance. However, as discussed in the introduction, an alternative to factorization (of both kinds) is the use of infrared safe quantities like the SW cross sections. These include all non-factorizable and interference terms - for example, there are $\ell n\, \varepsilon$, constant and $O(\varepsilon, \delta)$ terms of this type in F_2. These terms are important in determining the region of δ and ε in which the corrections are small. Gottschalk[6] has criticized the SW cross sections because of their lack of factorization (of both types, I think), but this "lack" means that SW cross sections go beyond the LL models. In fact it seems reasonable that a necessary condition for the applicability of the LL models is that the non-factorizable and interference terms calculated using a SW criterion are small. It is true, as Gottschalk also points out, that hadronization presents problems for the application of SW cross sections - this has been seen clearly above. But this is not a problem of principle - it will not be present at high enough energy - and, in any case, although hadronization is easily fitted into the LL models, this does require various assumptions.

Even assuming the validity of the approximations on which they are based, these LL models cannot test QCD at PEP and PETRA energies and below because the treatment of hadronization is a crucial ingredient at these energies. For instance the value of Λ_{QCD} found by Field and Wolfram[35] differs by a factor of 7 from that found by Gottschalk,[36] the main difference between the models being the way in which they hadronize soft partons. But it is interesting that some of these models[35,36] find that to fit the data they must allow partons to evolve perturbatively down to a virtualness of $\sim 1\ \mathrm{GeV}^2$. These models provide an adequate fit to the e^+e^- data for CM energies from 10 to 30 GeV, and in these fits a significant part of what I have implicitly assumed to be non-perturbative broadening comes from the perturbative evolution. If these models are correctly describing the physics, then the effects of

hadronization discussed throughout this dissertation will have been somewhat overestimated. It is not clear, however, that this is true because other LL models, using a different model of hadronization, need a cut off $q_0^2 \sim 10\ \mathrm{GeV}^2$ to describe the data.[37] The case for such a large cutoff has been made recently in some detail by Walsh and Zerwas.[38] In fact up to PEP/PETRA energies these models are very similar to the successful standard Monte-Carlo models discussed above. Most of the conclusions I present would not, in fact, be changed were hadronization a smaller effect as they are based on perturbative results, but the possibility should be born in mind during the discussion of hadronization in Section 5.

Finally I discuss inclusive quantities, i.e. those that assign a value of some quantity to every final state, for example Thrust[3] and energy-energy correlations.[39] The advantage of such quantities is that they are easily measured - the signal is large. The disadvantages are that they are sensitive to the smearing due to hadronization and that there is a lot of noise (from 2 jet events) from which one must disentangle the signal (3- and 4-jet events). The smearing problem also effects SW cross sections, as I discuss in Section 5, so that the advantage of the SW cross sections is that they look in more detail at the final state and thus can potentially extract more information. Given the statistics available at PEP and PETRA this may not in fact be an advantage because the signal is so small, but at a high statistics Z-factory this is, I think, important. There is, furthermore, a problem with some of these inclusive quantities which was noticed by Gottschalk,[6] and also is contained in the work of Kunszt.[40] In order to understand the apparent discrepancy between the results of ERT and FKSS - the former found large corrections to thrust-like distributions while the latter found fairly small corrections to the SW cross sections - Gottschalk looked at the dependence of the ERT result on soft momentum flows. He introduced a cut off (q_c) on the invariant mass of any two final state partons, such that if two partons had a mass less than q_c the two partons were treated as a single (massless) jet. This is, at least for 4 partons, similar to the SW criterion. He then calculated the distribution of the thrust-like variable C for various values of q_c, but in all cases using <u>all</u> 3 and 4 parton configurations. The ERT result is obtained at $q_c \to 0$. He

found that the size of the correction depended sensitively on the size of the cut off for $10^{-3} \leq y = q_c^2/Q^2 < 4.10^{-2}$, where Q is the CM energy and the ERT result is obtained at the lower limit while the FKSS result is obtained, approximately, at the upper limit. I think, though I have not proved this, that this sensitivity is not true for energy-energy correlations. It is certainly not true for the SW cross sections with ε and δ large enough that the sensitive range of y is contained with the cones (roughly $\delta^2 > y_{max}$, $\varepsilon > y_{max}$). The precise significance of this result is not clear. At PEP/PETRA energies the sensitive range corresponds to $1\ \mathrm{GeV} < q_c < 6\ \mathrm{GeV}$ which is arguably in the non-perturbative region so that the corrections to thrust-like distributions can probably not be reliably calculated. At Z-factory (Q = 100 GeV) energies this range becomes $3\ \mathrm{GeV} < q_c < 20\ \mathrm{GeV}$ so that the ERT result, which corresponds to the lower limit, is probably good. In any case this is one example of the "mines" discussed in the introduction.

3. CALCULATING THE LOGARITHMS AND CONSTANTS

In this section I present, in some detail, the calculation of the contribution to F_2 from the singular part of the 4-parton cross section for both the energies and angles cases. Such a calculation was also done, for the energies case, by FKSS and our results differ. Our methods of calculation are, however, different (e.g. we use different gauges) and a direct comparison is not easy. I have, though, found the sources of the differences and, I believe, strong arguments favoring my results. I should also mention that my result for the singular part of the matrix element squared, a significant part of the calculation, agrees with that of ERT.

Only the singular part of the 4-parton matrix element can produce logarithms and constants as nonsingular parts will integrate to give terms of $O(\varepsilon, \delta)$. One may approximate the matrix element and phase space in order to simplify the singular part, as long as the approximations only give rise to $O(\varepsilon, \delta)$ terms. The phase space integrations over the singular parts, and the singular parts themselves, must be regulated and the regulator must be the same as that used in the calculation of the loop diagrams. ERT and FKSS use dimensional continuation[41] for the loop diagrams (for both ultra-violet and infrared singularities) and so I use this regulator for the 4-parton diagrams. This allows the partons to be massless, which considerably simplifies the calculation. Ignoring quark masses for the known quarks will make only a small error at PEP/PETRA energies (apart from the quarks in the gluon vacuum polarization diagrams which I will discuss in Section 5) and a negligible error at Z-factory energies.[42] Of course if a heavy top quark is found the results presented here will probably not be applicable, and one must try to remove such events from the analysis.

The singularities of the matrix element fall into two classes - soft and collinear. The former occur when all the components of a parton's momenta vanish uniformly. The latter, also known as mass singularities, are found when two massless partons become collinear. These divergences occur because the sum of two collinear lightlike momenta is also lightlike. Both these divergences are well known in QED.

The source and nature of these singularities is best understood by considering an example. Figure 3.1 shows part of a squared amplitude in which a quark "emits" a gluon. The cross section for the whole process will thus contain a term:

$$\int \frac{d^{n-1}p}{2E_p} \frac{d^{n-1}k}{2E_k} \frac{(\not p+\not k)}{(p+k)^2} \gamma^\mu \not p \gamma^\nu \frac{(\not p+\not k)}{(p+k)^2} \Delta_{\mu\nu}(k) \tag{3.1}$$

where $\Delta_{\mu\nu}$ is the sum over gluon polarizations. Now $(p + k)^2 = 2\, p\cdot k = E_p E_k(\theta_{pk}{}^2 + O(\theta_{pk}{}^4))$ so as the gluon goes soft ($E_k \to 0$) we have:

$$\int \frac{d^{n-1}k}{E_k} \frac{1}{E_k{}^2} \propto \int dE_k\, E_k{}^{n-5} \tag{3.2}$$

Thus for $n \leq 4$ there is a divergence. It is regulated by taking $n > 4$ thoughout the calculation and then, after all poles at $n = 4$ have cancelled, setting $n = 4$. Notice that there is no divergence as the quark goes soft.

As the quark and gluon become collinear we have:

$$\int d\cos\Theta_{pk}\, (\sin^2\Theta_{pk})^{\frac{n-4}{2}} \frac{1}{\Theta_{pk}{}^2} (\not p+\not k)\, \not\varepsilon\, u(p)\, \bar u(p)\, \not\varepsilon\, (\not p+\not k) \frac{1}{\Theta_{pk}{}^2}$$

$$= \int d\Theta_{pk}\, \Theta_{pk}{}^{n-7}\, (\not p+\not k)\, \not\varepsilon\, u(p)\, \bar u(p)\, \not\varepsilon\, (\not p+\not k) \tag{3.3}$$

where I have written out explicitly the particle wavefunctions. Now $(\not p+\not k)\not\varepsilon\, u(p) = 2(p + k).\varepsilon\, u(p) - \not\varepsilon\, (\not p+\not k)\, u(p)$ and thus since $k.\varepsilon = 0$ and $\not\varepsilon u(p) = 0$ the numerator vanishes in the collinear limit. To see how fast it vanishes I write, using a Sudakov[43] decomposition:

$$k = \frac{E_k}{E_p} p + \frac{E_k}{E_1} \frac{\Theta_{pk}^2}{4} \bar{p} + E_k \Theta_{pk} \hat{k}_t + O(\Theta_{pk}^3) \tag{3.4}$$

where $p = (E_p, -\mathbf{p})$ and $k_t^2 = -1$, $k_t \cdot p = k_t \cdot p = 0$.

Thus the leading non-vanishing term in the numerator of Eq. (3.3) is proportional to θ_{pk}^2 - from the k_t term in Eq. (3.4) - so the collinear singularity becomes:

$$\int d\Theta_{pk} \, \Theta_{pk}^{n-5} \tag{3.5}$$

a logarithmic divergence for $n = 4$ as for the soft divergence.

This extra suppression factor is a consequence of helicity conservation in massless QCD. A quark cannot transmute into a collinear quark and gluon and conserve both spin and helicity. This is only true, though, if the gluon is physical, and so it is important to use only the physical polarization states in $\Delta_{\mu\nu}$.

Similar arguments apply to the other "branching" processes $G \to GG$ and $G \to Q\bar{Q}$, as long as a physical gauge propagator is used for the internal gluon lines. Using such a propagator ensures that the extra collinear suppression factor occurs. For example in the $G \to GG$ case spin conservation only suppresses collinear emission if the initial, internal, gluon propagator becomes physical as its mass goes to zero. There are collinear divergences for both $G \to GG$ and $G \to Q\bar{Q}$, but there are soft divergences only in the former case, and these occur when either gluon goes soft.

4-parton diagrams which contain these branching subprocesses are the only ones with collinear divergences. Thus, for example, the squared amplitude shown in Fig. 3.2, in which a gluon is "emitted" by a gluon but "absorbed" by a quark, does not have a collinear divergence. To see this recall that the propagator and helicity suppression factor from each "emission" gave a $\theta/\theta^2 = 1/\theta$ factor, while the phase space gives $\theta \, d\theta$. Thus both $1/\theta$ factors are necessary

for a divergence. However, there <u>will</u> be a soft divergences from such diagrams since the power counting is unchanged from the diagrams of the type Fig. 3.1. I reiterate that the absence of collinear divergences in the interference diagrams like Fig. 3.2, which I will call Ivy diagrams, is only true in physical gauges. Incidentally, the above reasoning shows why the leading collinear logarithms always come from "ladder" diagrams. In fact this result has been extended to all orders in collinear logarithms,[44] so that all such logarithms are factorizable, i.e. are associated with one particular jet. Clearly this is not the case for the soft logarithms from Ivy diagrams, but such logarithms can be factored into an overall multiplicative factor.[22] I return to these points below.

I now proceed to the details of the calculation. The above analysis has shown that all 4-parton diagrams contribute logarithms from some part of their phase space. The diagrams can, however, be divided into "ladders" and "ivy" and this division is shown in Fig. 3.3. I first consider the ladder diagrams and use as my example the first diagram of Fig. 3.3a which contains the subprocesses $Q \to QG$ (Fig. 3.1) discussed above.

Let me define $q = p + k$ (with p and k as above). I will do the phase space keeping E_q and the direction of $\mathbf{p}_q$ fixed. In the singular limit this corresponds to keeping the x_i' (or the θ) fixed, and I shall discuss the error made away from this limit below. Then it can be shown that the part of the phase space pertaining to the singular subprocess can be written:

$$PS \equiv \int \frac{d^{n-1}p}{(2\pi)^{n-1} 2E_p} \frac{d^{n-1}k}{(2\pi)^{n-1} 2E_k}$$

$$= \int \left(\frac{dE_q \, E_q^{n-2} \, d\Omega_q}{(2\pi)^{n-1} \, 2E_q} \right) \left\{ \left(\frac{Q^2}{4\pi}\right)^{\frac{d}{2}} \frac{1}{\Gamma(\frac{d+2}{2})} \frac{1}{8\pi^2} \right\} \times$$

$$\times \; 2E_q^2 \, x_j^d \, dx \, \frac{x^{1+d}}{1-x} \, du' \, (u'(1-u'))^{\frac{d}{2}} \, d\Omega_k' \, (1 + O(u'x)) \tag{3.6}$$

where $d = n - 4$, $x_j = E_q/E_{beam}$, $Q^2 = 4\,E_{beam}{}^2$, and $x = E_k/E_q$, $u' = (1 - \cos(\theta_{kq}))/2$, $\int d\Omega_q$ is the angular integral in n-1 dimensional space, and $\int d\Omega_k{}'$ is the n-2 dimensional angular average. The term in square brackets is the n-dimensional version of the jet's phase space, which I call PS_j. I have dropped terms of $O(u'x) = O(\theta^2 x)$ since they kill the singularities of the matrix element. This form of the phase space is useful in the angles case since it depends on θ_{kq}, and I return to it below. For the energies case I must change variables from u' to $u = (1 - \cos\theta_{kp})/2$, yielding:

$$PS = \int PS_J\, H\, 2E_q{}^2\, x_j{}^d\, dx\, (x(1-x))^{1+d}\, du\, (u(1-u))^{\frac{d}{2}}\, d\Omega_k{}'\, (1 + O(ux(1-x))) \qquad (3.7)$$

(H is the factor in curly brackets in Eq. 3.6) which shows the $x \to 1 - x$ symmetry. Notice that the angular average $d\Omega_k{}'$ is unchanged from Eq. (3.6).

Now I consider the relevant part of the amplitude squared which is (as in Eq. (3.1)):

$$M' = \not{q}\, \gamma^\alpha\, \not{p}\, \gamma^\beta\, \not{q}\, \frac{\Delta_{\alpha\beta}(k)}{(q^2)^2} \qquad (3.8)$$

I have correctly taken into account all factors of i in this expression - they cancel. I shall use two alternative forms for Δ:

$$\Delta_{\alpha\beta}(k) = -g_{\alpha\beta} + (k_\alpha \bar{k}_\beta + \bar{k}_\alpha k_\beta)/(k\cdot\bar{k}) \qquad (3.9a)$$

$$= -g_{\alpha\beta} + (k_\alpha t_\beta + t_\alpha k_\beta)/(k\cdot t) - k_\alpha k_\beta\, t^2/(k\cdot t)^2 \qquad (3.9b)$$

where $k = (E_k, -\mathbf{p}_k)$ and $t = (1, 0)$ so $t^2 = 1$. The second form is the denominator of the axial gauge propagator ($A_0 = O$, or temporal, guage) which is correct for both on and off shell gluons. The first form is only useful on shell. Useful properties of Δ are ($k^2 = O$):

$$\Delta_{\alpha\beta}\, k^\beta = 0 \quad ; \quad \Delta_{\alpha\beta}\, t^\beta = 0 \quad ; \quad \Delta^\alpha{}_\alpha = (2-n) \qquad (3.10)$$

Using the second form for Δ, and using also $\{\gamma^\alpha, \gamma^\beta\} = 2g^{\alpha\beta}$ and $g^\alpha{}_\alpha = n$, I find:

$$M' = (\not{q}\, q^2\, (4\frac{E_q}{E_k} - 2 - \frac{q^2}{E_k{}^2}) + \not{k}\, q^2\, ((n-2) - 2\frac{E_q}{E_k} + \frac{q^2}{E_k{}^2}) - \not{t}\frac{q^4}{E_k})\, \frac{1}{q^4} \qquad (3.11)$$

The factor of q^2 in the numerator is the suppression factor discussed above.

Using $q^2 = E_k E_p u$ and $E_k = xE_q$, $E_p = (1-x)E_q$ this can be rewritten as:

$$M' = \frac{1}{E_q{}^2}\, \frac{1}{4x(1-x)u} \left\{ \not{q}\, (\frac{4}{x} - 2 - \frac{4(1-x)u}{x}) + \not{k}\, (n - 2 - \frac{2}{x} + \frac{4(1-x)u}{x}) - \not{t}\, 4(1-x)u \right\} \qquad (3.12)$$

This is to be integrated over by $PS \propto dx\, du\, x(1-x)$ if $n = 4$ so, since $k \propto x$, the last term multiplying k and also the t terms give no singularities and may be dropped. In fact I can write $k = xq + O(x\sqrt{u})$, as in Eq. 3.4, and drop the $O(x\sqrt{u})$ terms since they kill the singularity. Furthermore I can replace q by $q_o = E_q, (1, q/|q|)$ and only make a harmless error of $O(ux(1-x))$. Thus I can write:

$$PS \times M' = \int PS_J \, \alpha_0 \, H \; 2x_j^{\,d} \; dx \; (x\,(1-x)\,)^{1+d} \; du \; (u\,(1-u)\,)^{\frac{d}{2}} \; d\Omega_k' \; \times$$

$$\times \quad \frac{1}{x(1-x)u} \left(\frac{1}{x} - 1 + \frac{(n-2)x}{4} - \frac{(1-x)u}{x} \right) + \text{non-singular} \qquad (3.13)$$

Of course as I do the x, u, and $d\Omega_u'$ integrations the remainder of the amplitude squared will vary. But this remainder is not singular and it approaches the same value when $x \to 0$ or $1 - x \to 0$ or $u \to 0$ so I can replace it by its limiting value and only make the harmless error $O(\sqrt{ux(1-x)})$. (Explicit evaluation shows that there are $O(\theta)$ i.e. $O(\sqrt{u})$ terms. Any power - and only integral powers of x and θ can appear from a matrix element - will kill the logarithmic singularity).

Thus the singular integral decouples (factorizes) from the remainder, and the remainder is exactly equal to a contribution to the 3 jet amplitude squared in n dimensions. Thus adding the four diagrams in Fig. 3a gives a contribution to the SW cross section:

$$\frac{d^2\sigma'}{dx_1' dx_2'} = \frac{\alpha_s}{2\pi} C_F \sigma_0 T(x_1', x_2') \left(\frac{Q^2}{4\pi\mu^2} \right)^{\frac{d}{2}} \frac{1}{\Gamma(1+\frac{d}{2})} \frac{\alpha_s}{2\pi} \times$$

$$\times \int I_J \frac{C_F}{x(1-x)u} \left(\frac{1}{x} - 1 + \frac{(n-2)x}{4} - \frac{u}{x} \right) \qquad (3.14)$$

where I have included the coupling constant ($g^2 \mu^{-d}$) and the appropriate color factor C_F, and where $T(x_1', x_2')$ is the lowest order qqg cross section (here x_1' is the energy of the quark, x_2' that of the antiquark) in n-dimensions.[8,9] I have defined the measure I_j to be:

$$I_J = 2x_j^{\,d} \; dx \; (x(1-x))^{1+d} \; du \; (u(1-u))^{\frac{d}{2}} \qquad (3.15)$$

where I have dropped the $\int d\Omega_k'$ since the integrand is azimuthally invariant.

Three things are of particular note in Eq. 3.14. Firstly, apart from the last term, the square bracket is proportional to the Altarelli-Parisi (AP) kernel for $Q \to QG$[45] in n dimensions.[46] Secondly, the first term in the square brackets, 1/x, has both soft and collinear divergences and gives rise to the leading double logarithm. Thirdly, the last term has a soft divergence but no collinear divergence. It is essential here but is not present in the AP kernel.

Exactly the same analysis applies to the $\bar{Q} \to \bar{Q}G$ ladder case giving exactly the same result except that x_j is now the antiquark jet scaled energy.

A similar analysis can be applied to the gluon jet ladder diagrams with quark loops. An example is shown in Fig. 3.3b, which explains the notation I use, and leads to a contribution to the matrix element:

$$M' = \frac{\Delta^{\alpha\mu}(q)}{q^2} \, Tr(\gamma_\mu \not{k} \gamma_\nu \not{p}) \, \frac{\Delta^{\nu\beta}(q)}{q^2}$$

$$= \frac{\Delta^{\alpha\mu}(q)}{q^2} \, 4(k_\mu p_\nu + p_\mu k_\nu - \frac{q^2}{2} g_{\mu\nu}) \, \frac{\Delta^{\nu\beta}(q)}{q^2} \qquad (3.16)$$

where I have used tr I = 4 which can be kept in n dimensions. Now I can expand k and p like:

$$k = x\,q + 2x(1-x)\sqrt{u}\,\hat{k}_t + O(xu)$$

$$p = (1-x)\,q - 2x(1-x)\sqrt{u}\,\hat{k}_t + O(\,(1-x)u\,) \qquad (3.17)$$

where C_A is the color factor (adjoint Casimir, $C_A = N_C = 3$) and the 1/2 is from statistics. Apart from the last term the square bracket is again proportional to the AP kernel.

Now I turn to the Ivy diagrams. Consider Fig. 3.3d. The part pertaining to the singularity is:

$$M' = \ldots \not{p}_1 \gamma^\mu \frac{\not{p}_1 + \not{k}}{(p_1+k)^2} \ldots\ldots\ldots(-\not{p}_2)\ \gamma^\nu \left(-\frac{\not{p}_2 + \not{k}}{(p_2+k)}\right) \ldots \Delta_{\mu\nu}(k) \tag{3.25}$$

where the sign of the antiquark propagator is important. Now the only soft singularity comes from the term in M'

$$\ldots \not{p}_1\ \gamma^\mu\ \not{p}_1 \ldots\ldots(-\not{p}_2)\ \gamma^\nu (-\not{p}_2) = \ldots\ 2p_1{}^\mu \not{p}_1 \ldots\ldots\ -2p_2{}^\nu(-\not{p}_2) \tag{3.26}$$

so that:

$$M' = (\text{Lowest order matrix element}) \times \frac{2\ p_1{}^\mu\ \Delta_{\mu\nu}(k)\ (-2\ p_2{}^\nu)}{2\ p_1\cdot k\ 2\ p_2\cdot k}$$

$$+\ \text{non-singular terms} \tag{3.27}$$

In this case we can simply use the gluon phase space PS_k since the p_1 and p_2 phase spaces differ from the lowest order phase space by singularity killing terms of O(x). Thus one gets:

$$(\text{Lowest order}) \times \int \frac{dE_k\ E_k{}^{n-3}\ d\Omega_k{}^{n-1}}{2\ (2\pi)^{n-1}} \times \left(-\frac{p_1{}^\mu \Delta_{\mu\nu} p_2{}^\nu}{p_1\cdot k\ p_2\cdot k}\right) \times (\text{color}) \tag{3.28}$$

In this case it is convenient to use the first form of $\Delta^{\mu\nu}$ so that

$$\frac{p_1{}^\mu\ \Delta_{\mu\nu}\ p_2{}^\nu}{p_1\cdot k\ p_2\cdot k} = \frac{-p_1\cdot p_2 + \dfrac{p_1\cdot k\ p_2\cdot \bar{k} + p_1\cdot \bar{k}\ p_2\cdot k}{k\cdot \bar{k}}}{p_1\cdot k\ p_2\cdot k}$$

$$= \frac{1}{2E_k{}^2}\ \frac{\left(-u_{12} + u_{1k}(1-2u_{2k}) + (1-u_{1k})\ u_{2k}\right)}{u_{1k}\ u_{2k}} \tag{3.29}$$

Notice that as $u_{1k} \to 0$ or $u_{2k} \to 0$ this expression is <u>not</u> singular.

The extra color factor associated with the soft gluon is:

$$\frac{\sum_{a,b} Tr(\ T^aT^bT^aT^b\ )}{\sum_a Tr(\ T^aT^a)} = \frac{2C_F - C_A}{2} \tag{3.30}$$

There is also a factor of 2 from the hermitean conjugate graph. Including all these factors, and rearranging the phase space, I find:

$$\frac{d^2\sigma}{dx_1{}'dx_2{}'} = \sigma_0 C_F \frac{\alpha_s}{2\pi} T(x_1{}',x_2{}') \left(\frac{Q^2}{4\pi\mu^2}\right)^{\frac{d}{2}} \frac{1}{\Gamma(1+\frac{d}{2})} \frac{\alpha_s}{2\pi} (-1)\times 2\times \frac{(2C_F - C_A)}{2}$$

$$\int 2\ dx'\ x'^{n-5}\ du\ (u(1-u))^{\frac{n-4}{2}}\ d\Omega_k{}'\ \frac{u_{1k}(1-u_{2k}) + u_{2k}(1-u_{1k}) - u_{12}}{2\ u_{1k}\ u_{2k}} \tag{3.31}$$

where the dropped term are nonsingular.

Furthermore since:

$$q^{\nu}\,\Delta_{\nu\beta}(q) = O(q^2) \quad ; \quad t^{\nu}\,\Delta_{\nu\beta}(q) = 0 \tag{3.18}$$

I can rewrite M' as:

$$M' = \Delta_{\alpha\mu}(q)\left[-2x(1-x)\,\hat{k}_t^{\,\mu}\,\hat{k}_t^{\,\nu} + \frac{1}{2}\,\Delta^{\mu\nu}(q_0)\right]\frac{\Delta\nu\beta(q)}{x(1-x)u} \tag{3.19}$$

where $q_0 = E_q(1, q/|q|)$ as defined above. To do the azimuthal averaging contained in PS I use:

$$\int d\Omega_k{}'\,\hat{k}_t^{\,\mu}\,\hat{k}_t^{\,\nu} \equiv \frac{\int d\Omega_k{}^{n-2}\,\hat{k}_t^{\,\mu}\,\hat{k}_t^{\,\nu}}{\int d\Omega_k{}^{n-2}} = \frac{\Delta^{\mu\nu}(q_0)}{n-2}$$

$$\Delta^{\alpha}{}_{\beta}(q_0)\,\Delta^{\beta\gamma}(q) = -\Delta^{\alpha\gamma}(q_0) + O(\,ux(1-x)\,) \tag{3.20}$$

The result is:

$$PS \times M' = \int PS_J\,H\,I_j\,\Delta^{\alpha}{}_{\mu}(q)\,\Delta^{\mu\nu}(q_0)\,\Delta_{\nu}{}^{\beta}(q)\,\frac{1}{2x(1-x)u}\left(1-\frac{4x(1-x)}{n-2}\right)$$

$$= \int PS_J\,H\,\Delta^{\alpha\beta}(q_0)\,I_j\,\frac{(1-4x(1-x)/(n-2))}{2x(1-x)u} + \text{non-singular} \tag{3.21}$$

where H is defined in Eq. 3.6. But again the first two terms in 3.21 are precisely those needed for the lowest order 3-jet calculation, and so, making the same approximation as above for the rest of the matrix element, I find again factorization:

$$\frac{d^2\sigma}{dx_1{}'dx_2{}'} = \sigma_0 C_F\,\frac{\alpha_s}{2\pi}\,T(x_1{}',x_2{}')\left(\frac{Q^2}{4\pi\mu^2}\right)^{\frac{d}{2}}\frac{1}{\Gamma(1+\frac{d}{2})}\,\frac{\alpha_s}{2\pi}$$

$$\int I_j\,\frac{T_R}{x(1-x)u}\left[\frac{1}{2}\left(1-\frac{4x(1-x)}{n-2}\right)\right] \tag{3.22}$$

where I have included the coupling constant and color factor ($T_R = N_{flavors}/2$). In this result the square bracket is again proportional to the AP kernel, but here there are no soft divergences.

The final ladder diagram is $G \to GG$ (see Fig. 3.3c for notation) and one finds:

$$M' = \frac{\Delta^{\alpha\mu}(q)}{q^2}\,(\text{MESS})_{\mu\nu}\,\frac{\Delta^{\nu\beta}(q)}{q^2} \tag{3.23}$$

The only important terms in MESS are proportional to $g^{\mu\nu}$ and $k^{\mu}k^{\nu}$ as shown above. The extraction of these terms is messy but straightforward, and, proceeding as in the $G \to Q\bar{Q}$ case I find:

$$\frac{d^2\sigma}{dx_1{}'dx_2{}'} = \sigma_0 C_F\,\frac{\alpha_s}{2\pi}\,T(x_1{}',x_2{}')\left(\frac{Q^2}{4\pi\mu^2}\right)^{\frac{d}{2}}\frac{1}{\Gamma(1+\frac{d}{2})}\,\frac{\alpha_s}{2\pi}$$

$$\int I_j\,\frac{C_A}{2}\,\frac{1}{x(1-x)u}\left[\frac{1}{x(1-x)} - 2 + x(1-x) - \frac{u}{x(1-x)}\right] \tag{3.24}$$

where $x' = E_k/E_{beam}$. In this case there are <u>two</u> non trivial angular integrations to be done as opposed to only one in the ladder cases.

The other Ivy diagrams (Figures 3.3e and 3.2), i.e. a soft gluon connecting a quark and gluon or an antiquark and gluon, give the same results as above except for color and sign factors. In both cases the results are obtained by replacing $(-1) \times 2 \times (2C_F - C_A)/2 = -(2C_F - C_A)$ by $-C_A$. Also, of course, the subscripts 1 and 2 in the integrand are changed appropriately.

This completes the calculation of the singular matrix element. My results agree (after some manipulations) with those of ERT, but not with those of FKSS. The disagreement with FKSS is, however, only in the O(n - 4) terms. FKSS do <u>not</u> find a form in which, apart from the poles, there is an overall factor of the n-dimensional 3-jet cross section $T(x_1, x_2)$. In my analysis, however, this is a very general feature of the results. For this reason, and because of my agreement with ERT, I think it most likely that FKSS are in error. It should be noted, furthermore, that FKSS did the calculation in Feynman gauge in which the origin of the collinear singularities is not simple as in a physical gauge.

I now proceed to the integrations. I organize the integrals into 4 standard types. To do this I note that the integration is symmetric under $x \to 1 - x$ so that I can replace x by $(x + (1 - x))/2 = 1/2$, and $1/x(1-x) = 1/x + 1/1-x$ by $2/x$. This leaves me with the standard forms (I_i is defined in 3.15):

$$J_i = \int I_i \frac{1}{x(1-x)u} \frac{1}{x}$$

$$K_i = \int I_i \frac{1}{x(1-x)u}$$

$$L_i = \int I_i \frac{1}{u} \tag{3.32}$$

I can also combine the soft-singular-only terms in Eqs. 3.14 and 3.24 ($Q \to QG$, $G \to GG$) with the Ivy contributions (changing variable $x = x'x_J$ and noting that $(1-x)^d - 1$ gives <u>no</u> contribution to softly divergent integrals) such that I have a final standard form:

$$I_{ij} = \int 2\, dx'\, x'^{n-5}\, du\, (u(1-u))^{\frac{d}{2}}\, d\Omega_k' \left(\frac{u_{ik}(1-u_{jk}) + u_{jk}(1-u_{ik}) - u_{ij}}{2\, u_{ik}\, u_{jk}} + 1 \right)$$

$$= \int 2\, dx'\, x'^{n-5}\, du\, (u(1-u))^{\frac{d}{2}}\, d\Omega_k' \frac{u_{ik} + u_{jk} - u_{ij}}{2\, u_{ik}\, u_{jk}} \tag{3.33}$$

This form has the property that as $u_{ij} \to 1$ (i.e. 2 back to back jets), $I_{ij} \to 0$.

Collecting the above results I find:

$$\frac{d^2\sigma^{sing}}{dx_1' dx_2'} = \sigma_0 C_F \frac{\alpha_s}{2\pi} T(x_1', x_2') \left(\frac{Q^2}{4\pi\mu^2}\right)^{\frac{d}{2}} \frac{\Gamma(1+\frac{d}{2})}{\Gamma(1+d)} \left(1 + \frac{d^2}{4}\frac{\pi^2}{6}\right) \frac{\alpha_s}{2\pi}$$

$$\Big\{ C_F \left(2J_1 + \frac{d-6}{4} K_1 + 2J_2 + \frac{d-6}{4} K_2 - 2I_{12} \right)$$

$$+ N_C \left(2J_3 - 2K_3 + L_3 - I_{13} - I_{23} + I_{12} \right)$$

$$+ T_R \left(K_3 - \frac{4}{2+d} L_3 \right) \Big\} \tag{3.34}$$

where I have changed the Γ factors to conform with the prefactor in ERT's and FKSS's loop calculation results to which (3.34) must be added.

The integration region for the J, K and L integrals is

$$I(1,\eta) + I(\varepsilon_i,1) - I(\varepsilon_i,\eta)$$

$$I(a,b) = \int_0^a dx \int_0^b du \quad ; \quad \eta = \frac{1-\cos 2\delta}{2} \quad ; \quad \varepsilon_i = \frac{\varepsilon}{x_i} \tag{3.35}$$

Using the following expansion of the incomplete β-function:

$$\int_0^a du\, u^{\alpha-1} (1-u)^{\alpha} = \frac{a^{\alpha}}{\alpha} \left(1 - \alpha^2 \, Li_2(a) + O(\alpha^3) \right) \tag{3.36}$$

where

$$Li_2(a) = -\int_0^a dx \frac{\ln(1-x)}{x}$$

is the dilogarithm,[47] I find:

$$J_i = \frac{2}{d^2} + \frac{2}{d} \ln x_i - \ln \eta \ln \varepsilon_i + \ln^2 x_i - \frac{5\pi^2}{12} \tag{3.37}$$

For K and L only $I(1,\eta)$ gives singular terms ($I(\varepsilon_i, 1) - I(\varepsilon_i, \eta)$ gives terms of the form $\varepsilon \ln \eta$) and I find

$$K_i = \frac{2}{d} + \ln \eta + 2 \ln x_i - 4$$

$$L_i = \frac{1}{3d} + \frac{1}{6} \ln \eta + \frac{1}{3} \ln x_i - \frac{5}{9} \tag{3.38}$$

These integrals agree with the similar ones done by FKSS.

The integrals I_{ij} need only be integrated over the soft region, i.e.

$$I_{12} = 2 \int_0^{\varepsilon} dx' \, x'^{d-1} \int_0^1 du \, (u(1-u))^{\frac{d}{2}} \int_0^1 du_{\phi} \, (u_{\phi}(1-u_{\phi}))^{\frac{d-1}{2}}$$

$$\frac{1}{\{\int_0^1 du_{\phi} \, (u_{\phi}(1-u_{\phi}))^{\frac{d-1}{2}}\}} \frac{u_{1k} + u_{2k} - u_{12}}{2\, u_{1k}\, u_{2k}} \tag{3.39}$$

where $u_{\phi} = 1 + \cos(\phi)/2$, and note that the limit on x' is ε. If I choose to expand k about jet 1, then the integrand becomes

$$\frac{u - u_{12}}{2\, u\, u_{2k}} + \frac{1}{2u} = \frac{u - u_{12}}{2u\, (A+B)(1-zu_{\phi})} + \frac{1}{2u} \tag{3.40}$$

where $A = 1 - c_{1k}c_{12}$, $B = s_{1k}s_{12}$, and $z = 2B/(A+B)$ with $0 \le z \le 1$. Using the formulae in Lebedev[48] I find

$$\frac{1}{\{\int_0^1 du_{\phi} \, (u_{\phi}(1-u_{\phi}))^{\frac{d-1}{2}}\}} \int_0^1 du_{\phi} \, (u_{\phi}(1-u_{\phi}))^{\frac{d-1}{2}} \frac{1}{(A+B)(1-zu_{\phi})}$$

$$= (1-y)^{-1+d} \left(\frac{1+\sqrt{(1-z)}}{2}\right)^{-2} \frac{1}{(A+B)} F\left(\frac{d}{2}, d ; 1+\frac{d}{2}, y\right) \tag{3.41}$$

where $y = ((1-\sqrt{(1-z)})/(1+\sqrt{(1-z)}))^2$. Expanding this to O(d) and noting that (after some algebra):

$$1 - y = \frac{2\,|u - u_{12}|}{u + u_{12} - 2\,u\,u_{12} + |u - u_{12}|}$$

$$(1-y)^{-1}\left(\frac{1+\sqrt{(1-z)}}{2}\right)^{-2}\frac{1}{(A+B)} = \frac{1}{\sqrt{(A^2-B^2)}} = \frac{1}{2|u-u_{12}|} \tag{3.42}$$

I find

$$I_{12} = \frac{\varepsilon^d}{d}\int_0^1 du\,(u(1-u))^{\frac{d}{2}}\,\frac{1}{u}\left(1+\frac{u-u_{12}}{|u-u_{12}|}\,(1+d\,\ln(1-y))\right) \tag{3.43}$$

Fairly straightforward integration finally gives:

$$I_{12} = -\frac{2\,\ln u_{12}}{d} - 2\,\ln\varepsilon\,\ln u_{12} + I_{12}'$$

$$I_{12}' = Li_2(u_{12}) - \frac{1}{2}\ln^2 u_{12} - \frac{\pi^2}{6} + \ln u_{12}\,\ln(1-u_{12}) \tag{3.44}$$

FKSS, however, obtain an answer that differs by not having the last term in I_{12}'. This can be traced to their exclusion of the $[u_\phi(1-u_\phi)]^{(d-1)/2}$ term i.e. they have not done the ϕ integral in n dimensions as is necessary for consistency. (This can be seen explicitly in their Eq. D.1). Thus I believe that FKSS are in error.

Combining all these standard integrals I obtain my final answer for the logarithms and constants in the "energies" case:

$$\frac{d^2\sigma^{\text{sing.}}}{dx_1'dx_2'} = \sigma_0 C_F\,\frac{\alpha_s}{2\pi}\,T(x_1',x_2')\left\{\left(\frac{Q}{4\pi\mu^2}\right)^{\frac{d}{2}}\frac{\Gamma(1+\frac{d}{2})}{\Gamma(1+d)}\right\}\frac{\alpha_s}{2\pi}$$

$$\left[\frac{4}{d^2}\,(2C_F + N_C) + \right.$$

$$\frac{1}{d}\left(C_F(4\ln x_1x_2 - 6 + 4\ln u_{12}) + N_C(4\ln x_3 - \frac{11}{3} + 2\ln(\frac{u_{13}u_{23}}{u_{12}})) + T_R\frac{4}{3}\right)$$

$$+ C_F\left(-2\ln\eta\,(\ln\varepsilon_1 + \ln\varepsilon_2 + 1.5) + 4\ln\varepsilon\,\ln u_{12} + \right.$$

$$\left. 2\ln^2 x_1 + 2\ln^2 x_2 - 3\ln x_1x_2 - \frac{4\pi^2}{3} + 13 - 2I_{12}'\right)$$

$$+ N_C\left(-2\ln\eta\,(\ln\varepsilon_3 + \frac{11}{12}) + 2\ln\varepsilon\,\ln(\frac{u_{13}u_{23}}{u_{12}}) + \right.$$

$$\left. 2\ln^2 x_3 - \frac{11}{3}\ln x_3 - \frac{4\pi^2}{6} + \frac{67}{9} - I_{13}' - I_{23}' + I_{12}'\right)$$

$$\left. + T_R\left(\frac{2}{3}\ln\eta + \frac{4}{3}\ln x_3 - \frac{23}{9}\right)\right] \tag{3.45}$$

(The explicit differences with FKSS (see their Eqs. 4.2-4.5) are as follows.

1. In I'_{ij} they do not have the term $\ln u_{ij}\ln(1-u_{ij})$.
2. In (3.25) they have terms $C_F\,(4B^v + 2B^s) + 4\,N_C(B^g - 11/6\,B^s) + 4/3\,T_RB^S$ which I claim should be $C_F\,4\,nB^V + 4/3\,n\,T_RB^V$

[I think their lack of n's is a typographical error]).

The singular cross section (3.45) should be added to the 1-loop result of ERT or FKSS. Using $u_{12} = (1-x_3)/x_1x_2$ etc. I find that the poles cancel as they should. I can then take the limit $d \to 0$ so that the factor in curly brackets becomes 1, and $T(x_1', x_2')$ reverts to the $n = 4$ form given in Eq. 2.2.

Apart from terms involving $\ell n\, x_i$ this result is proportional to the lowest order angular distribution. But these $\ell n\, x_i$ terms do change the angular distribution. Associated with the logarithms of ε and δ there are two such effects:

(a) The $\ell n\, \varepsilon_i\, \ell n\, \eta = \ell n\, \varepsilon/x_i\, \ell n\, \eta$ terms, which come from the ladder diagrams and which correspond to the fact that ε_i is the maximum fractional energy loss from the ith jet. Put another way these ladder diagrams only involve the scale E_q, the jet energy, and not E_{beam}.

(b) The $\ell n\, \varepsilon\, \ell n\, u_{ij}$ terms, which came from the Ivy diagrams. These occur because the soft gluon "remembers" the direction of the jets it couples to.

There are also $\ell n\, x_i$ terms in the constants (i.e. terms independent of ε and δ). The combination:

$$\frac{\alpha_s}{2\pi}\left(-\frac{11}{3}C_A + \frac{4}{3}T_R\right)\ell n\, x_3 \tag{3.46}$$

is of the form expected if the correct scale of the lowest order coupling constant is Qx_3, rather than Q. This is reasonable since this coupling constant comes with the gluon bremmstrahlung and the gluon energy fraction is x_3. I return to this point in Section 5.

It is worthwhile considering the corresponding result in the two jet (original SW) case. There, too, there are ladder and Ivy diagrams and the soft-only divergencies combine to give I_{12}'. But for two jets $I_{12} \propto (1-u_{12}) = 0$, so that there are no terms involving $\ell n\, \varepsilon$ alone. This comes from a cancellation of ladder and Ivy $\ell n\, \varepsilon$ contributions and not from an absence of Ivy contributions - this was somewhat misstated in SS. Furthermore the ladder contributions involve $\ell n\, \varepsilon$ since $x_1 = x_2 = 1$. I have checked that one obtains the correct SW result if one

uses the above results for the Q ladders. I have also checked my result for gluon ladders with the calculations of Einhorn and Weeks[49] and Shizuya and Tye.[50] My results also satisfy all the tests used by FKSS to check their results.

My calculation gives all the logarithms of ε and δ but only some of the constant terms; it also gives some of the $O(\varepsilon, \delta)$ terms which I have not displayed. The remaining constant terms come from the 1 loop diagrams calculated by ERT and FKSS (their results agree) and these terms are not in general proportional to the lowest order cross section. In fact they differ by more than logarithmic factors, although, it turns out that this is not a very large effect.

It is worthwhile noting that the above method could be easily generalized to any number of jets and to other processes. Such a generalization was actually done by Smilga and Vysostsky,[51] who considered only the logarithmic terms.

Finally I explain how these results are changed if I use the angles definition of the SW cross section. The important difference, as noted above, is that all the angular integrals are now with respect to the direction of the momentum sum of the jet rather than the last integral being over the angle between the two partons comprising the jet. Furthermore the limit on this angular integral is changed to $\eta' = (1 - \cos\delta)/2$ rather than $\eta = (1 - \cos 2\delta)/2$. The fact that the angles between the jets are held fixed rather than the energies is irrelevant for the singular integrations. Thus I must use the form of the phase space involving u', Eq. 3.6, make the replacement $u \to u'/(1-x)^2\,(1 + O(u'x))$ in the integrand, and change the upper limit of the angular integral. The total effect is to make the replacement:

$$\int_0^{\frac{1}{2}} dx\ (x(1-x))^{1+d} \int_0^{\eta} du \ \to\ \left(\int_0^{\frac{1}{2}} dx\ x^{1+d}(1-x) + \int_{\frac{1}{2}}^{1} dx\ x(1-x)^{1+d}\right)\int_0^{\eta'} du \tag{3.47}$$

in the collinear integrals, the soft integrals being unaffected. The x integral has to be broken up as shown because u' is only the larger of the two partons' angles to the jet direction for $x < 1/2$. Thus only J, K, and L are effected and I find:

$$J_i \to J_i + \frac{\pi^2}{6}$$

$$K_i \to K_i + 2\,(1 - \ln 2)$$

$$L_i \to L_i + \frac{1}{3}\left(\frac{13}{12} - \ln 2\right) \tag{3.48}$$

Recalling that K_i and L_i were the integrals producing $\ln \delta$ terms, these changes can be understood as an increase in the "effective" δ when not in the soft region, which is precisely the effect of the "angles" definition. It is notable that J is changed by a π^2 term since π^2 terms have been the subject of much speculation concerning their exponentiation or otherwise (e.g. the infamous K factor in Drell-Yan theory and experiment). I return to this point later. Finally I should emphasize that, although the <u>form</u> of the result is the same, apart from the changes indicated in J, K and L, in the angles case, the <u>numerical</u> value of the result is substantially different because η is replaced by η' i.e. $\ln 2\delta$ by $\ln \delta$.

4. NUMERICAL EVALUATION OF NON-SINGULAR PARTS

The complete $O(\alpha_s)$ corrected jet angular distribution is

$$d\sigma_3(\varepsilon,\delta) = \lim_{n\to 4}\Big[d\sigma_3{}^n(\text{ 1 loop }) + \int PS_n \sum_n \delta(\text{kinematic constraints})$$

$$\theta(\varepsilon,\delta \text{ constraints})\Big] \tag{4.1}$$

in a schematic notation, with Σ_n the matrix element squared evaluated in n dimensions. The kinematic constraints enforce overall momentum conservation and the precise definitions of the energies or angles cross sections.

There are only 5 independent Lorentz scalars on which Σ_n depends, two of these being the jet variables, the remaining 3 requiring integration. Doing all the other integrations leads to:

$$d\sigma_3(\varepsilon,\delta) = \lim_{n\to 4}\Big[d\sigma_3{}^n(1 \text{ loop}) + \int_{\varepsilon,\delta \text{ constraints}} dx \int du \int d\phi \quad (\text{JAC})_n \sum_n\Big]$$

$$= \lim_{n\to 4}\Big[d\sigma_3{}^n(1 \text{ loop}) + \int_{\varepsilon,\delta \text{ constraints}} dx \int du \int d\phi \quad (\text{JAC})_n{}' \sum_n{}'$$

$$+ \int_{\varepsilon,\delta \text{ constraints}} dx \int du \int d\phi \quad \left((\text{JAC})_n \sum_n - (\text{JAC})_n{}' \sum_n{}'\right)\Big] \tag{4.2}$$

where in the second form I have extracted the singular approximations to the matrix element squared and the jacobian. The first term is that discussed in detail in Section 3 and the second is finite as $n \to 4$. Thus I must evaluate:

$$N = \int_{\varepsilon,\delta} dx \int_{\text{constraints}} du \int d\xi \quad \left((JAC)_{n=4} \Sigma_{n=4} - (JAC)_{n=4}' \Sigma_{n=4}' \right) \tag{4.3}$$

and, because of the length of Σ and the ugliness of JAC, I did so numerically. It is possible to choose the variables x, u, θ such that the limits are the same for both terms in the integrand, and I made such a choice to simplify the calculation. I used the result of ERT for $\Sigma_{n=4}$ which has been checked with the result of Ali et al.[52]

Although this method of evaluation leads to a straightforward numerical problem it does involve analytic calculation of the jacobian, which is nontrivial in the angles case. It may be possible to devise a method involving binning in x_1' and x_2' as opposed to taking account of fixed x_i' or θ_i' analytically, which evades the calculation of the jacobian, but I did not find such a method. Furthermore a binning method was used by ERT in a related calculation and they found large numerical fluctuations.

I did the numerical evaluation of N (4.3) in the energies and angles cases completely separately. I did the energies case first and the results were reported in I. The angles case was done more recently and incorporated various improvements. As explained in Section II one of my reasons for repeating the calculation was as a check, there being significant overlap between the two cases. In fact I did find errors in the energies computation as discussed above.

As becomes obvious below there are few checks on my results that I can perform, except for repeated rederivation of ugly jacobians and repeated rechecking of the transcriptions of long expressions. I can, fortunately, check the singular terms, but as I am claiming that the nonsingular term are important the lack of a significant check of these is unfortunate. Consequently I have taken extreme care and multiply checked every formulae and derivation. I drew inspriation in this task from Charles Delaunay who between 1847 and 1867 calculated algebraically the moon's orbit in gravitational perturbation theory, a

calculation not checked for 100 years until the advent of computer algebra. Only 3 minor errors were found and the calculation is now used to test computer algebra systems![53]

I now describe some aspects of the evaluation of N (4.3). Configurations of 4 particles satisfying the ε, δ criteria are either "cone-like" or "soft". These two types are shown in Figs. 4.1a and b which establish the notation that I shall use. In each case there are 3! = 6 ways of assigning the three jets to the energies or angles which have been chosen (and are held fixed). Next, the partons ($Q\bar{Q}GG$ or $Q\bar{Q}Q\bar{Q}$) have to be assigned to the particles. There are 4! = 24 ways of doing this but some of these permutations have already been taken into account. (This is in fact ony true of the integration and not of the integrand since the jet assignment permutations correspond to parton assignment permutations together with a change in the azimuthal angle $\phi \to \pi - \phi$). In the cone-like cases the permutation of the particles not in the cone (2 and 4) have already been accounted for. This leaves 12 permutatons - the number of ordered pairs of partons. This ordering is necessary in the angles case if one wants simple limits for the integrals (just as in the analytical calculation described in Section 3), and I chose to use it in the energies case also. In the soft cases only 4 of the 24 permutations remain - the choice of which parton is soft. Thus in total there are 6 × 12 cone integrations and 6 × 4 soft integrations to be done for each value of the energies or angles.

The 4-parton cross secton in 4 dimensions can be written, if the beam direction is averaged over,

$$d\sigma = \frac{1}{\int PS_2} \sigma_0 \frac{1}{C_A} \frac{1}{4Q^2} PS_4 \, H^{\mu}{}_{\mu} \, S \tag{4.4}$$

where

$$\sigma_0 = \frac{1}{Q^2} \frac{4\pi\alpha_{EM}^2}{3} C_A \sum_i e_{q_i}^2 \tag{4.5}$$

is the Born cross section, S is the statistical factor, and $H_\mu{}^\mu$ is the contracted hadronic tensor, which has been calculated by ERT and Ali et al.[52] If I extract the g^4 from $H_\mu{}^\mu$, and integrate out all but the variables on which Σ depends I find:

$$d\sigma = \sigma_0\, C_F\, Q^2\, S \left(\frac{\alpha_s}{2\pi}\right)^2 dx_2\, dx_4 \int_0^{\frac{x_J}{2}} dx_3 \int_0^{\eta} du_{13} \int_0^{\pi} \frac{d\phi}{\pi} \times$$

$$\times \frac{x_1\, x_3}{\sqrt{((x_1+x_3)^2 - 4x_1x_3u_{13})}} \left[\frac{H^\mu{}_\mu}{16C_AC_F} \right] \tag{4.6}$$

where the expression in square brackets is given by ERT as Eqs. B.3 - B.7. Here ϕ is the azimuthal angle with respect to the jet, i.e. $\mathbf{p}_1 + \mathbf{p}_3$, direction, and its range is taken (using the $\phi \rightarrow -\phi$ symmetry if $H_\mu{}^\mu$) to be $0 - \pi$. This is the expression applicable to the energies cone-like case. The integration to be done is that in curly brackets and comparison with Eq. 3.7 shows that the jacobian is very simple in this case. For the energies soft case the only differences are that

$$dx_2\, dx_4 \int_0^{\frac{x_J}{2}} dx_3 \int_0^{\eta} du_{13} \rightarrow$$

$$dx_2'\, dx_4' \int_0^{\epsilon} dx_3 \left(\int_\eta^1 du_{13} - \int_0^{\eta} du_{34} - \int_0^{\eta} du_{23} \right) \left(1 - \frac{x_3}{2}\right)^2 \tag{4.7}$$

where I have used $x_2' = x_2/(1-x_3/2)$, etc. which defines the "energy" variables, and the subtracted u integrals remove the cone-like regions where partons 3 and 4 or 3 and 2 are

nearly collinear. Of course thoughout these integrations the dependent variables are set consistent with the kinematic constraints, which is in this case fairly trivial.

In the angles case the kinematics are less trivial. I find, using the notation shown in Fig. 4.1a:

$$d\sigma = \sigma_0 C_F\, Q^2\, S \left(\frac{\alpha_s}{2\pi}\right)^2 d\Theta_2\, d\Theta_4 \int_0^{\eta'} du \int_0^{x_3{}^0} dx_3 \int_0^{\pi} \frac{d\phi}{\pi}$$

$$\frac{x_3\,(x_3c + x_1c')}{x_1c'} \quad \frac{z_1x_2x_4c'}{2\,(c' + (1-c')(1-z_1/2))} \left[\frac{H^\mu{}_\mu}{16\, C_A\, C_F}\right] \tag{4.8}$$

where:

$$c = \cos\Theta_{32} \quad ; \quad s = \sin\Theta_{32} \quad ; \quad u = (1-c)/2$$

$$c' = \cos\Theta_{12} \quad ; \quad s' = \sin\Theta_{12} = s\, x_3/x_1 \quad ; \quad x_3{}^0 = \frac{z_1}{2\,(1-u(2-z_1))}$$

$$x_1 = \frac{z_1{}^2}{2(1-z_1)} \left(\frac{2-z}{z} \times \left[\left(1 - \frac{x_3}{2x_3{}^0}\right)^2 + \frac{(x_3z_1s)^2}{16(1-z_1)} \right]^{\frac{1}{2}} + \frac{x_3}{2x_3{}^0} - 1 \right)$$

$$x_i = \frac{(2 - x_1 - x_3)}{(2 - z_1)}\, z_i \qquad i = 2,4 \tag{4.9}$$

The upper limit or x_3 depends on u. To make the range of variables as in the analytic calculation I used the variable $t = x_3/2x_3{}^0$ which ranges from 0 to 1/2.

The soft case is even worse - one has to solve a quartic equation rather then a quadratic. I find (see Fig. 4.1b for notation):

$$d\sigma = \sigma_0\, C_F\, Q^2\, S \left(\frac{\alpha_s}{2\pi}\right)^2 d\Theta_2'\, d\Theta_4' \fint_0^{\varepsilon} dx_3 \fint_0^{1} du_{13} \fint_0^{\pi} \frac{d\phi}{\pi} \times$$

$$\times \frac{1-u_2}{2u_1} \frac{1}{\left(1 + \frac{(1-u_2)(1-u_2')(s_\phi Y)^2}{(1-u_2+Yc_\phi s_2/2)^3}\right)} \left[\frac{H^\mu{}_\mu}{16\, C_A\, C_F}\right] \tag{4.10}$$

where:

$$u_i' = (1-\cos\Theta_i')/2 \quad , \quad u_i = (1-\cos\Theta_i)/2 \quad i = 1,2,4$$

$$u_2'/u_2 = u_4'/u_4 = u_1'/u_1$$

$$Y = \frac{x_3 s_{13}}{2(1-x_3 u_{13})} \quad ; \quad s' = \frac{4\sqrt{(u_2'-u_2)u_1 u_4}}{s_2 s_4} \quad ; \quad x_4 = \frac{x_3 s_{13} s_\phi}{s_4\, s'}$$

$$x_2 = \frac{x_3 s_{13}(s_\phi c' - c_\phi s')}{s_2\, s'} \quad ; \quad x_1 = -x_3 c_{13} - x_2 c_2 - x_4 c_4 \tag{4.11}$$

and u_2' is obtained from u_2 by solving:

$$\sqrt{(1-u_2)(u_2'-u_2)} + Y\left(c_\phi\sqrt{u_2(u_2'-u_2)} - s_\phi\sqrt{u_2(1-u_2')}\right) = 0 \tag{4.12}$$

the quartic equation referred to above. Here ϕ is the azimuthal angle of 3 with respect to the 1, 2 plane, ϕ'($c' = \cos\phi'$) is the azimuthal angle of 4 with respect to the 1, 2 plane, the θ_i' are

projected angles as explained in section 2 ($\Sigma\theta_i' = 2\pi$), and the z_i are the energies of the jets for the given θ_i' in the three jet limit ($x_3 \to 0$).

The slashed integration symbols represent the fact that the integrals exclude the regions where particle 3 can form a jet with one of 1, 2 and 4. I do not need to calculate the limits analytically because, as will be explained below, I use Monte-Carlo integration.[2]

In both cone-like and soft configurations the jacobians reduce to the correct from in the 3 jet limit, namely the expressions 3.7 and 3.6 used to do the singular integrals, except for an overall factor $z_1 z_2 z_4/2$. This factor is the jacobian to transform from energies to angles in the three jet limit.

As discussed in Section 2 there are problems with the jet definitions for large ε and δ. For large ε the least energetic jet may have energy less then εE_{beam}, and for large δ there may be an ambiguity in assigning partons to jets. In the angles case for each θ_1 and θ_2 I only consider values of ε and δ for which these problems do not arise. In fact I build the limits into the program to provide a check on the kinematics used. In the energies case I respect the limit on ε but not that or δ, and for large δ I associate always the two partons closest in angle as described in Section 2.

To calculate N (4.3) I have to subtract the singular part of the integrand calculated in Section 3. To simplify this subtraction I make two changes.

(i) I choose a slightly different form for the singular part of the matrix element from that calculated in Section 3, the difference, however, being nonsingular. I then integrate this analytically over all the regions, two partons collinear and <u>each</u> parton soft, not only over the regions which give logarithms and constants. Thus I obtain some $O(\varepsilon, \delta)$ terms. I do this separately for both the energies and angles cases, but it turns out that the only differences are the change from η to η' and the changes to the constants given in Eq. 3.48. The advantage of this <u>complete</u> integration is that I can subtract the <u>entire</u> singular integrand in all cases where subtraction is necessary.

(ii) I permuted the parton labels in the exact and approximate integrands so that the only singularities are associated with two of the partons. This allows a simplification logistics of the programs since I only need to subtract when either or both of these partons are in a cone or when either was soft.

I then subtract the singular matrix element squared in the appropriate cases using the same approximate jacobians and kinematics that I used in the analytic calculation. The resulting subtracted integrand has $1/\sqrt{u}$ singularities as $u \to 0$, but no singularities as $x \to 0$. To deal with these integrable singularities I change variables from u to y with $u = e^{A(1-1/y)}$ with A = 1 or 2 - a "Hinchliffe transform".[54] I also set the integrand to zero somewhat before the point at which the cancellation of divergent terms become numerically unstable. I stress that I cancel the integrands point by point to avoid numerical fluctuations.

In the energies case I do the integration using a mixture of trapezoidal integration and Simpson's rule. In the angles case I use a simple Monte-Carlo method for all three integrals (i.e. x, u and ϕ) except for a $\phi \longleftrightarrow \pi - \phi$ symmetrization to remove $\cos\phi$ terms. The disadvantages of Monte-Carlo integration as compared to the standard methods are its slower convergence, larger errors, and "metastable" false answers. The great advantage, however, is the possibility of doing many integrals simultaneously. In this case I can obtain the corrections for many values of ε and δ and fixed θ_i in one integration. The standard methods, especially if one uses Hinchliffe transforms, are much less amenable to such a procedure. Given the computer time taken to do the integrations, this is an important advantage. Furthermore in the angles case, as discussed above, the Monte-Carlo method allows the limits in the soft integrals to be calculated numerically rather than analytically.

In the energies case I find that 5^3 points give ~ 5% accuracy, which I consider adequate. Thus for each value of ε, δ, x_1' and x_2' I use ~ 50, 000 points. In total I do the integration for 18 values of ε and δ for each of which I used at least 30 pairs of x_1', x_2' values.

In the Monte-Carlo integration I require the error in <u>each</u> cone or soft integration to correspond to a contribution to F_2 of less than 0.02 or that the number of points not exceed

20,000. Because I brake the integration up into so many pieces in effect I create an adaptive Monte-Carlo routine! I calculate the error by breaking up the points into groups of 30 and calculating the standard deviation for the answers so obtained. I combine all the errors in quadrature to give a final error estimate and find that with 150,000 - 200,000 points I can obtain results for ~ 50 different ε, δ pairs with an error in F_2 ranging up to ~1. This is small since it multiplies $\alpha_s/2\pi$ which is 0.025 - 0.04. In the Monte Carlo case I check for "metastable states" by using different numbers of points and by different boxing in ε and δ.

As discussed at the beginning of this section there are few checks I can perform. The cancellation of singularities between exact and approximate integrands is the only significant check I perform in the energies case. In the angles case, however, I include a new feature that allows me to broaden one or more of the cones (e.g. that of the jet opposite the largest angle). To do this I keep the subtractions as if the jet is not broadened, but do the integration of the exact integrand over the larger region. There are two reasons for doing this. Firstly, it allows me to study perturbative jet broadening jet by jet - possibly useful at very high energies. Secondly, and more importantly, if I broaden all three jets equally I should obtain the same total result as with no broadening but with appropriately larger δ. However, the split between analytical and numerical evaluation will be different in the two cases and if the results agree it checks both my analytic and numerical integration. For large enough δ this check tests the integration of both singular and nonsingular parts. In fact, broadening all jets by a factor of 2 or 3 gives the same answers as with an appropriately larger δ, within the errors.

Finally, having obtained the numerical answer I combine it with the analytic results (logarithms, constants and $O(\varepsilon, \delta)$ parts) summed over the six permutations of assigning partons to jets. The errors I have described above occured in transcribing the analytic formulae on to the computer code.

5. RESULTS

I break up the presentation and discussion of my results into three sections. I firstly discuss the size and nature of the corrections to the 3-jet cross section without considering the effects of hadronization or possible perturbative improvements of the results - I call this the straightforward analysis. Secondly, I discuss the effects of hadronization on the perturbative results. Thirdly, I use the recent proof of Mukti and Sterman[22] that all the logarithms of ε and δ can be resummed to "improve" the perturbative results.

In presenting these results I use $N_f = 5$. The dependence on N_f comes from quark "bubbles" in the gluon jet (real and virtual) and thus the appropriate N_f to use is determined by the energy of the gluon jet. At PEP/PETRA energies $N_f = 4$ should probably be used. At Z-factories $N_f = 5$ (or 6?) is appropriate. However, the N_f terms contribute only a small percentage to the final result so using $N_f = 5$ thoughout involves only a small error, an error that effects none of the conclusions.

(a) Straightforward Analysis

Figures 5.1 and 5.2 show the "allowed regions" of the ε and δ plane for the energies and angles cases respectively. These allowed regions are defined by the requirement that the correction (F_2) have an absolute value less than 10(15) for all values of $x_i' \leq .85$ (or the equivalent θ_i). This corresponds to a 33% correction for $\alpha_s = .21(.14)$. The figure for the energies case shows the limit discussed in Section 2 on ε and δ required for the consistency of the 3-jet definition. That for the angles case shows the consistency limit following from the requirements that the third jet have more energy than $\varepsilon\, E_{beam}$, and also shows the "limit" which follows from the requirement that there be no ambiguity in the assignments of partons to jets. As discussed in Section 2 I do not calculate results beyond this "overlap" limit in the angle case. I shall refer to all these limits as "kinematic limits".

If I consider the enlarged 3-jet region $x_i' \leq .9$ then the allowed region of ε and δ is much reduced, in fact disappearing in the angles case. This is because of the more stringent

kinematic limits and because of the increased range of x_i' for which the corrections must be small. Thus I only consider the region $x_i' \leq .85$ for the remainder of this subsection.

As discussed in Section 2 it is reasonable to require that the corrections for both the energies and angles cases be small in order that the lowest order result be applicable. The allowed region of ε and δ is, as the figures show, rather small because of the small allowed regions in the angles case. Had I extended the angles calculation into the overlap region then no doubt the size of the angles allowed region would be increased. However, most of the increase would be outside the allowed region for the energies case, so that the overall perturbative situation would improve little. It can be improved, as we see below, by resummation and so I do not dwell on these straightforward results. For the remainder of this subsection I comment on various interesting features of the results which survive the improvement.

The first such feature is the rapid variation of the correction with ε and δ, which is shown by the proximity of the $|F_2| < 10$ and $|F_2| < 15$ contours. The correction becomes large and negative for small ε and δ because of the leading double logarithmic term. For large ε and δ the correction becomes large and positive. This is probably related to the large corrections to thrust-like distributions found by ERT and VGO. This effect occurs in both energies and angles cases - it cannot be seen from Fig. 5.2 for the angles case but for configurations with approximately equal θ_i the kinematical constraints on ε and δ are much weaker and this effect can be seen.

In Tables 5.1 and 5.2 I show a breakdown of the contributions to F_2 for a number of ε and δ values and for $x_i' = .85, .85, .3$ (point I), $x_i' = .85, .6, .55$ (point II), and $x_i' = .7, .7, .6$ (point III). Points I, II and III are at the corners of the triangular $x_i' \leq .85$ region. The variation of F_2 between these points is monotonic. The angles points are on an ε, δ grid, while the energy points have been chosen to lie as close to the grid as possible. The $O(\varepsilon, \delta)$ parts of the breakdown are the sum of the analytical and numerical $O(\varepsilon, \delta)$ contributions.

The domination of the logarithms for small ε and δ is clear in both cases. The logarithms are more negative in the angles case because the limit on the angular integral is δ rather than 2δ. This behavior is somewhat compensated for by the larger constants but the total angles result is necessarily smaller as the phase space is smaller. Thus the angles allowed region is pushed to larger ε and δ.

For the larger values of ε and δ the $O(\varepsilon, \delta)$ parts form a substantial fraction of the total answer, being themselves as large as a 30% correction to the lowest order with $\alpha_s \sim .2$. They play an important part in determining the allowed region. This result should be compared to the 2-jet cross sectionwhere the $O(\varepsilon, \delta)$ terms become a 25% correction to the logarithms and constants only for very large ε and δ, $\varepsilon \geq .4$ and $\delta \geq 30^0$.

It is interesting to look at the variation of the correction with the x_i' at fixed ε and δ. For both energies and angles cross sections the pattern is the same: the constants are nearly independent of the x_i', while the $O(\varepsilon, \delta)$ parts increase from point I through point II to point III. The largest effects, however, come from the logarithmic terms, with the corrections increasing from III through II to I. This latter pattern remains in the total correction. Since the lowest order cross section increases from III to II to I, this correction enhances the lowest order shape. The effect is true for the entire ε, δ plane and although the size of the correction varies rapidly with ε and δ the shape of the corrected distribution varies much more slowly. This is illustrated for the energies case in Figs. 5.3 and 5.4. Figure 5.3 shows the corrected x_1' distribution (i.e. x_2' has been integrated over) at Z-factory energies (E_{CM} = 90 GeV) for various ε, δ values that fall within the allowed region with $|F_2| < 16$. (16 rather then 15 was chosen for convenience given the limited number of ε, δ values available - the maximum correction was 41%). I take the scale of the α_s multiplying the correction to be the beam energy, whereas that for the α_s multiplying the lowest order is, according to Eq. 2.4, E_{CM}. I use the form $\alpha_s(Q) = 6\pi/((11C_A - 4T_R)\,\ell n\, Q/\Lambda)$ with Λ = .24 GeV which gives α_s(30, 45, 90 GeV) = .170, .157, .138 respectively. The lowest order curve is also shown for comparison. Figure 5.4 shows the difference is shape between the normalized lowest order and normalized

corrected distributions, the normalization being to an average value of 1 in the range $2/3 \leq x_i' \leq .85$. Figure 5.4a shows the quotient and Fig. 5.4b shows the difference. Both are shown because the quotient displays the possible percentage differences while the difference shows the differences in terms of numbers of events. Also shown in these figures is the lowest order result with the scale of α_s charged from E_{CM} to $E_{CM}x_3$, in order to give an idea of the type of term in the correction (see Equation 3.4b) that gives rise to the effects shown. The corrected curves have a systematically different shape from the lowest order throughout the allowed region.

Finally I compare my results with those quoted by FKSS. FKSS show x_1' distributions only for $\varepsilon = 0.1, \delta = 15^0$ and $\varepsilon = 0.2, \delta = 22.5^0$. (Notice that in their paper they define δ to be twice what I use.) For the first point they find large negative corrections ($\sim -25\,\alpha_s/2\pi$) while the second has corrections ranging from $-5\,\alpha_s/2\pi$ for $x_i' \approx 2/3$ to zero for $x_i' \approx .85$. For both of these points the correction becomes more positive as x_i' increases in agreement with my results, an agreement that is to be expected because this effect is dominated by the logarithms on which we agree. I cannot compare the absolute magnitudes for the first point since I have not calculated the correction for these values of ε and δ, but it is clear from Table 5.1 that we roughly agree. I do have results for $\varepsilon = 0.2$, $\delta = 21^0$, very close to their second point, and I find corrections varying from zero at $x_i' \approx 2/3$ to $5\,\alpha_s/2\pi$ at $x_1' \approx .85$. Thus, for this point my results are larger than those of FKSS by $\approx 5\alpha_s/2\pi$ for all x_1'. Half of this difference is explained by the error in the n-dimensional azimuthal integration made by FKSS. The remaining difference is presumably accounted for by the difference in the n-dimensional matrix elements discussed above and/or by a numerical error made by one or both of us. However, this remaining discrepancy is sufficiently small so as not to effect the following discussion and conclusions.

(b) Hadronization

As explained in Sections 1 and 2, in order to convert the perturbative results into experimental numbers it is essential to take hadronization into account at presently available

energies and even at Z-factory energies. To do this I made a simple model which included both the perturbative and non-perturbative broadening. I have given a brief discussion of the problem of hadronization in Section 2, but I shall be more thorough here.

In order to measure the 3-jet angular distribution one must use an experimental criterion to select events containing three jets, because, for example, one must specify when a broad jet becomes two jets. A number of different criteria have been used experimentally, ranging from simple extensions of thrust [55] - to complex cluster algorithms.[28,29] Some of the criteria have been quite similar to the SW criterion.[56] Non-perturbative jet broadening, however, obscures the connection between the experimental criterion and the perturbative cross section in two ways. Firstly, the experimental criterion rather than corresponding to a perturbative jet cross section with particular values of ε and δ, will correspond to a weighted average of perturbative cross sections with various ε and δ. It is this weighting function that I have estimated. Secondly, the energies and relative angles of the jets will change from their perturbative values, an effect that is particularly sensitive to experimentally undetected particles. This effect is more important if one uses the x_i' rather than the θ_i. I return to this "smearing" problem after describing the hadronization model and the results obtained with it.

In order to estimate the weighting function I have to model the hadronization of jets already perturbatively broadened. Such a model is different from standard Monte-Carlo models which hadronize partons rather than jets, although there is some overlap between these approaches because the standard Monte-Carlos do introduce a cut off on the nearly collinear or soft 3 parton events, as discussed above, which is similar to a 2 jet SW criterion. But this is a somewhat ad hoc way of dealing with the singularities whereas the SW cross sections provide a systematic approach and so it is better to attempt to hadronize the SW cross sections directly. No doubt by suitably altering a standard Monte-Carlo a model more accurate and reliable than the one I describe could be made, but mine suffices for the reasonably reliable quantitative estimates of hadronization that I require. A model of some

kind is, I think, necessary because the hadronization of three jets is sufficiently complex that crude estimates are not useful.

I choose to imagine using an experimental SW criterion with parameters δ_{exp} and ε_{exp}. However, I also imagine using some sort of cluster algorithm to separate real jets from soft "noise" because I allow ε_{exp} to go beyond the kinematical consistency limit (i.e. softest jet not too soft) discussed above. The weighting function W is defined by:

$$\sigma_{exp}(\delta_{exp},\varepsilon_{exp}) = \int d\delta \int d\varepsilon \; \sigma_{th}(\delta,\varepsilon) \; W(\delta_{exp},\varepsilon_{exp};\delta,\varepsilon) \tag{5.1}$$

where σ_{exp} and σ_{th} are respectively the experimental and theoretical three jet cross sections. I have suppressed the dependence of the σs and W on the x_i' - in fact we shall find later that W is nearly independent of the x_i' so that this notation is appropriate. Both σ_{exp} and σ_{th} are chosen to be cross sections whose variables are the jet energies rather than angles - this makes no difference at this stage.

The weighting function defined by Eq. 5.1 is clearly a simplification. It does not include the smearing in the x_i', it does not address the related problem of possible weight for SW criteria with different sized cones, and it only allows one theoretical SW cross section to be a "basis" although, as discussed in Section 2, a number should perhaps be used. Nevertheless the important point is to obtain an idea of the "smearing" in ε and δ due to hadronization and these criticisms concern details that do not effect this aim. The use of a simple approach means, furthermore, that the results should be general and apply to the angles as well as the energies cross sections. In fact, although I designed the model with the energies cone definition in mind it is clear below that there is no reason to associate the model with any particular theoretical cone definition. Similarly the fact that I use the energies as variables rather than the angles is not a crucial feature.

I cannot directly estimate W using a hadronization model since $\sigma(\delta, \varepsilon)$ is an inclusive cross section. However, I can write

$$\sigma_{th}(\delta,\varepsilon) = \int d\phi \int dz \frac{d^2\sigma_{th}(\phi,z)}{d\phi dz} \theta(\delta-\phi)\ \theta(\varepsilon-z) \tag{5.2}$$

where ϕ is the half-breadth of the largest cone in the perturbative configuration and $z\,E_{beam}$ is the energy lying outside the cones. This is an ambiguous definition since I can trade off larger ϕ for smaller z or visa-versa. I can remove this ambiguity, however, by requiring ϕ x z to be minimal or by some similar requirement. This bizarre decomposition of $\sigma_{th}(\delta, \varepsilon)$ allows me to write the SW criterion in terms of step functions and it gives me a quantity, $d\sigma/d\phi\, dz$, which I can hadronize. To proceed I assume that all perturbative configurations with the same z and ϕ hadronize such that a fraction F are accepted by the experimental criterion, i.e.

$$\sigma_{exp}(\delta_{exp},\varepsilon_{exp}) = \int d\phi \int dz \frac{d^2\sigma}{d\phi dz} F(\delta_{exp},\varepsilon_{exp};\phi,z) \tag{5.3}$$

Now, provided F and its derivatives go to zero for large ϕ and z, which they do, I can write

$$F(\delta_{exp},\varepsilon_{exp};\phi,z) = \int d\delta \int d\varepsilon\ \theta(\delta-\phi)\ \theta(\varepsilon-z) \left(\frac{\partial^2}{\partial\delta\partial\varepsilon} F(\delta_{exp},\varepsilon_{exp};\delta,\varepsilon)\right) \tag{5.4}$$

which, up on substitution in Eq. 5.3 and comparison with Eq. 5.1 shows that

$$W(\delta_{exp},\varepsilon_{exp};\delta,\varepsilon) = \frac{\partial^2}{\partial\delta\partial\varepsilon} F(\delta_{exp},\varepsilon_{exp};\delta,\varepsilon) \tag{5.5}$$

To calculate W I first calculate F and then take the derivative numerically. To calculate F I must model a typical z, ϕ configuration and its hadronization. I take the typical configuration to have one thick jet and two thin jets - following perturbation theory. I then proceed in two steps. Firstly, for each jet I determine the average energy lost outside the

experimental cone ($\langle E_{lost,i}\rangle$) with parameters δ_{exp}, ε_{exp}. I assume independent hadronization of each jet. For thin jets with energy 10 GeV I use the angular profile for a jet produced by the Monte-Carlo "tubes"[57] (not including detection efficiencies). This is shown in Fig. 5.5. For jets with other energies I modify this profile, putting extra energy into the first 4^0 bin, and removing energies so as to flatten the angular profile - this is illustrated in the figure. I keep the same large θ profile in all cases since the distribution in rapidity is experimentally uniform and for energetic particles $y = -\ell n \tan\ \theta/2 + 0\ (M^2/E^2)$. For the perturbatively thickened jet I use the same angular profile, but I put the axis of the Monte Carlo jet on a cone of half angle δ with respect to the experimental cone and average the energy distribution over the azimuthal angle. This clearly leads to a broadened jet and a larger energy lost outside the experimental cone.

The second step is to distribute the amount of energy lost non-perturbatively from each of the jets according to a function with the correct average, which I call $f_i(E_{lost,i})$, and calculate the fraction of events with an energy outside the cones of less than $\varepsilon_{exp}E_{beam}$. One must, of course, take account of the perturbatively lost energy and I do this either by saying it is entirely outside the experimental cones or by saying that the energy is distributed uniformly in the 4π solid angle so that some energy flows back into the cones. Thus I have:

$$F(\delta_{exp},\varepsilon_{exp};\phi,z) = \int \prod_i \left(dE_{lost,i}\ f_i(E_{lost,i})\right)$$

$$\theta(\varepsilon_{exp}E_{beam} - \sum_i E_{lost,i} - z'E_{beam}) \tag{5.6}$$

where z' = z in the first case and z' = z x (solid angle outside the experimental cones) in the second.

I use various forms for $f_i(E_{lost,i})$ but my preferred form is:

$$f_i(E_i) = A \left((1-c)E_i \exp(-\frac{E_i}{B}) + c(E-E_i)\exp(-\frac{E-E_i}{B}) \right)$$

$$\frac{1}{c} = 1 + \exp\left[-2 \left(\frac{1.5}{\Delta} \left(\frac{\langle E_{lost,i} \rangle}{E_i} - \frac{1}{2} \right) \right) \right]$$

$$\int f_i(E_i)\, dE_i = 1 \quad , \quad \int f_i(E_i)\, E_i\, dE_i = \langle E_{lost,i} \rangle \tag{5.7}$$

where the parameters A and B are determined by the last two conditions, and Δ is a parameter determining the rate of transition between the two exponentials in f. This form is motivated by a calculation of f in an uncorrelated particle model done by Furmanski.[2]

The final step is to calculate W by numerical differentiation of F calculated on a grid in ϕ and z with spacing 4^0 and 0.025 respectively. The weighting functions so calculated shows for PEP/PETRA energies a significant shift from δ and ε to δ_{exp} and ε_{exp} and a substantial smearing, i.e. the total weight for a given δ_{exp} and ε_{exp} is spread over a sizeable region in the δ, ε plane. In fact the size of a region containing 80% of the weight is $\Delta\delta \sim 20^0, \Delta\varepsilon \sim .175$, an area larger than the energies allowed region! Thus, even ignoring the problem of the smaller angles allowed region, the angular distribution measured experimentally will have contributions from regions of the δ, ε plane where the straightforward perturbation expansion is not well behaved. Nevertheless, the sum of these weighted contributions may have a well behaved perturbation expansion. It turns out that the region in the $\delta_{exp}, \varepsilon_{exp}$ plane for which this is true depends little on the choices of f, Δ and z, This "experimentally allowed region" is shown in Fig. 5.6 for the energies case with f given by Eq. 5.7 ($\Delta = 0.2$) and using the z definition which includes the flow of soft energy back into the cones. The errors in the curves due to the small number of ε, δ points are comparable to those for the perturbative result shown in Fig. 5.1. The overall shift in the allowed region is by $\Delta\delta \sim 8^0$ and $\Delta\varepsilon \sim .1 - .15$, and

the variation in this shift from different choices of f, Δ and z is less than 4^0 in $\Delta\delta$ and 0.025 in $\Delta\varepsilon$. The experimental allowed region has roughly the same shape and size as the perturbative allowed region. The total fraction of 3-jet events accepted by the experimental criterion (given by $F(\phi = 0, z = 0)$) does vary substantially with different choices for f, Δ and z, however, which shows again the difficulty of measuring α_s from the 3 jet fraction. Finally, as claimed above, I find that the weighting function varies little with the x_i' for my preferred form of f . There is more variation with other forms of f, but these other forms are not physically motivated and I use them only to obtain estimates of the uncertainties due to hadronization.

At Z-factory energies one would expect jet broadening effects to be roughly three times smaller. Thus, one would expect the shift from perturbative to experimental allowed regions to be $\Delta\delta \sim 3^0$ and $\Delta\varepsilon \sim 0.05$. This is in fact what I find by repeating the above analysis. I also find that the size of the region in the ε, δ plane that contains 80% of the weight is reduced to $\Delta\delta \sim 8^0, \Delta\varepsilon \sim .1$.

It is worth pointing out that although the shift due to hadronization is fairly small the smearing in ε and δ is significant: $\Delta\delta/\delta \sim \Delta\varepsilon/\varepsilon \sim 0.5\text{-}1$ for the allowed region. Thus, I expect the uncertainty in the choice of correct cone definition discussed in Section 2 to remain at Z-factory energies because the two definitions that I have used differ by $\Delta\delta$ such that $\Delta\delta/\delta < 1$. This substantiates the claim that I made frequently in Section 2, based partly on the work of Furmanski[2] and of Walsh and collaborators[25] that even at Z-factory energies the effects of hadronization are important. In fact I probably understated the effects of hadronization as found by these authors because they considered 2-jet events whereas I am dividing the CM energy between three jets.

A final effect of going to Z-factory energies is that there is a small increase in the size of the allowed regions since α_s is decreased.

I now turn to the smearing of the x_i' and θ_i due to hadronization. This occurs because non-perturbative jet broadening necessarly throws some particles outside the experimental

cone. This, together with the fact that not all particles are experimentally identified, will cause the experimental and partonic x_i' and θ_i to differ. This difference will include a random component and, as discussed above, in the energies case there will also be a systematic increase in x_1' and decrease in x_3'. This systematic effect will be smaller for cluster algorithms than experimental SW criteria because the former can identify more of a broad third jet than the latter. I roughly estimate these effects with the aid of Monte-Carlo events and analysis provided by W. Chinowsky.[58] Three parton events are hadronized and put through a Monte-Carlo simulation of the Mark II detector. Jets are then identified with the cluster algorithm of J. Dorfan.[29] Finally an experimental SW criterion is applied. The systematic increase in x_1' and decrease in x_3' is found to be ~ 0.1, with fluctuations of $\pm$ 0.1. A more detailed study by Daum et al.,[56] using an algorithm containing features of both cluster and SW methods, finds a somewhat smaller systematic effect and fluctuations in the x_i' of $\sim \pm$ 0.05. They also find fluctuations in the angle between the parton and reconstructed jet of $\sim 5^0$ for the first jet and 10 - 15^0 for the 3rd jet, so that the fluctuations in the θ_i will be $\sim 10^0$ - 15^0. These results do not include detector efficiencies, however. Using a cluster algorithm alone (i.e. with no SW component) Dorfan[29] finds similar fluctuations in the angles without the inclusion of detector effeciencies but also finds that inclusion of these efficiences increases the fluctuations by roughly 5^0. Now the $x_i' \leq .85$ region is a triangle of length .325 and height $\sim$ .2, or, in terms of angles, $\Delta\theta_1 \sim \Delta\theta_2 \sim 40^0$, although the region has a peculiar shape in terms of the angle variables so this gives an overestimate of its size. Clearly, then, the fluctuations make a test of the angular distribution very difficult at PEP/PETRA energies since they are comparable to roughly half of the x_i' region that perturbation theory forces one to use. The situation is worse still if one uses the energies as variables because of the large systematic effects. At Z-factory energies, however, both the fluctuations and the systematic effects should be significantly smaller - roughly by a factor of three - and these smearing problems should not prevent a test of the angular distribution.

These results show that a test of the QCD prediction for the 3-jet angular distribution at PEP/PETRA energies is difficult for two reasons. Firstly, the combined energies/angles allowed ε, δ region ($|F_2| < 10$ for PEP/PETRA energies) is not much larger than the uncertainty in the shift in the allowed region due to hadronization. Thus, one cannot identify with certainty the experimental parameters for which the correction is small, although they are most likely close to $\delta = 35^0$, $\varepsilon = .25$ - .3. Secondly, the smearing in the x_i' is not much smaller than the region that the perturbative results force us to consider, i.e. $x_i' \leq .85$. Since the lowest order cross section varies fairly rapidly within this region (by up to a factor of 4) this smearing is particularly difficult to deal with. This has been shown clearly by analyses of Mark II data done by H. Schellman[59] using a cluster algorithm to identify the jets. At Z-factory energies the smaller hadronization effects improve the situation substantially. Because the uncertainties in the effects of hadronization are much smaller, one can claim with some confidence that for $\delta_{exp} \approx 30^0$, $\varepsilon_{exp} \approx .2$ the corrections are small, while the problem of x_i' smearing is significantly eased. Both the problems afflicting PEP/PETRA energies can perhaps be alleviated by further work. Improving the perturbative results by resummations can, as we shall see, have dramatic effects. In fact the improvements I make greatly improve the situation at Z-factories but make that at PEP/PETRA energies worse. However, further improvements may well be possible in the future as our understanding of perturbative resummations improves. The x_i' smearing problem can perhaps be corrected for - this has recently been attempted by the JADE collaboration[60] - but any such correction will rely on some assumptions concerning hadronization. This problem seems to me the more intractable, though whether or not it can be corrected for it is, of course, a question to be decided by detailed Monte Carlo work. It is clear, though, that using the angles between the jets as variables rather than the jet energies is much preferable, particularly at PEP/PETRA energies. Given these negative conclusions concerning the possibility of testing QCD using the 3-jet angular distribution at PEP/PETRA energies, it is ironic that a recent JADE analysis[60] which looks at the distribution with respect to the angles using the partial cluster,

partial SW algorithm of Reference 56 with parameters corresponding approximately to ε_{exp} = .2, $\delta_{exp} = 35^0$, and which corrects for the θ_i smearing, and, furthermore, which only uses $x_i' \leq$ .85, finds good agreement with the lowest order angular distributions!

(c) Improved results

There are various terms in the SW cross section that have a well understood origin and may be in some way "resummed". The most obvious such term is that corresponding to a change in scale of the coupling constant associated with the gluon jet bremmstrahlung vertex from Q to Qx_3. Of course we can choose this scale to be anything we like but a "good" choice is one that does not give rise to large logarithms like $\ell n\ x_3$ in higher orders. Since x_3Q is roughly the large momentum flowing through the vertex, and since the $\ell n\ x_3$ terms with the correct coefficients appear in the correction, it is reasonable to resum these terms.

The terms multiplying $\ell n\ \delta$ and thus corresponding to collinear divergencies have, as the explicit calculations in Section III showed, a close relationship to the Altarelli-Parisi kernels and these kernels generate all the leading logarithms in deep inelastic scattering. Thus, it is to be expected that an Altarelli-Parisi equation would apply to the leading collinear singularities and this in fact has been shown to be true.[61] Roughly speaking the leading $\ell n\ \delta$ terms exponentiate so that the logarithms, rather then becoming infinitely negative as ε and $\delta \rightarrow 0$, go to zero as a power. This has the potential for greatly improving the perturbative convergence, but it is essential in order for such an improvement to occur that renormalization group equations are found that control the nonleading logarithms. This is because we are summing terms of the form $(\alpha_s\ \ell n\ \delta)^n$, when they became large, to make a small answer, so $\alpha_s(\alpha_s \ell n\ \delta)^n$ terms cannot be ignored. In deep inelastic scattering we have the classsic renormalization group analysis which tells us that such non-leading terms are also exponentiated and are thus supressed in the exponent by powers of α_s. Thus, we have an ordered renormalization group improved expansion. Recently an analysis was presented by Mukti and Sterman,[22] based on the earlier work of Collins, Soper and Sterman,[62] which showed that essentially the same result applies to 2-jet SW cross section. Their analysis,

moreover, shows exponentiation of all logarithmic terms - not only of the $\ell n\ \delta$ terms but also of the $\ell n\ \varepsilon$ terms. Essentially the soft terms can be factored from the whole amplitude. To be precise, they find that the 2-jet SW cross section may be written as:

$$\sigma(\varepsilon,\delta) = \exp\left(\int_Q^{\varepsilon Q} \frac{d\mu'}{\mu'} V_s(g(\mu'))\right) \exp\left(2\int_\zeta^{\varepsilon} \frac{d\varepsilon'}{\varepsilon'} \int_{\delta\varepsilon' Q}^{\varepsilon' Q} \frac{d\mu'}{\mu'} p(g(\mu'))\right)$$

$$\times \exp\left(2\int_{\zeta Q}^{\delta Q} \frac{d\mu'}{\mu'} \gamma(g(\mu'),\zeta)\right) \times F(g(\delta Q),\zeta) + \text{non-logarithmic terms} \tag{5.8}$$

where V_s, p and γ are functions of g of the form $1 + 0(g^2)$, and ζ is a small parameter on which the cross section does not depend. Expanding V_s, p and γ one finds, respectively, the soft $\ell n\ \varepsilon$ terms (which actually cancel in leading order for two jets), the $\ell n\ \delta\ \ell n\ \varepsilon$ terms and the $\ell n \delta$ terms as found above. Notice the appearence also of $g(\delta Q)$, which can be expanded as $g(Q) \times (1 + 0(g^2\ \ell n\ \delta))$ and thus does represent a resummation of non-leading logarithms.

The three jet case was not studied by Mukti and Sterman but it appears that their analysis also applies there. The only differences in the result for three jets are that there is an extra exponential factor for the third jet and that the "appropriate" ε is changed. For the $\ell n\ \varepsilon$ terms associated with one jet alone - the generalizations of the ladder diagrams - the "appropriate" ε is certainly ε/x_j since the only energy scale that such diagrams contain is E_{jet} - not E_{beam}. (For the same reason $g(\delta Q)$ should be changed to $g(\delta x_{jet}\ Q)$ but this only affects higher order terms.) Thus the terms in Eq. 3.45 of the form $\ell n\ \delta\ \ell n\ x_i$ should be exponentiated.

The remaining $\ell n\ \varepsilon$ terms, which multiply $\ell n\ u_{ij}$, should also be exponentiated. The dependence of such terms on the angles between the jets is natural in the treatment of Mukti and Sterman because the soft gluon "remembers" the direction of its jet. (Actually this is just

another demonstration of the suppression factor associated with spin and helicity conservation discussed in Section 3). There remains the question of the appropriate ε to use. Some of the $\ell n\ \varepsilon$ terms come from ladder diagrams for which ε/x_j is appropriate , while the remainder come from the ivy diagrams. I have not carried out a detailed analysis to determine the correct form to use, but a simple analysis suggests $\varepsilon/\min\{x_i,x_j\} \sim \varepsilon(x_i + x_j)/x_i x_j$ is correct. In fact, using these forms instead of ε leads to numerically small changes. Thus, I choose to exponentiate these terms using ε itself.

It is fortunate that I can make this choice as it removes a potential source of ambiguity. Had I used ε/x_j etc. I would have been exponentiating terms like $\ell n\ x_j\ \ell n\ u_{ij}$, i.e. constant terms. But the methods of Mukti and Sterman no doubt also exponentiate constant and $O(\varepsilon, \delta)$ terms. No detailed analysis of this exponentiation has been given, and so I prefer to exponentiate none of the constants, apart from those associated with the change of scale in α_s. I should note, though, that large n^2 terms coming from the mismatch of spacelike momenta (from loops) and timelike momenta (from real diagrams) in double logs have been shown to form a major component of the large corrections to thrust-like distributions found by ERT.[63] However, the explicit calculation given above shows that there are other n^2 terms that come from the singular integrals, being produced, for example, by the mismatch of gamma functions. Furthermore, there are n^2 terms appearing in the difference between the constants in the energies and angles cases. Lacking a detailed analysis I shall, therefore, not exponentiate any n^2 terms.

The above considerations mean that I can rewrite the 3 jet SW cross sections as

$$\frac{d^2\sigma}{dx_1' dx_2'} = \sigma_0 C_F \sum_{\text{permutations}} \left\{ \frac{\alpha_s(Qx_g)}{2\pi} \frac{x_q^{\ 2} + x_{\bar{q}}^{\ 2}}{(1-x_q)(1-x_{\bar{q}})} \times \left(\exp(\text{LOGS}) + \frac{\alpha_s(E_{beam})}{2\pi} \text{CORR}' \right) \right\}$$

$$= \sigma_0 C_F \left\{ \sum_{\text{perms}} \frac{\alpha_s(Qx_g)}{2\pi} \frac{x_q^{\ 2} + x_{\bar{q}}^{\ 2}}{(1-x_q)(1-x_{\bar{q}})} \exp(\text{LOGS}) + \left(\frac{\alpha_s(E_{beam})}{2\pi}\right)^2 \sum_{\text{perms}} \frac{x_q^{\ 2} + x_{\bar{q}}^{\ 2}}{(1-x_q)(1-x_{\bar{q}})} \text{CORR}' \right\}$$

$$\equiv \sigma_0 C_F \frac{\alpha_s(E_{beam})}{2\pi} F_1(x_1', x_2') \left\{ \exp(\text{LOGS}') + \frac{\alpha_s(E_{beam})}{2\pi} F_2'(x_1', x_2'; \varepsilon, \delta) \right\} \tag{5.9}$$

where LOGS means the logarithms of ε and δ calculated in Section 3, CORR′ is the correction term, <u>before</u> the sum over permutations, with these logarithms removed and with the term corresponding to a charge in the scale of the overall coupling constant removed. The scale of α_s multiplying CORR′ is undetermined - for simplicity I have taken it to be E_{beam}. The approximation made to obtain the second line-changing $\alpha_s(Qx_g)$ to $\alpha_s(E_{beam})$ in the correction term - is necessary because of the way I do the numerical calculation. I sum over the permutations in that calculation <u>without</u> using $\alpha_s(Qx_g)$ as a weighting factor. The final line, which defines LOGS′ and F_2', shows the resummed result in a form as close as possible to that used for defining the original correction F_2 (i.e. Eq. 2.4). The effect of resumming the logarithms and the change of coupling constant scale is contained, suitably adjusted for the sum over permutations, in LOGS′. The lowest order result is the 1 in the expansion of the exponential. Although this 1 has been engulfed in the exponential I shall compare the improved correction, $F_2'\ \alpha_s/2\pi$, to 1. Notice that it has <u>not</u> been proven that the exponential is a prefactor to the entire cross section, although it may be to some or all of it - a point to which I return below. There is some uncertainty in the precise form of exponentiation, e.g. the scales of the α_s factors in the exponent are undetermined. This and the undetermined scale of α_s multiplying the correction are higher order effects, but they introduce some uncertainty into

the results presented below. In fact these uncertainties are roughly of the same size as the error which I have estimated is caused by the approximation made to obtain the second line of Eq. 5.9. I shall comment on the size and effects of these uncertainties below.

F_2' is shown for points I, II and III in Tables 5.1 and 5.2 for the energies and angles cases respectively. The corresponding allowed regions are shown in Figs. 5.7 and 5.8. The improvement due to the resummation is substantial in both cases. In the energies case the $|F_2'| < 10$ allowed region is slightly enlarged, but the size of the $|F_2'| < 15$ region is substantially increased. This large difference between these two regions reflects the much slower variation of F_2' with respect to ε and δ than that of F_2. In the angles case there is no $|F_2'| < 10$ region, but the $|F_2'| < 15$ region has grown dramatically as compared to the $|F_2| < 15$ region. Again the variation of F_2' with ε and δ is much slower than that of F_2. Furthermore, within the kinematically allowed region shown in Fig. 5.8, the $|F_2'| < 15$ contour applies also to the x_i' region $x_i' \leq 0.9$. The extension to $x_i' \leq 0.9$ may also be possible in the energies case but I do not have the results necessary to check whether this is true. Notice that although there is no region for which both angles and energies obey $|F_2'| < 10$, there is a sizeable region where $|F_2'| < 15$ in both cases. This is the dramatic improvement in the results for Z-factory energies which I mentioned above.

In Figs. 5.9 and 5.10 I show the corrected results for $d\sigma/dx_i'$ for various ε and δ using the resummed form Eq. 5.9 at Z-factory energies for the energies and angles cases respectively. Notice that the exponentiation reduces the cross section as compared to the lowest order curve at small ε and δ so that the cross section varies move rapidly with ε and δ than in the unimproved case. Figures 5.11 and 5.12 show how the shape of the x_1' distributions varies with ε and δ. The peculiar behavior of some of the curves in Fig. 5.12 is due to Monte-Carlo integration errors. The main point of interest, which can also be seen in Tables 5.1 and 5.2, is that for all the allowed ε and δ values in the energies case and for the larger ε, δ values in the angles case the corrected x_1' distribution is steeper than the lowest order curve. For small ε and δ in the angles case, however, the curves have a slope

comparable to or less than that of the lowest order result. The division between these two regions fall roughly along the boundary of the $x_i' \leq .9$ kinematically allowed region shown in Fig. 5.8.

It is easy to understand the flattening of the curves for small ε and δ in the angles case. As Tables 5.1 and 5.2 show, the logarithms and "scale changing" terms both tend to make the curves steeper than the lowest order, while F_2' has the opposite effect. The exponentiation of the logarithms and the incorporation of the scale changing terms into the argument of α_s weakens the effect of both of these terms. This is particularly true of the logarithms for small ε and δ since a large negative number is being changed to a number between 0 and 1. Thus the F_2' term eventually dominates and the curves become less steep than the lowest order result. This effect is more pronounced in the angles case because the logarithms are larger. Clearly this effect is very dependent upon the exponentiation or otherwise of terms in F_2', and thus it is not a reliable prediction. However, for larger ε and δ, where the log terms are not so large, the results are not very sensitive to possible exponentiation of terms in F_2'. I should also mention that using other forms of exponentiation gives results that vary from those shown by no more than the variation between the curves in the energies case shown in Fig. 5.11.

These improved results do not, unfortunately, improve the situation at PEP/PETRA energies. At Z-factory energies there is, however, significant improvement I summarize the Z-factory results and discuss the effects of hadronization on them. The $|F_2'| < 15$ allowed region for the angles case, which is shown in Fig. 5.8, is contained within that for the energies case and thus is the region of ε and δ for which the corrections are firmly under control. Hadronization will shift this region by $\Delta\varepsilon \sim 0.05$ and $\Delta\delta \sim 3^0$ with its shape and size remaining nearly the same, <u>giving a range of experimental parameters of roughly $5^0 \leq \delta_{exp} \leq 35^0$, $.1 \leq \varepsilon_{exp} \leq .2$ for which the lowest order angular distribution is a reliable prediction of QCD</u>. For the smaller allowed values of ε and δ, and thus of ε_{exp} and δ_{exp} this result can probably be extended to $x_i' \leq .9$. Given the much smaller x_i' smearing ($\approx \pm$ (0.01 - 0.03)) it

should be possible to measure this distribution and test QCD. For medium and large allowed values of ε and δ both the energies and angles cases have corrected x_1' distributions steeper than the lowest order result. Thus it seems to be a very solid prediction that in the corresponding shifted region of δ_{exp} and ε_{exp} the measured angular distribution should be steeper than the lowest order result. Unfortunately there is variation of the steepness of the corrected distributions within this region and between the angles and the energies cases (the angles corrected curves are less steep), so a more precise prediction is not possible. There are two obstacles to measuring this difference between corrected and lowest order distribution shapes. Firstly, there is the remaing x_i' smearing. A detailed Monte-Carlo study, which I have not done, is needed to see whether this smearing will wash out any small difference or whether the smearing can be corrected for. Secondly, there is the problem of statistics. Take the α_s scale-changed lowest order result as an example (See e.g. Fig. 5.11). If I divide the x_1' interval into the two bins 2/3 - 0.8, and 0.8 - 0.85, there will be roughly equal numbers of events in these two bins and the difference between the numbers of events in the lowest order case as opposed to the scale-charged lowest order case will be ~ 2% in each bin. To distinguish by four standard deviations these two situations would require ~ 10^4 three jet events. Thus, 10^5 Zs might give enough statistics for such a test, assuming that the x_i' smearing corrections are manageable.

6. CONCLUSIONS

I have presented a detailed account of the corrections to the 3-jet Sterman-Weinberg cross sections in e^+e^- annihilation, and of the effects of hadronization on this cross section. I find that

(a) at PEP/PETRA energies there is at best a very small region of the parameters for which the correction is under control;

(b) at PEP/PETRA energies the effects of hadronization are substantial and would make a test of the angular distribution difficult even if point (a) were not true;

(c) at Z factory energies there is a substantial region of experimental parameters for which the lowest order angular distribution should be measurable. The use of the angles between the jets as variables is preferred to the energies of the jets; and

(d) there is a somewhat smaller region of parameters in which the corrections to the lowest order result may be measureable.

The results show a suprisingly sharp division between the bad news ((a) and (b)) and the good news ((c) and (d)). It is worthwhile dwelling on this point. The dramatic improvement on going from PEP/PETRA to Z-factory energies is due to two factors. Firstly, there is the decrease in the size of hadronizaton effects (point (b) above) which is a rock solid result. Secondly, there is the decrease in α_s which, since the maximum (over the x_i' range) improved correction F_2 is a slowly varying function of ε and δ with a magnitude close to 15 over a large area, causes a substantial increase in the perturbative allowed region. This result would be much less dramatic if F_2 were increased by a uniform factor of five. Conversely, a reduction in F_2 due to further exponentiation would greatly improve the perturbative PEP/PETRA results, although the non-perturbative effects would still make a test difficult. One might also query my choice for the maximum allowable correction, any change in which would have a significant effect on the size of the allowed regions, although I think my choice is reasonable and fairly conservative. Thus, there are caveats attached to the good news and the final judgement is not yet, and may never be, in. A major step would,

however, be a systematic treatment of the exponentiation of the non-logarthmic terms. Of course, one could argue that since F_2' is large and positive in the more sensitive angles case, the exponentiation of non-logarithmic terms will most likely reduce F_2' thus improving the situation. I have criticized such specious arguments in the introduction and so I do not indulge in them now.

Finally, I should comment on similar work done by other authors. Sharpe[11] finds small corrections for a range of ε and δ in the energies case. This work is, however, superseded by that presented here because he does not discuss the uncertainty in cone definitions, he does not improve the perturbative cross section, and he does not discuss Z-factory results.[64] There are also various errors in his work.[65]

Chainawitch[66] has not done any useful work in this field, but I mention him because he cannot be left out.

REFERENCES

1. See e.g. D. H. Perkins, lecture at the 1981 Banff Summer Institute (C.A.P.) on Particles and Fields, Banff, Canada.
2. W. Furmanski, *Nucl. Phys.* B158, *429 (1979).*
3. E. Farhi, *Phys. Rev. Lett.* 39, *1587 (1977).*
4. H. Georgi and M. Machacek, *Phys. Rev., Lett.* 39, *1237 (1977).*
5. G. Sterman and S Weinberg, *Phys. Rev. Lett.* 39, *1436 (1977).*
6. T. D. Gottschalk, *Phys. Lett.* 109B, *31 (1982).*
7. I. Hinchliffe, private communication.
8. K. Fabricius et al., *Z. Phys. C-Particles and Fields* 11, *315 (1982).*
9. R. K. Ellis et al., *Phys. Rev. Lett.* 45, *1226 (1980), Nucl. Phys* B178, *421 (1981).*
10. J. A. M. Vermaseren et al., *Nucl. Phys.* B187, *301 (1981).*
11. S. Sharpe, *Phys. Lett.* 106B, *331 (1981).*
12. R. M. Barnett et al., *Phys. Rev.* D22, *594 (1980)*, see also G. Wolf, Ref. 16.
13. G. Hanson et al., *Phys. Rev. Lett.* 35, *1609 (1975);*
    R. F. Schwitters - Proc. Int. Symp. on Lepton and Photon Interactions at High Energy, Stanford, CA (1975) (ed. W. T. Kirk).
14. See e.g. D. P. Barber et al., *Phys. Lett.* 89B *139 (1980).*
15. See e. g. G. Goldhaber, talk given at the 1981 Banff Summer Institute (C.A.P.) on Particles and Fields, Banff, Canada.
16. See e.g. G. Wolf, Rapporteur talk, XXI Int. Conf. on High Energy Physics, Paris, July 1982 (DESY preprint 82-077).
17. T. Kinoshita, *J. Math. Phys.* 3, *650 (1960).*
    T. D. Lee and M. Nauenberg, *Phys. Rev.* 133, *1594 (1960).*
18. G. Sterman, *Phys. Rev.* D17, *2789 (1978).*
    J. C. Collins and G. Sterman, *Nucl. Phys.* B185, *172 (1981).*

19. P. M. Stevenson, *Phys. Lett.* 78B, 451 (1978);
B. G. Weeks, *Phys. Lett.* 81B, 377(1979).
20. S. Nandi and W. W. Wada, *Phys. Rev.* D21, 76 (1978)
21. P. E. L. Rakow and B. R. Webber, *Phys. Rev. Lett.* 43, 1695 (1979); *erratum, ibid* 44, 764 (1980).
22. S. Mukti and G. Sterman, *Nucl. Phys.* B206, 221 (1982).
23. See e.g. Reference 2.
24. K. Kinoshi, et al., *Nucl. Phys.* B157, 45 (1979).
25. T. Walsh et al., *Nucl. Phys.* B173, 244 (1980).
26. J. Ellis et al., *Nucl. Phys.* B111, 253 (1976).
27. K. Hagiwara, U. Wisconsin preprint, M4D/PH/56, May 1982.
28. H. J. Daum et al., *Z. Phys. C - Particles and Fields* 8, 167 (1981);
K. Lanius et al., *ibid*, 8, 251 (1982).
29. J. Dorfan, *Z. Phys. C - Particles and Fields* 7, 349 (1981).
30. See e.g. W. Bartel et al. (JADE collaboration), *Phys. Lett.* 119B, 239 (1982).
31. H. J. Behrend et al.(CELLO Collaboration), *Acta. Phys. Polon* B14, 193 (1983).
32. In addition to References 33-37 see:
G. C. Fox and S. Wolfram, *Nucl. Phys.* B168, 285 (1980);
R. Odorico, *Nucl. Phys.* B172, 157 (1980);
Phys. Lett. 102B, 341 (1981).
33. G. Marchesini and B. R. Webber, CERN preprint TH3525 (Feb. 1983).
34. A. H. Mueller, *Phys. Lett.* 104B, 161 (1981)
A. Bassetto et al., *Nucl. Phys.* B207, 189 (1982).
35. R. D. Field and S. Wolfram, *Nucl. Phys.* B213, 65 (1983).
36. T. D. Gottschalk, *Nucl. Phys.* B214, 201 (1983)
37. P. Mazzanti and R. Odorico, *Z. Phys.* C7, 61 (1980)
38. T. F. Walsh and P. Zerwas, SLAC-PUB 2939, June 1982.

39. C. L. Basham et al., *Phys. Rev. Lett.* 41, 1585 (1979);
Phys Rev. D19, 2018 (1979);
D. G. Richards et al., *Phys. Lett.* 119B, 193 (1982).
40. Z. Kunszt, *Phys. Lett.* 99B, 429 (1981).
41. G. 't Hooft and M. Veltman, *Nucl. Phys.* B44, 189 (1972).
C. G. Bollini and J. J. Giambiagi, *Nuovo Cimento* 12B, 20 (1972);
W. J. Marciano, *Phys. Rev.* D12, 3861 (1975).
42. See e. g. H. P. Nilles and K. H Streng, *Phys. Rev.* D23, 1944 (1981).
43. V. Sudakov, *Zh eksp Theor. Fiz*, 30 ,87 (1956).
44. R. K. Ellis et al, *Phys. Lett.* 78B, 281 (1978); *Nucl. Phys.* B152, 285 (1979).
45. G. Altarelli and G. Parisi, *Nucl. Phys.* B126, 298 (1977).
46. See also ERT (Reference 9).
47. See e.g. L. Lewin, Dilogarithms and Associated Functions, MacDonald, London, 1958.
48. N. N. Lebedev, Special Functions and their Applications, Dover, New York, 1972.
49. M. B. Einhorn and B. G. Weeks, *Nucl. Phys.* B146, 445 (1978).
50. K. Shizuya and S. -H. H. Tye, *Phys. Rev. Lett.* 41, 787 (1978); *erratum, ibid* 41, 1195 (1978); *Phys. Rev.* D20, 1101 (1979); *erratum, ibid* D21, 313 (1979).
51. A. V. Smilga and M. I. Vy sotsky, *Nucl. Phys.* B150, 173 (1979).
52. A. Ali et al., *Nucl. Phys.* B167, 454 (1980); Phys. Lett. 82B, 285 (1979);
K. J. F. Gaemers and J. A. M. Vermaseren, *Z. Phys.* C7, 81 (1980).
53. R. Pavelle et al., "Computer Algebra", *Scientific American, Dec. 1981, p. 136.*
54. J. Sheiman et al, *Nucl. Phys.* B183, 397 (1981).
55. S. L. Wu and G. Zobernig, *Z. Phys.* C2, 107 (1979).
56. See the first Reference in 28.
57. I thank Chris Day for providing me with Monte-Carlo "data".
58. W. Chinowsky, private communication.
59. H. Schellman, private communication.

60. W. Bartel et al. (JADE Collaboration), *Phys. Lett.* 119B, 239 (1982).

61. See e.g. Reference 2.

62. G. Sterman, *Phys. Rev.* D17, 2773 and 2789 (1978);

S. Libby and G. Sterman, *Phys. Rev.* D18, 3252 (1978);

J. C. Collins, *Phys. Rev.* D22, 1478 (1980);

A. Sen, *Phys. Rev.* D24, 3281 (1981);

J. C. Collins and D. Soper, *Nucl. Phys.* B193, 381 (1981).

63. D. Ross, *Nucl. Phys.* B188 109 (1981).

64. What does he do?

65. S. Sharpe, very private communication.

66. M. T. ("vacuous") Chainawitch, no communication.

Tables 5.1: Breakdown of F_2 for various ε, δ and x_i' in the energies case. Points I, II and III are respectively, $x_i' = .85, .85, .3$; $x_i' = .85, .6, .55$; $x_i' = .7, .7, .6$. The breakdown is LOGARITHMS / CONSTANTS / $O(\varepsilon, \delta)$ / TOTAL / IMPROVED CORRECTION (F'_2). The improved correction has the logarithms and the scale change terms (the latter are 8, 4 and 3 for points I, II and III respectively) removed. The ε and δ values are within 0.1 and 2^0 of the values shown. The numbers shown have been rounded off and thus may not sum exactly to the total.

ε	$\delta \simeq 10^0$			$\delta \simeq 20^0$			$\delta \simeq 30^0$		
	I	II	III	I	II	III	I	II	III
				-24	-31	-36			
				6	7	7			
≈0.05				4	5	4			
	-30	-39	-44	-14	-19	-25			
	6	7	7	1	7	8			
0.075	-4	-2	-2				-3	-8	-11
	-28	-34	-39				6	7	7
	-7	0	3				5	6	9
≈0.1							8	5	4
							2	8	12
	-15	-24	-28	-3	-9	-12	1	-3	-7
	6	7	7	6	7	7	6	7	7
≈0.15	-9	-7	-7	-1	1	0	2	4	5
	-18	-24	-28	2	0	-5	9	7	5
	-12	-5	-3	-4	4	4	0	6	9
				2	-3	-6			
≈0.2				6	7	7			
				-3	0	-1			
				6	4	0			
				-5	3	3			

TABLE 5.2: Breakdown of F_2 for various ε and δ and x_i' in the angles case. The format is as in Table 5.1, except that in this case the ε and δ values shown are exactly correct.

ε	$\delta=10^0$			$\delta=20^0$			$\delta=30^0$		
	I	II	III	I	II	III	I	II	III
	-74	-88	-94	-49	-58	-65	-34	-42	-47
0.05	19	20	20	19	20	20	19	20	20
	-4	-3	-3	-4	-2	-1	-2	+1	0
	-59	-84	-76	-33	-40	-45	-17	-21	-27
	7	13	15	8	11	17	9	17	17
	-40	-53	-58	-25	-34	-40	-16	-23	-29
	19	20	20	19	20	20	19	20	20
0.10	-7	-6	-6	-5	-5	-4	-7	-3	-4
	-28	-39	-44	-13	-19	-23	-4	-7	-12
	4	10	11	4	11	14	4	12	14
	-20	-32	-37	-12	-21	-25	-7	-14	18
0.15	19	20	20	19	20	20	19	20	20
	-10	-8	-9	-10	-7	-6	-11	-6	-7
	-11	-21	-25	-3	-8	-10	2	0	-4
	1	7	9	1	9	12	1	10	11

FIGURE CAPTIONS

Fig. 2.1. Matrix elements for $\gamma^* \to q\bar{q}g$ in lowest order in α_s.

Fig. 2.2. A 4 parton configuration which for $\delta \geq 25^0$ has an ambiguous cone assignment. Scaled energies (E_{jet}/E_{beam}) are shown by each parton.

Fig. 2.3. Figures (a) and (b) show two configurations accepted as jets by a perturbative Sterman-Weinberg criterion; (c) and (d) show possible configurations of particles resulting from the hadronization of (a) and (b) respectively. The length of the lines is proportional to the energy of the particles, which are assumed massless.

Fig. 3.1. Part of a squared amplitude contributing to the 4 parton cross section (see e.g. Fig. 3.3a). This figure establishes some notation used in the text.

Fig. 3.2. A contribution to the squared amplitude for 4 partons (i.e. a "cut diagram") containing, in a physical gauge, no collinear divergences, but having soft divergences when either gluon running across the cut goes soft. This is an example of an "Ivy" diagram.

Fig 3.3. Cut diagrams contributing to the 4 parton cross section. (a) shows all the quark "ladder" diagrams; these are singular when the gluon labeled SC is either soft or collinear with the quark. (b) and (c) show examples of gluon ladder diagrams - which also have soft and collinear singularities - and establish some notation used in the text. (d) and (e) show ivy diagrams - those with only soft divergences when the gluons marked S go soft. (d) also establishes some notation.

Fig. 4.1. Notation used in Section 4 for discussing the numerical integration of the 4 parton cross section. (a) shows a configuration with partons 1 and 3 forming a jet with momentum sum $\bar{J}$. (b) shows a configuration with parton 3 going soft. θ_{23} and θ_{34} are defined analagously to θ_{13}.

Fig. 5.1. Perturbatively allowed regions for the energies case. The singly hatched strips bound the area in which the magnitude of the correction, for all $x_i' \leq .85$, is less

than 10 $\alpha_s/2\pi$, i.e. $|F_2| < 10$. The doubly hatched strips bound the $|F_2| < 15$ region. The width of the strips reflects the uncertainty in the position of the boundaries due to the relatively small number of ε, δ values for which results were obtained. The solid line is the kinematic boundary beyond which the 3-jet definition is not consistent.

Fig. 5.2. The perturbatively allowed region in the angles case, using the same format as in Fig. 5.1. The allowed regions are to the lower right of the boundaries shown. The dashed vertical line delimits the region which has no cone overlap ambiguity (that to the left). As discussed in the text, I did not extend my calculations across this boundary.

Fig. 5. 3. Corrected three jet cross sections with respect to x_1' for various allowed (ε, δ) values in the energies case. Also shown is the lowest order curve. These curves are for Z-factory energies, the precise values of α_s used being discussed in the text.

Fig. 5.4. Graphs showing the difference between the shape of the lowest order and corrected x_1' distributions for various allowed ε and δ in the energies case. (a) shows the normalized (to an average value of 1) corrected distribution divided by the lowest order normalized result; (b) shows the difference between the corrected and lowest order normalized curves. Also shown is the lowest order distribution with the scale of the overall α_s changed to Qx_3'. These results are for Z-factory energies.

Fig. 5.5. The average energy profile of a Monte-Carlo jet after integration over the azimuthal angle. The unbroken histogram corresponds to a 10 GeV jet - data from the Monte-Carlo "tubes". The dashed lines show the modifications made for 11 GeV and 4.5 GeV jets and illustrate the procedure used for jets with other energies. The curve is a plot of the distribution resulting from a constant

rapidity (y) density of massless particles with fixed transverse momentum (p_t) such that $p_t\, dN/dy = .71$.

Fig. 5.6. This figure shows the perturbatively allowed regions (upper left) and the corresponding experimental allowed regions (lower right) for the energies case. The latter were found using the hadronization model discribed in the text. The dashed curves are for $|F_2| < 10$, the dot-dashed curves for $|F_2| < 15$. The solid line shows the boundary of the consistently defined perturbative 3-jet SW criterion. I did not consider $\varepsilon_{exp} > .325$. The uncertainties in these curves are not shown but are comparable to those in Fig. 5.1.

Fig. 5.7. Perturbatively allowed regions for the improved corrections (F_2') in the energies case. The notation is as in Fig. 5.1. Notice that the presence of $\varepsilon\, \ell n\, \delta$ and $\delta\, \ell n\, \varepsilon$ terms in F_2' forbids the boundaries to touch the axes.

Fig. 5.8. The perturbatively allowed region for the angles case using the improved correction. There is no $|F_2'| < 10$ region, so only the $|F_2'| < 15$ region is shown.The notation is as in Figure 5.2 except that the consistency and overlap boundaries for the $x_i' < 0.9$ region are shown in addition to those for $x_i' < 0.85$ - the former are the more stringent ones. The $|F_2'| < 15$ boundary applies to <u>both</u> these x_i' regions. The hatched region is that for which the corrected x_i' distributions are more steep then the lowest order result.

Fig. 5.9. Improved corrected x_1' distributions for the energies case at Z-factory energies.

Fig. 5.10. Improved corrected x_1' distributions for the angles case at Z-factory energies.

Fig. 5 11. Curves showing the difference in shape between the corrected and lowest order normalized distributions in the energies case. (a) quotient; (b) difference.

Fig. 5.12. Curves showing the difference in shape between the corrected and lowest order normalized distributions in the angles case. (a) and (b) quotient; (c) and (d) difference.

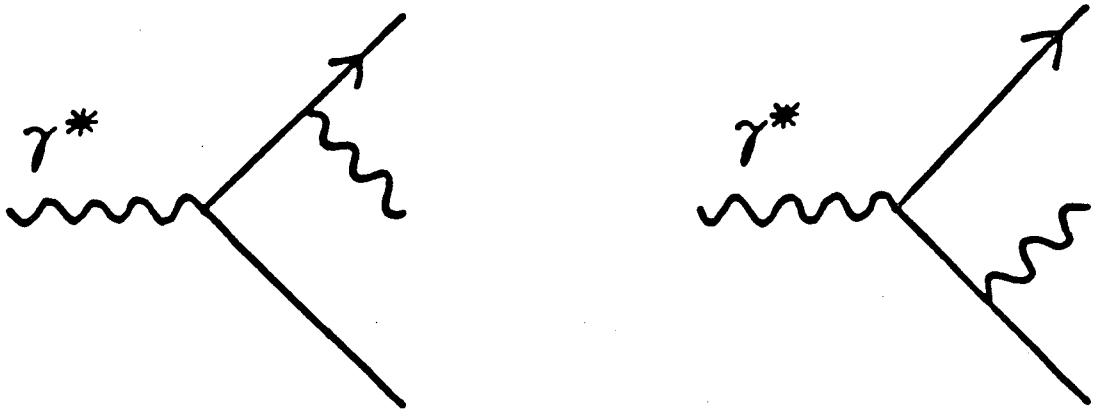

Fig. 2.1

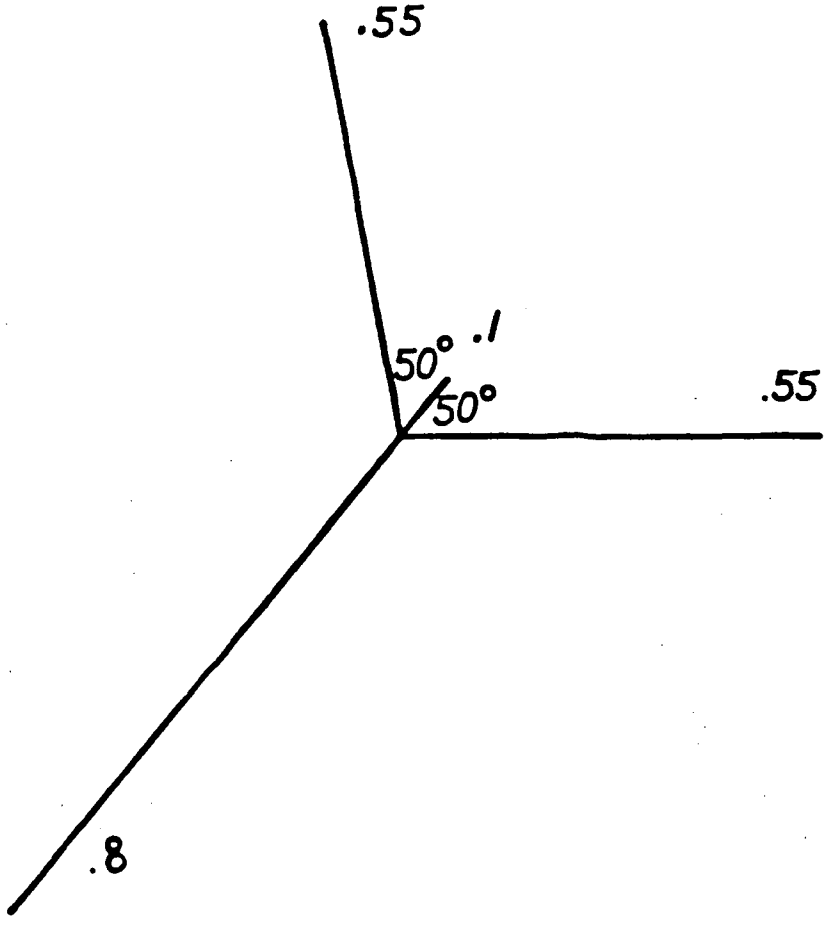

Fig. 2.2

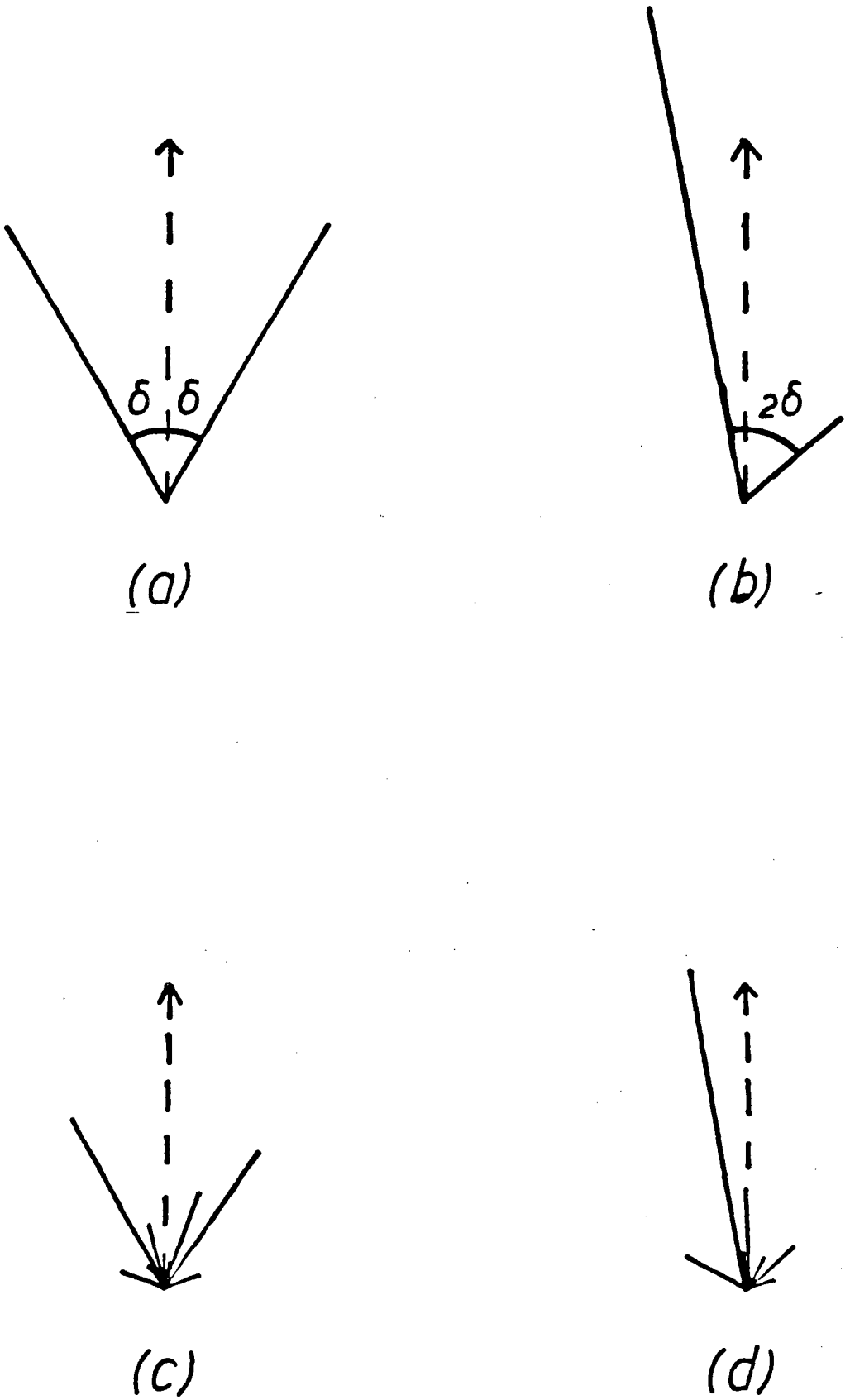

Fig. 2.3

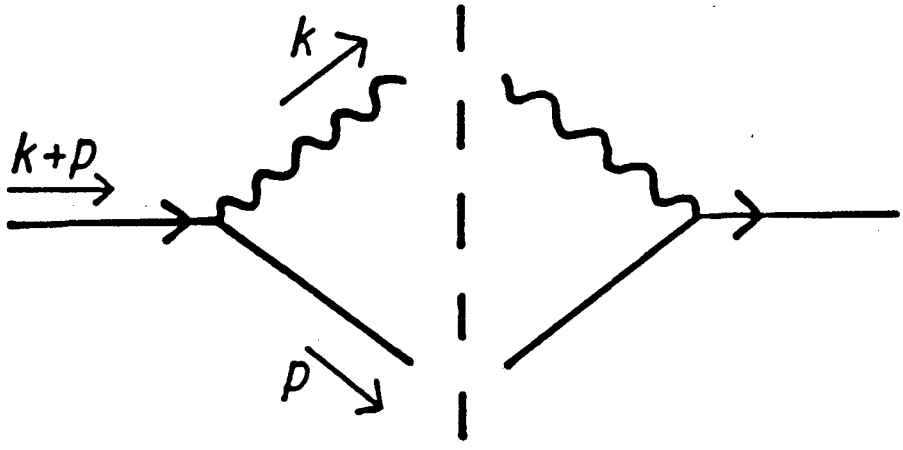

Fig. 3.1

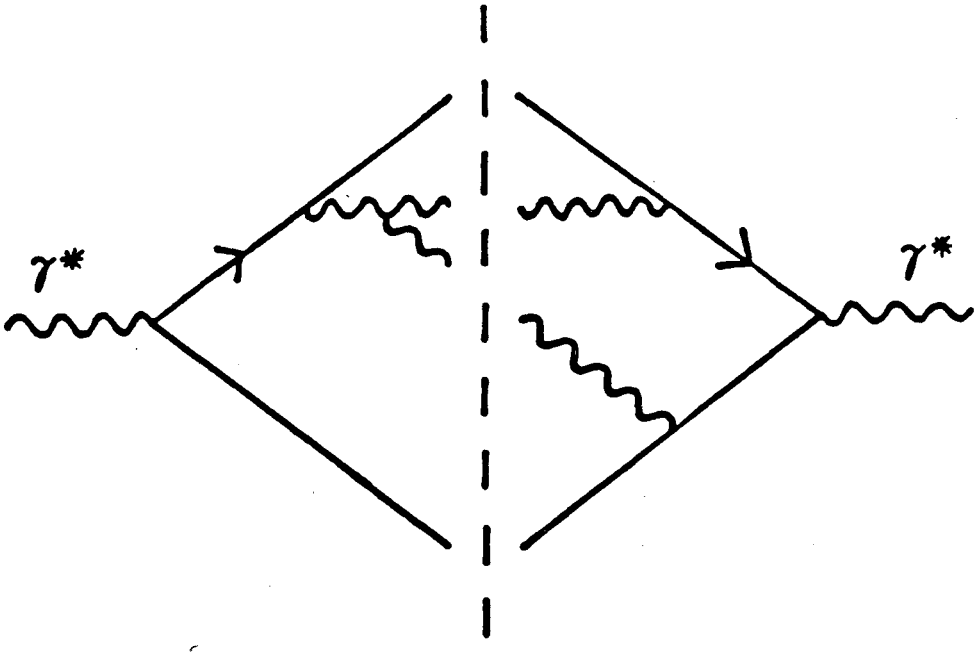

Fig. 3.2

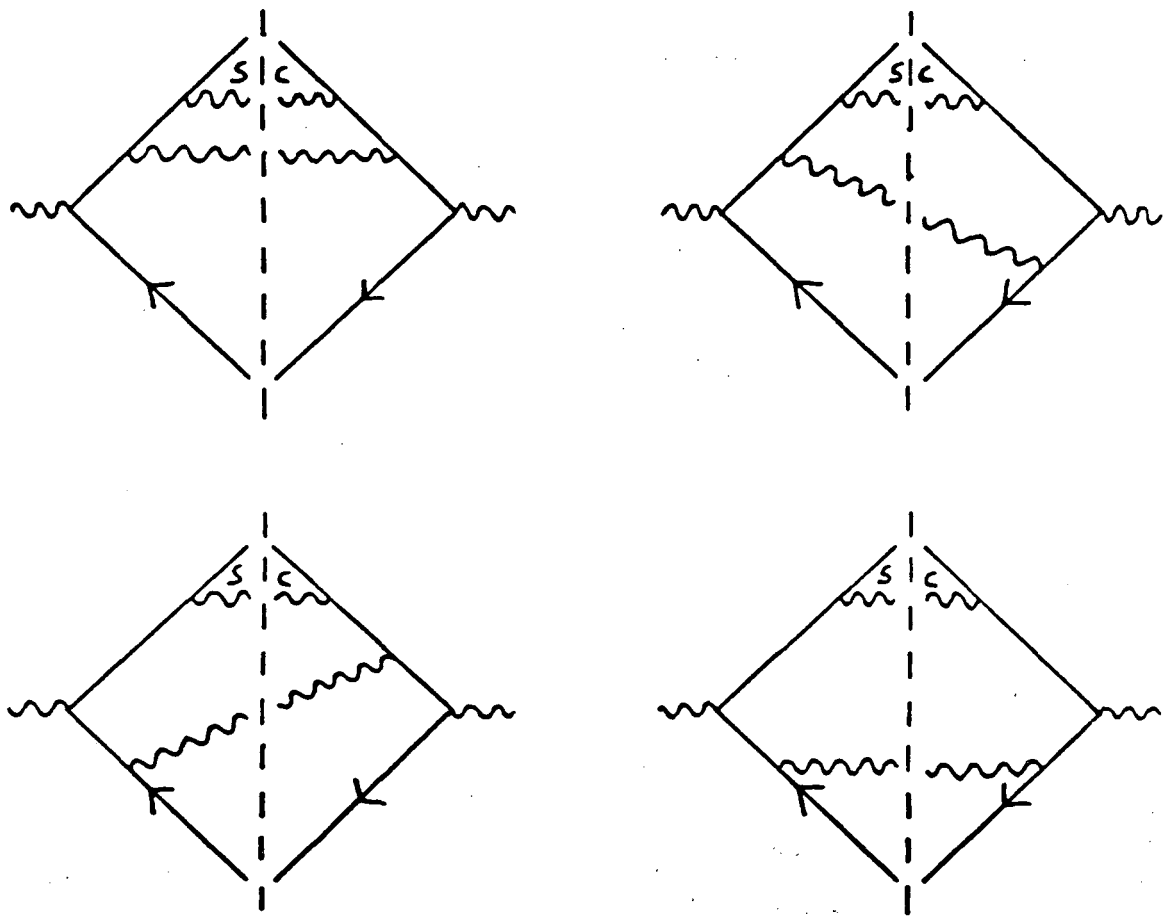

(a)

Fig. 3.3

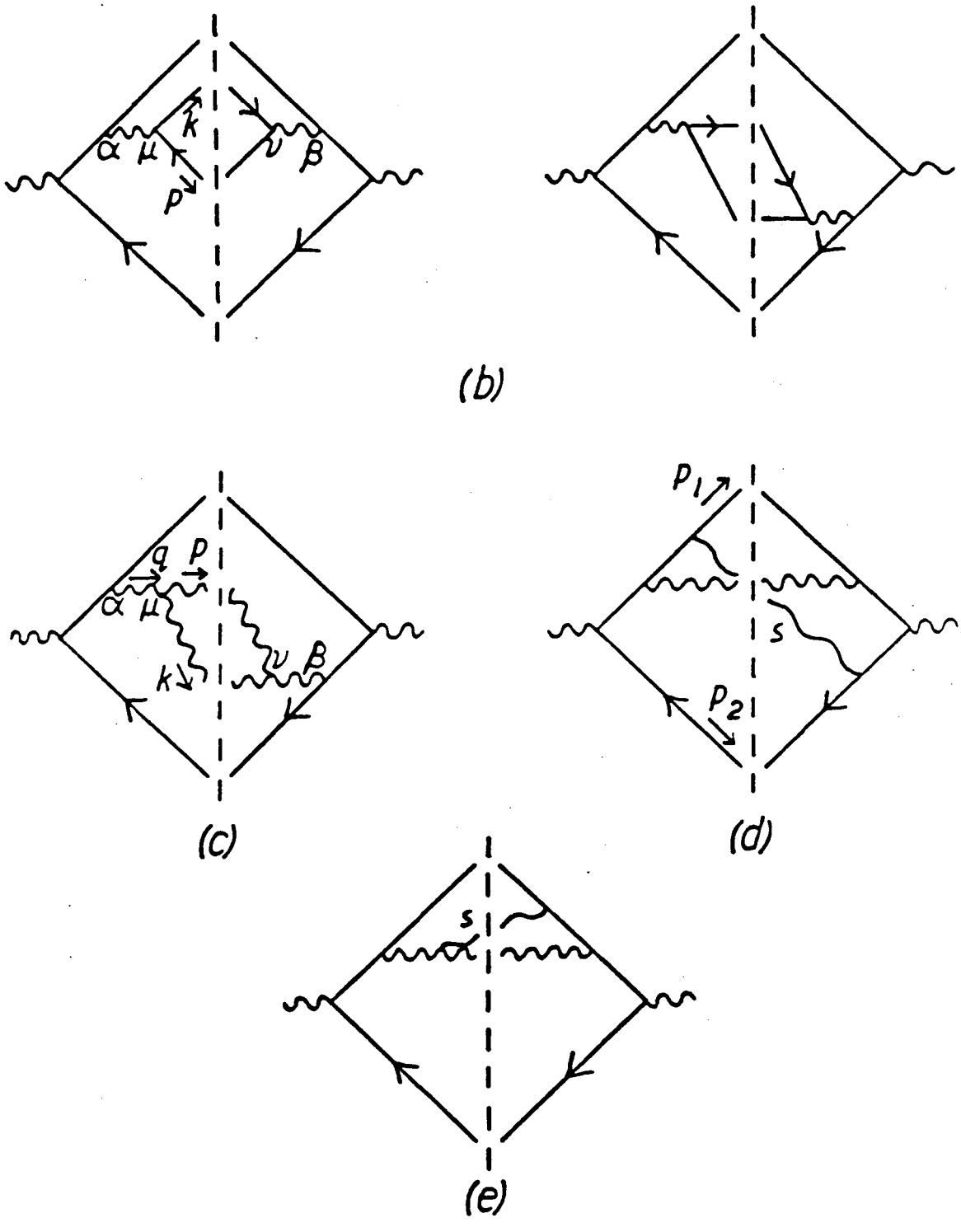

Fig. 3.3

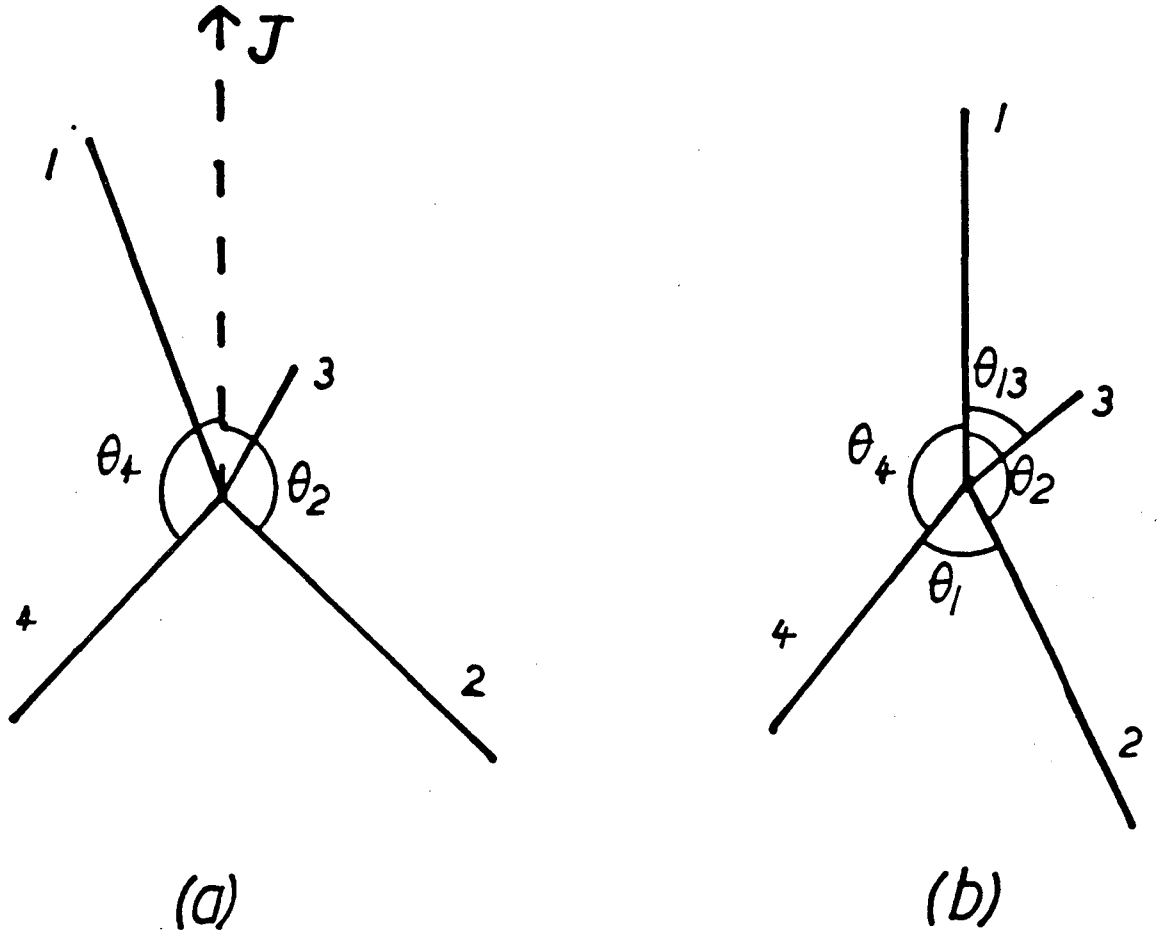

Fig. 4.1

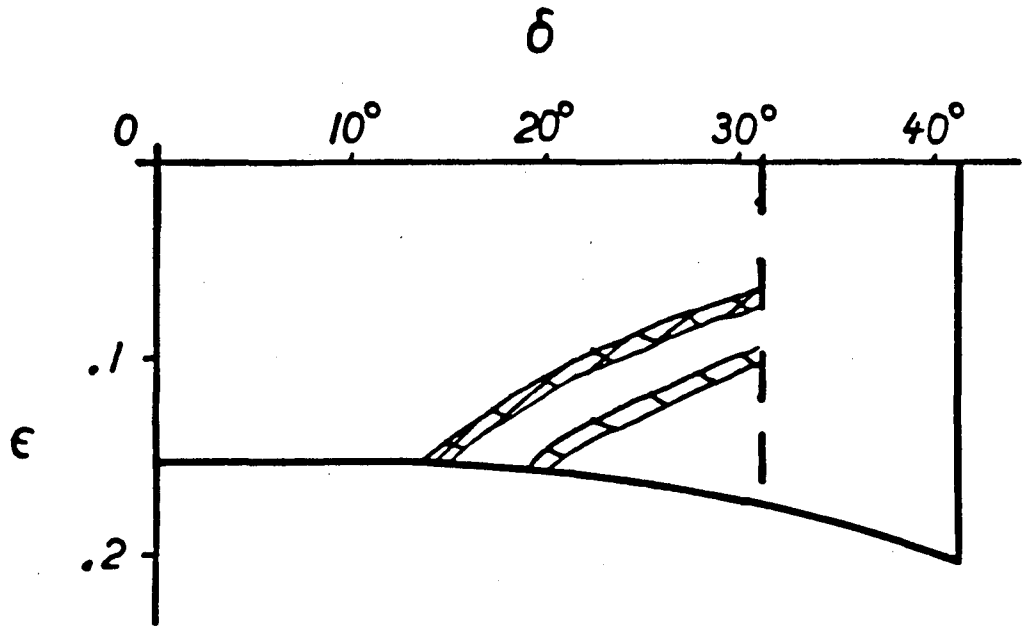

Fig. 5.1

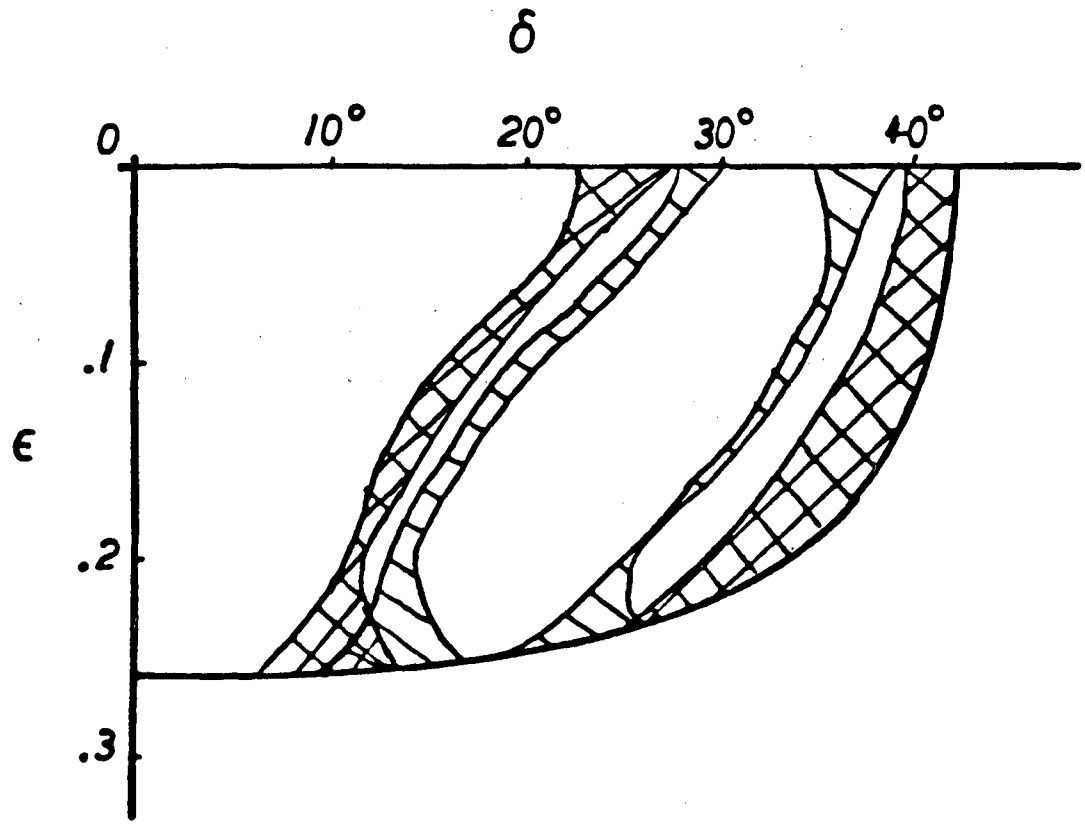

Fig. 5.2

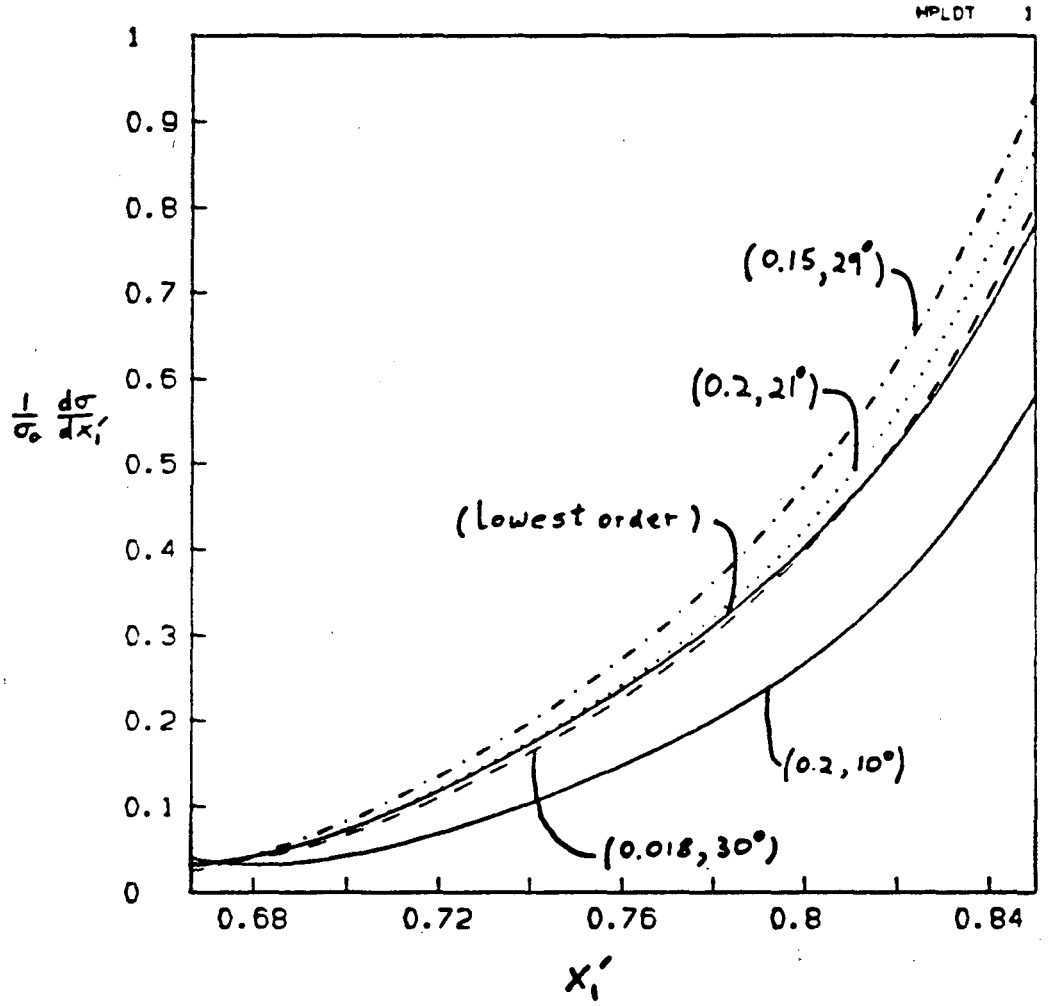
MPLDT 1
1
0.9
0.8
0.7
0.6
0.5
0.4
0.3
0.2
0.1
0
0.68
0.72
0.76
0.8
0.84
$\frac{1}{\sigma_0}\frac{d\sigma}{dx_1'}$
x_1'
(0.15, 29°)
(0.2, 21°)
(lowest order)
(0.2, 10°)
(0.018, 30°)

Fig. 5.3

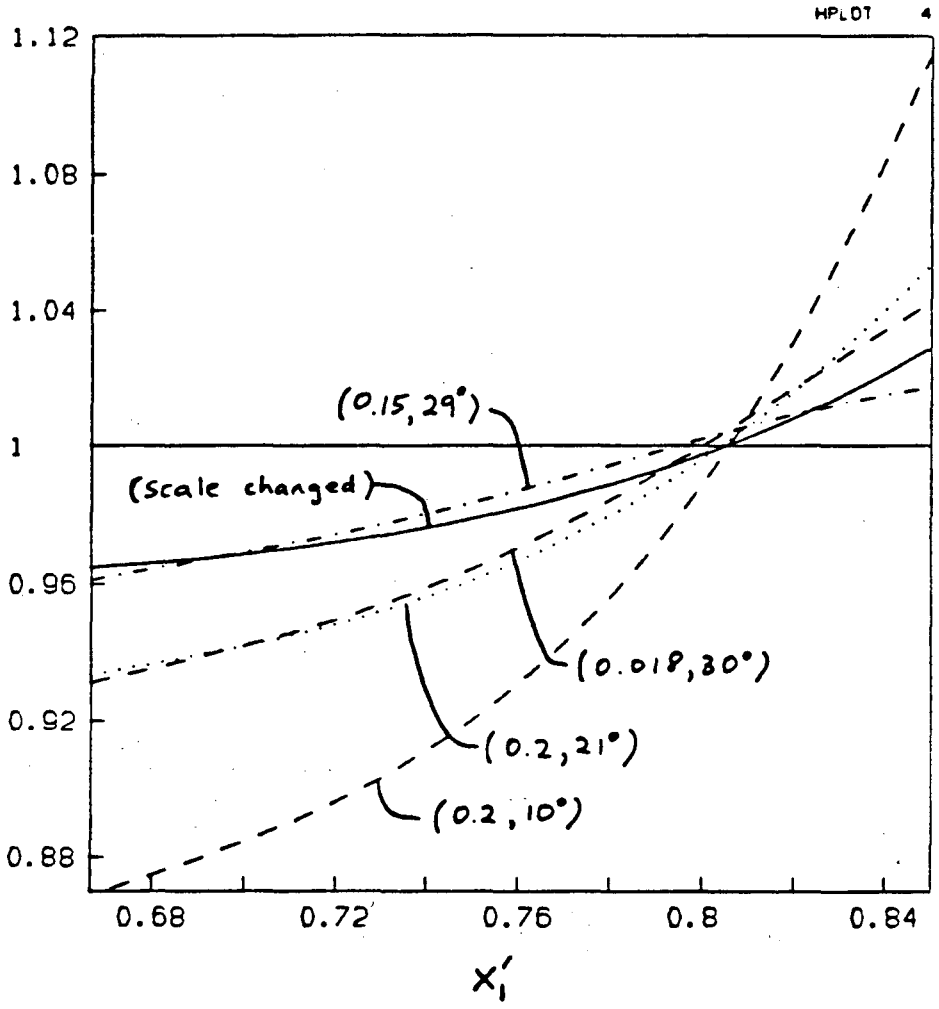
HPLOT 4
1.12
1.08
1.04
1
0.96
0.92
0.88
0.68
0.72
0.76
0.8
0.84
X_1'
(0.15, 29°)
(scale changed)
(0.018, 30°)
(0.2, 21°)
(0.2, 10°)

Fig. 5.4a

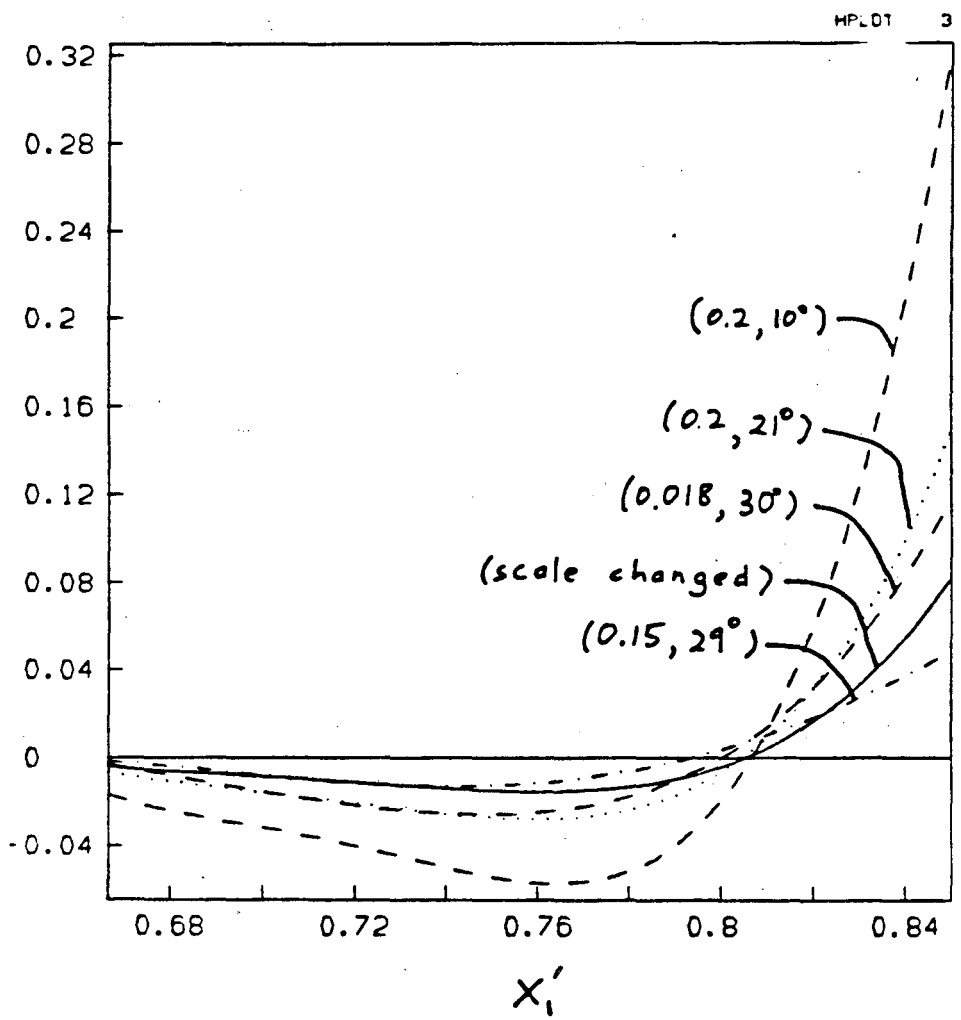
HPLOT 3
0.32
0.28
0.24
0.2
0.16
0.12
0.08
0.04
0
-0.04
0.68
0.72
0.76
0.8
0.84
X_1'
(0.2, 10°)
(0.2, 21°)
(0.018, 30°)
(scale changed)
(0.15, 29°)

Fig. 5.4b

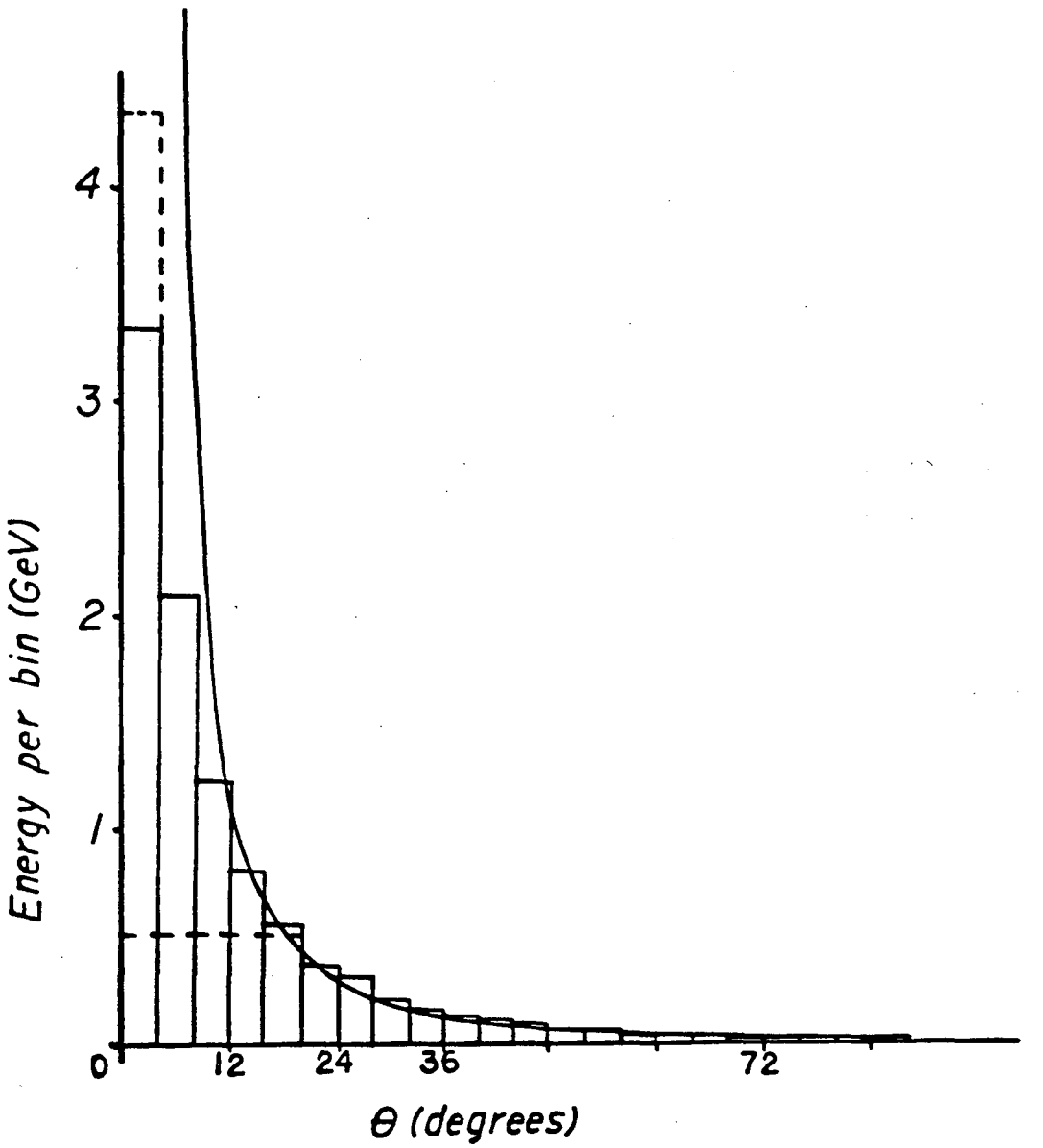

Fig. 5.5

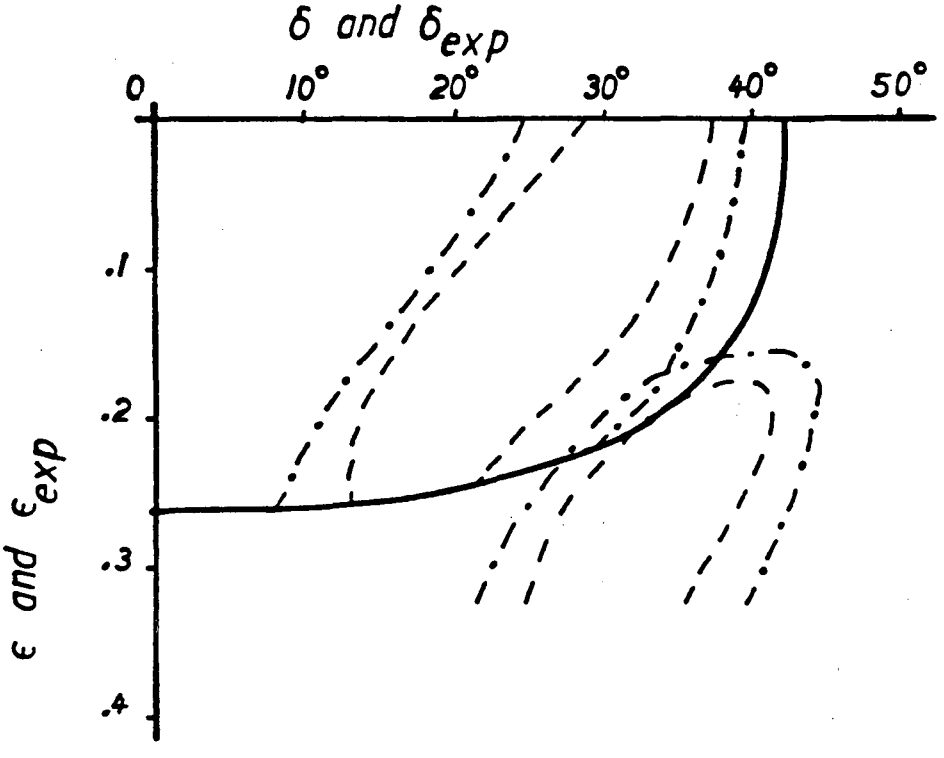

Fig. 5.6

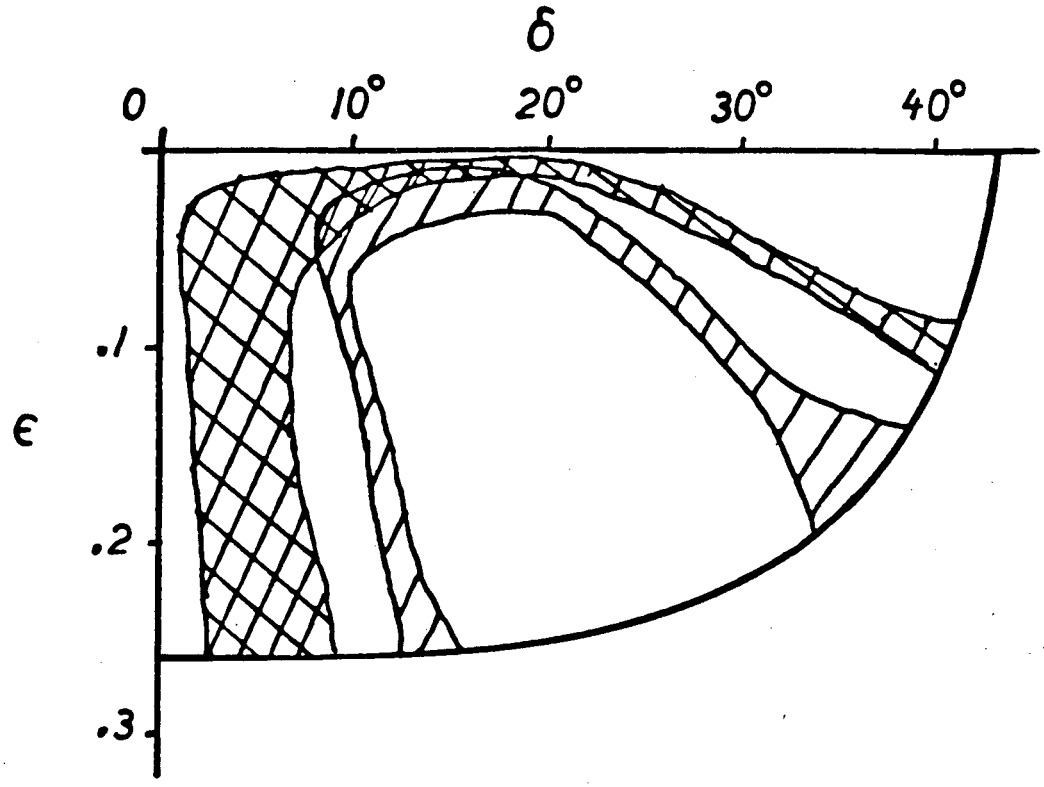

Fig. 5.7

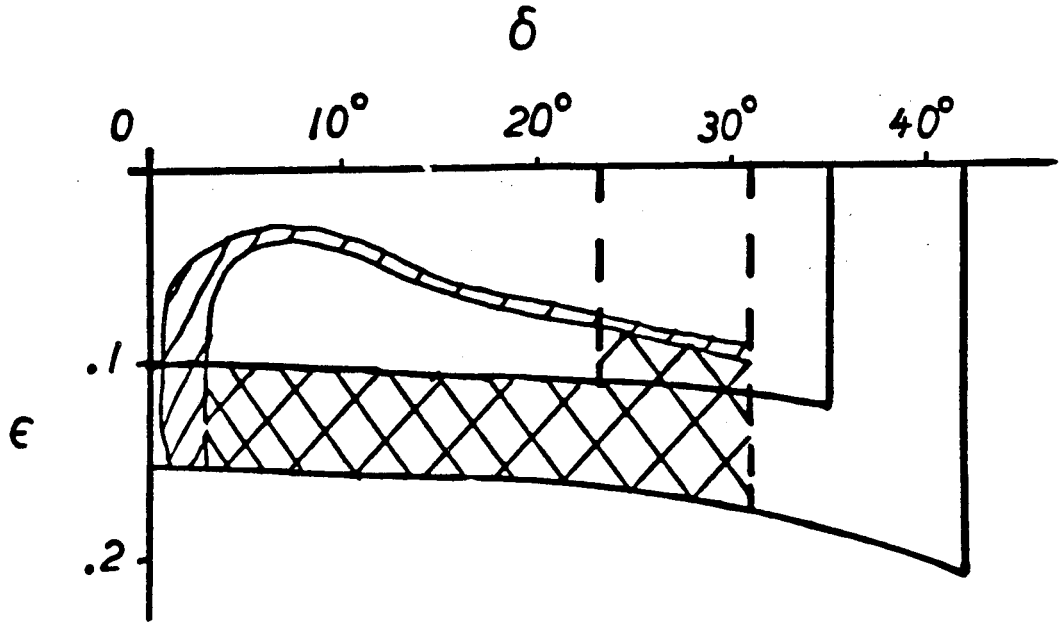

Fig. 5.8

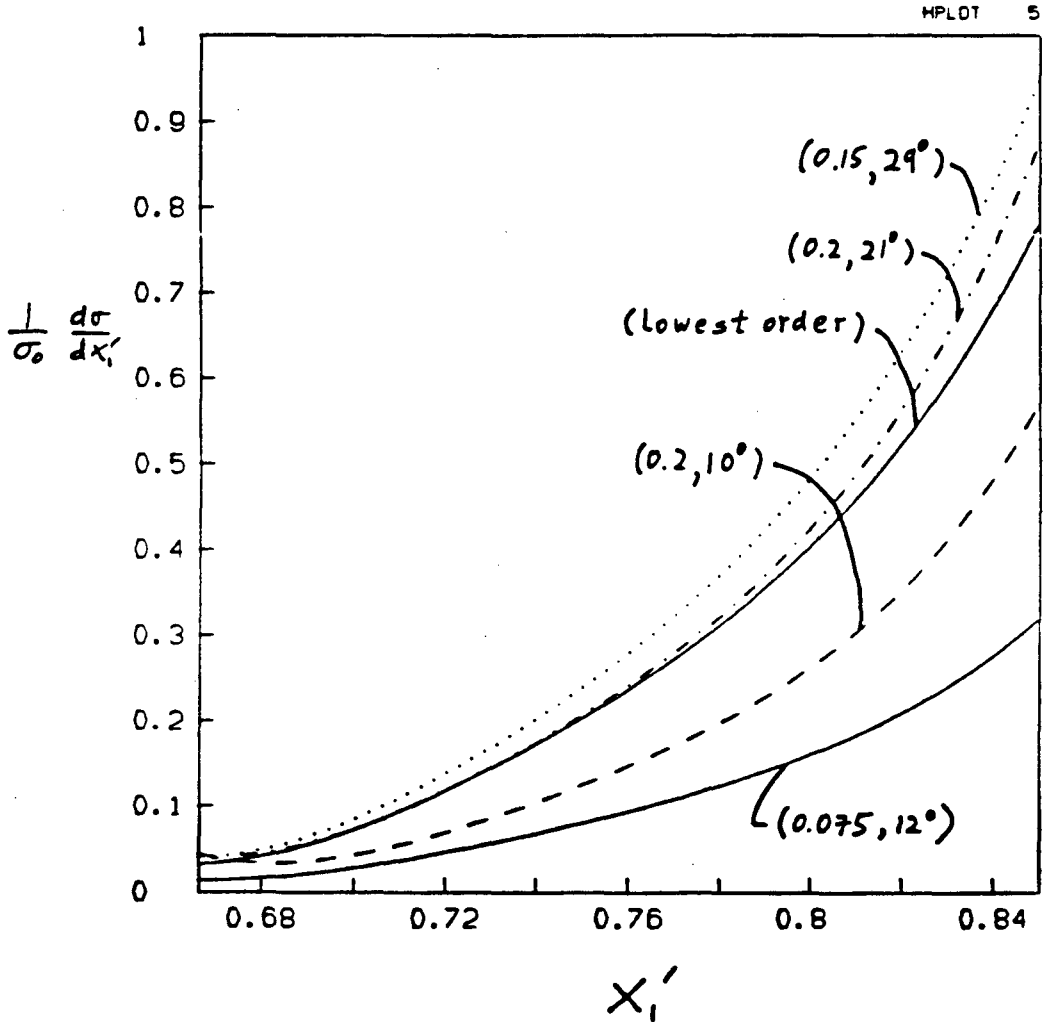
HPLOT 5
1
0.9
0.8
0.7
0.6
0.5
0.4
0.3
0.2
0.1
0
0.68
0.72
0.76
0.8
0.84
$\frac{1}{\sigma_0}\frac{d\sigma}{dx_1'}$
x_1'
(0.15, 29°)
(0.2, 21°)
(lowest order)
(0.2, 10°)
(0.075, 12°)

Fig. 5.9

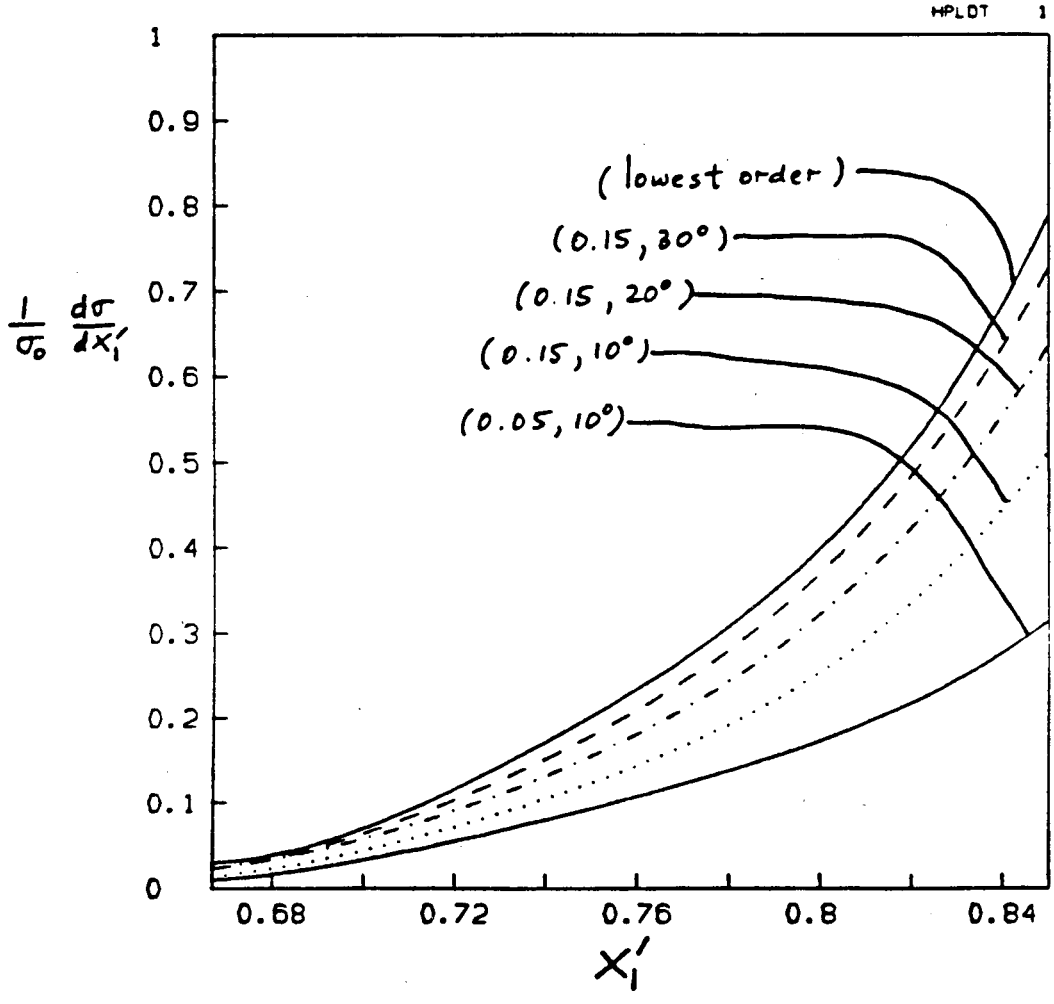
HPLOT 1
1
0.9
0.8
0.7
0.6
0.5
0.4
0.3
0.2
0.1
0
0.68
0.72
0.76
0.8
0.84
$\frac{1}{\sigma_0}\frac{d\sigma}{dx_1'}$
x_1'
(lowest order)
(0.15, 30°)
(0.15, 20°)
(0.15, 10°)
(0.05, 10°)

Fig. 5.10

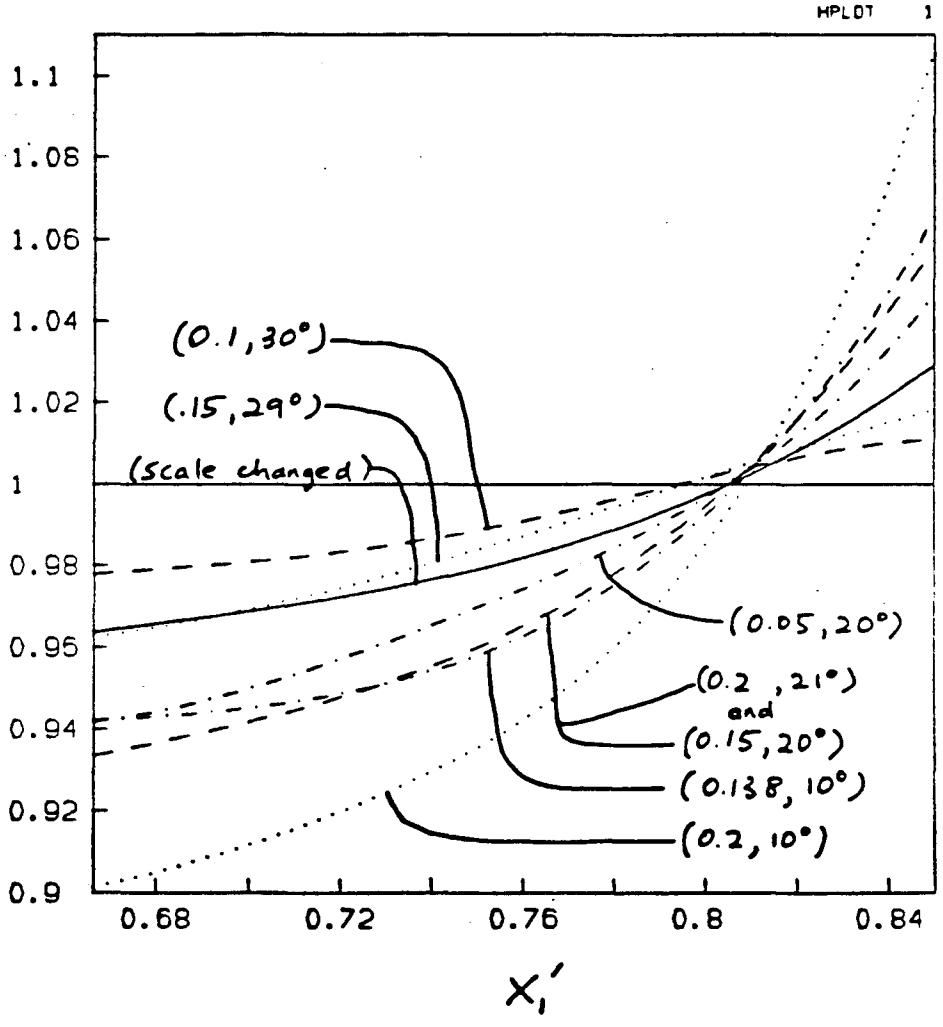
HPLOT 1
1.1
1.08
1.06
1.04
1.02
1
0.98
0.96
0.94
0.92
0.9
0.68
0.72
0.76
0.8
0.84
X_1'
(0.1, 30°)
(.15, 29°)
(scale changed)
(0.05, 20°)
(0.2 , 21°)
and
(0.15, 20°)
(0.138, 10°)
(0.2, 10°)

Fig. 5.11a

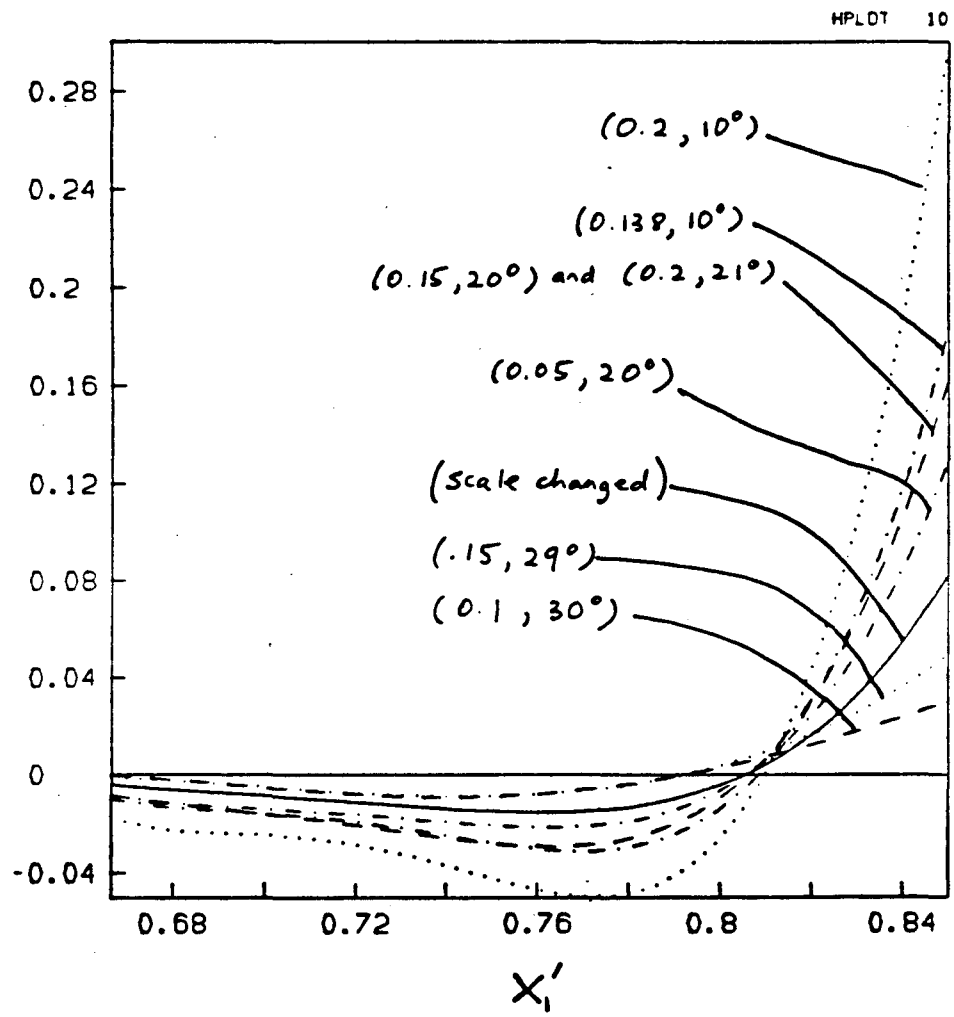
HPLOT 10
0.28
0.24
0.2
0.16
0.12
0.08
0.04
0
-0.04
0.68
0.72
0.76
0.8
0.84
X_1'
(0.2, 10°)
(0.138, 10°)
(0.15, 20°) and (0.2, 21°)
(0.05, 20°)
(scale changed)
(.15, 29°)
(0.1, 30°)

Fig. 5.11b

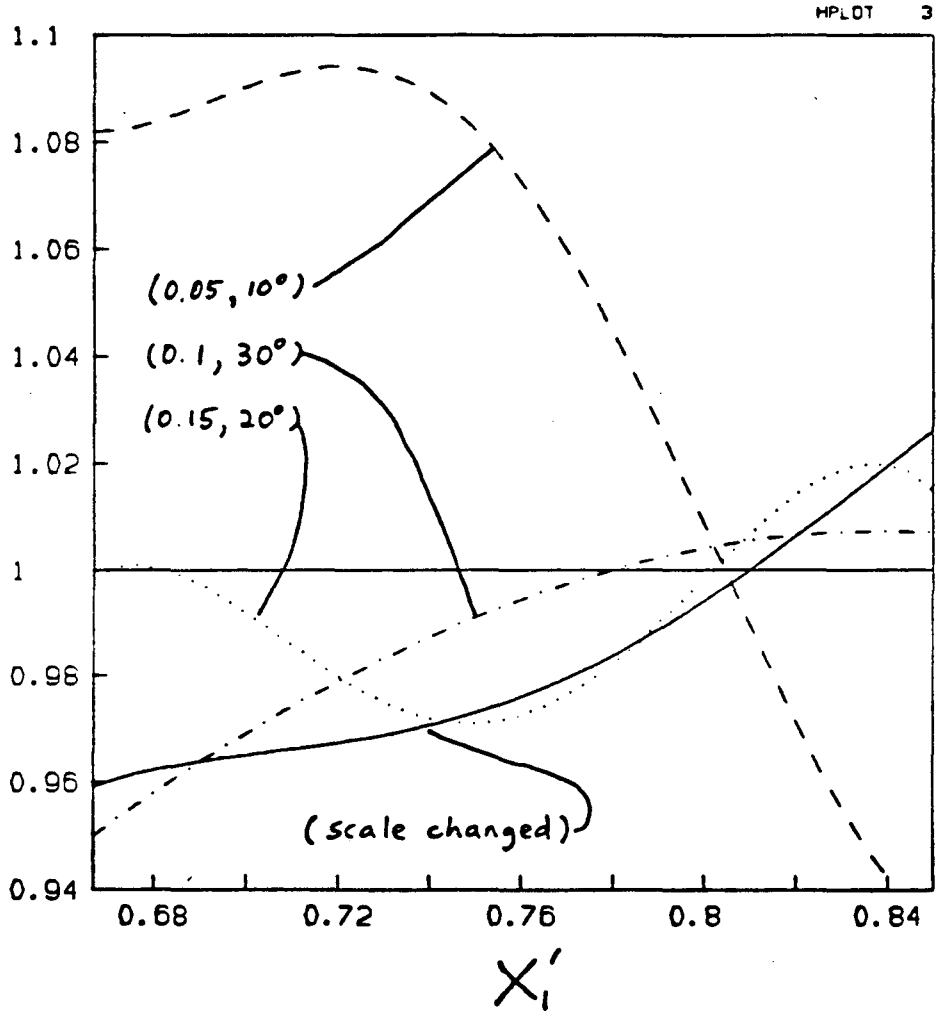
HPLOT 3
1.1
1.08
1.06
1.04
1.02
1
0.98
0.96
0.94
0.68
0.72
0.76
0.8
0.84
(0.05, 10°)
(0.1, 30°)
(0.15, 20°)
(scale changed)
X_1'

Fig. 5.12a

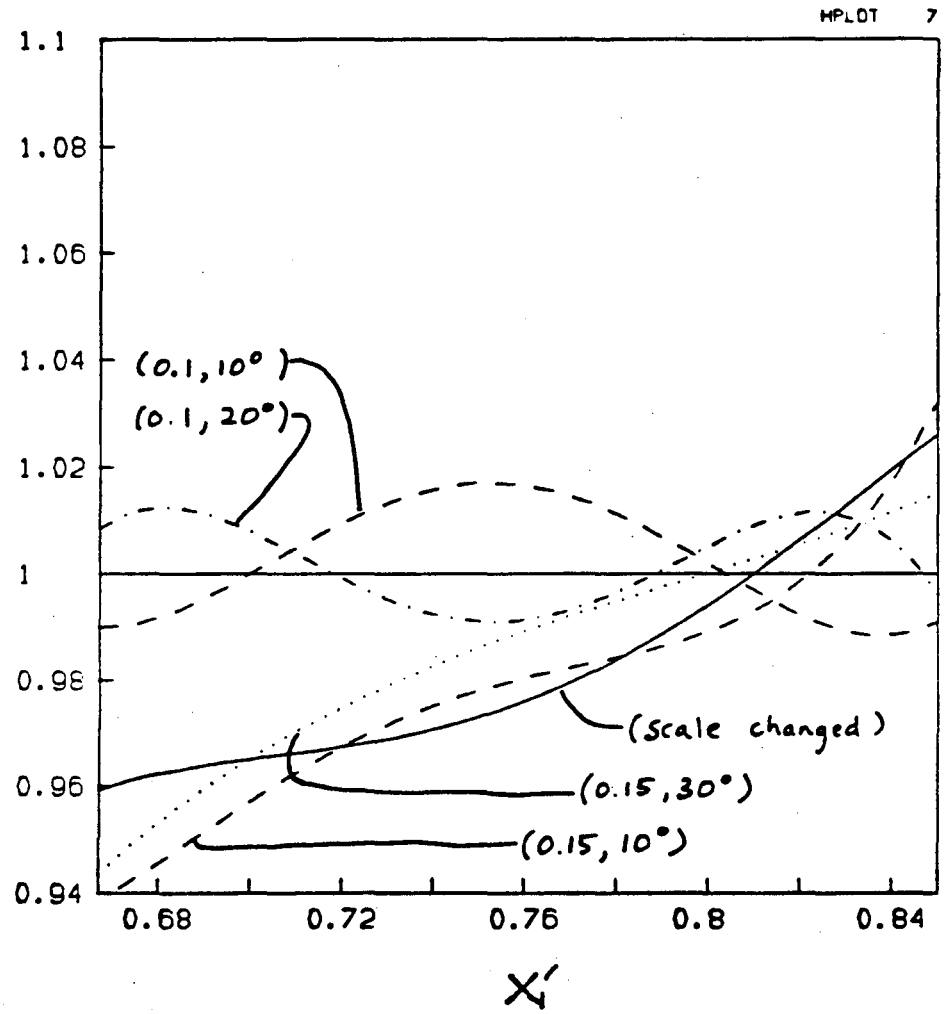
HPLOT 7
1.1
1.08
1.06
1.04
1.02
1
0.98
0.96
0.94
0.68
0.72
0.76
0.8
0.84
(0.1, 10°)
(0.1, 20°)
(Scale changed)
(0.15, 30°)
(0.15, 10°)
X'

Fig. 5.12b

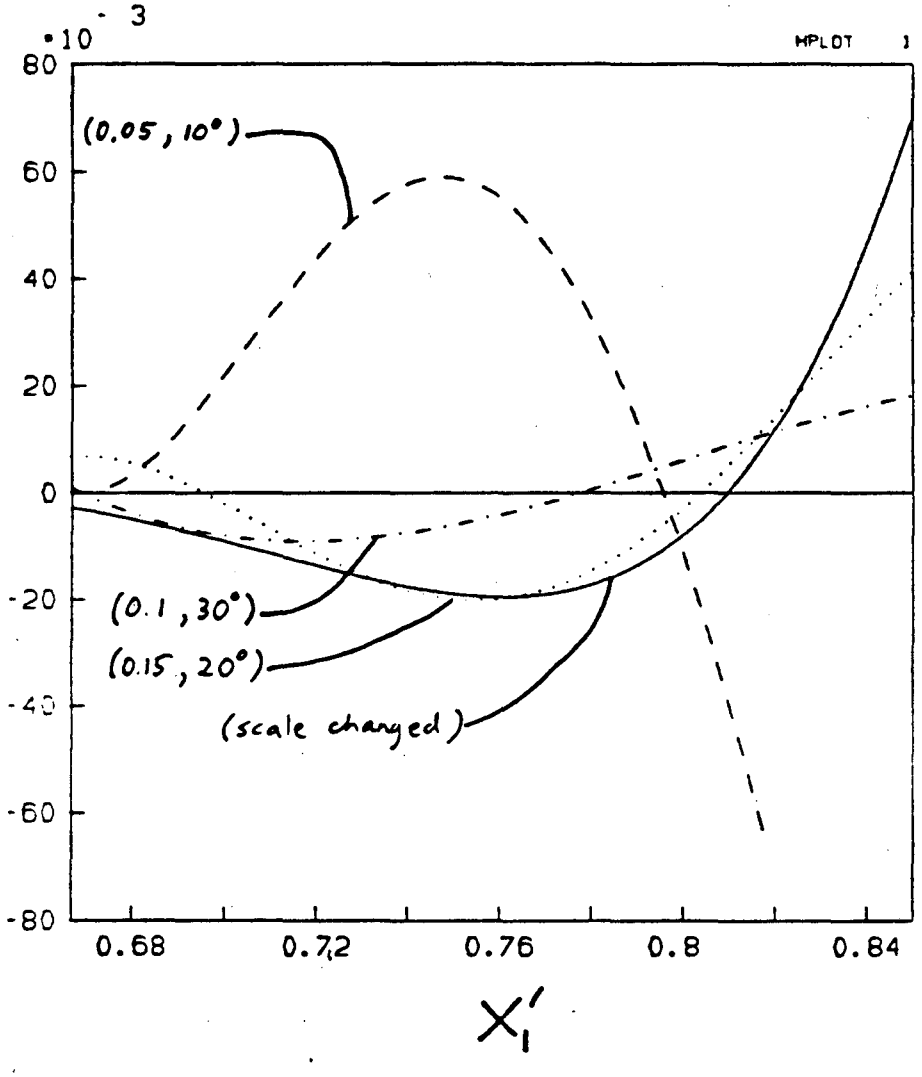
•10 - 3
MPLOT 1
80
60
40
20
0
-20
-40
-60
-80
0.68
0.72
0.76
0.8
0.84
(0.05, 10°)
(0.1, 30°)
(0.15, 20°)
(scale changed)
X'1

Fig. 5.12c

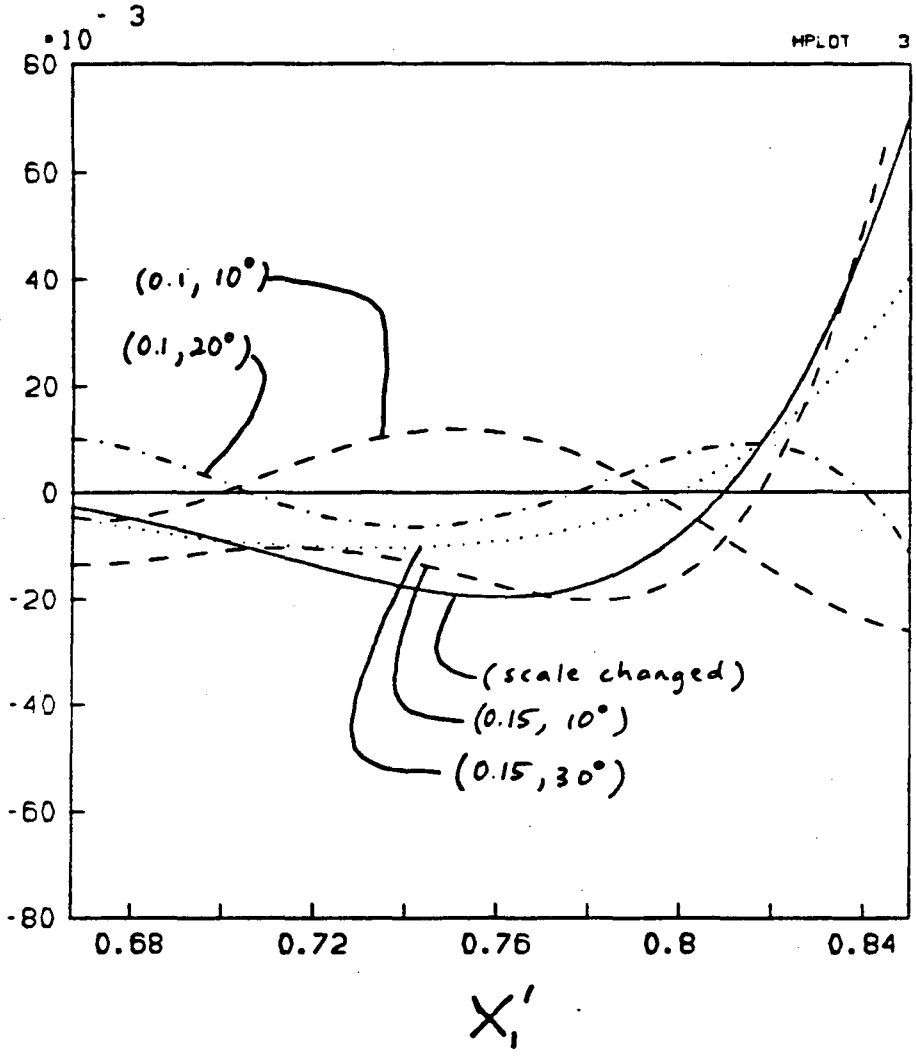
$\cdot 10^{-3}$
HPLOT 3
80
60
40
20
0
-20
-40
-60
-80
0.68
0.72
0.76
0.8
0.84
X_1'
(0.1, 10°)
(0.1, 20°)
(scale changed)
(0.15, 10°)
(0.15, 30°)

Fig. 5.12d

This report was done with support from the Department of Energy. Any conclusions or opinions expressed in this report represent solely those of the author(s) and not necessarily those of The Regents of the University of California, the Lawrence Berkeley Laboratory or the Department of Energy.

Reference to a company or product name does not imply approval or recommendation of the product by the University of California or the U.S. Department of Energy to the exclusion of others that may be suitable.

TECHNICAL INFORMATION DEPARTMENT
LAWRENCE BERKELEY LABORATORY
UNIVERSITY OF CALIFORNIA
BERKELEY, CALIFORNIA 94720